NASA CR 114521
Aerotherm Report No. 72-56, Vol. I

V. 1 - NASA CR-114,521
V. 2 - NASA CR-114,522

THERMAL SCREENING OF SHUTTLE ORBITER VEHICLE TPS MATERIALS UNDER CONVECTIVE HEATING CONDITIONS

Volume I

Final Report

by

John W. Schaefer

August, 1973

Contract NAS2-6445

NASA Ames Research Center
Moffett Field, California
Nick S. Vojvodich, Technical Monitor

AEROTHERM
ACUREX Corporation
485 Clyde Avenue
Mountain View, California

FOREWORD

This report is Volume I of a two volume report prepared by the Aerotherm Division of Acurex Corporation under National Aeronautics and Space Administration Contract No. NAS2-6445 which describes an extensive screening test program under convective heating conditions for the complete spectrum of candidate shuttle orbiter vehicle TPS materials. Volume I (this report) serves as the final report under the contract and also presents representative test results. Volume II is a complete tabulation of all test results on all test samples, and because of its limited general interest is available only from the NASA Technical Monitor. This work was sponsored by the Ames Research Center with Mr. Nick S. Vojvodich as the NASA Technical Monitor. The Aerotherm Program Manager and principal investigator was Mr. John W. Schaefer. The author gratefully adknowledges the support of the Technical Monitor and the Aerotherm personnel who contributed to the program.

SUMMARY

A low cost cyclic test procedure for screening candidate shuttle orbiter TPS materials was developed and employed in an extensive screening test program. The test program was performed in the Aerotherm arc plasma test facility:

- Under multiple cycle convective heating conditions which simulated the shuttle vehicle reentry
- For all candidate TPS material concepts - metallics, surface insulators, carbon-carbon composites, and ablators.

The test procedure maximized efficiency and minimized cost by utilizing multiple test samples - up to six - in each test model, and by employing continuous testing of two models which were alternately exposed to the test stream. The test model and test sample designs allowed a quick change of test samples, which employed common instrumentation, to minimize turn around time between each series of cyclic tests. At maximum testing efficiency the demonstrated cost was as low as $70 per hour of exposure which, with a six sample model configuration, resulted in a cost of roughly $10 per sample hour. The test configuration was a flat face stagnation point model which was 4 3/4 inches in diameter and which was immersed in an 8-inch diameter supersonic air test stream. The TPS material concepts and types which were tested and the corresponding exposure hours were as follows:

Concept and Type	Facility Hours	Sample Hours
• Metallics	82-1/4	487-1/2
TD nickel chrome Coated columbium Coated tantalum		
• Surface Insulators	131-1/2	288
LI-1500 (silica system) HCF (mullite system) REI (mullite system) Silicon carbide foam		
• Carbon-Carbon Composite	54-1/4	91
Truss core and conventional, various coating systems		
• Ablators	3-1/3	3-1/3
SS41		

The total facility test time for all materials was 271-1/3 hours and the total sample hours of exposure time was 870 hours. The test conditions covered the spectrum of surface temperature and heat flux appropriate to the application of these materials to the shuttle orbiter vehicle. The test samples were nominally exposed to from 1 to 50 half hour cycles. Measurements were made during exposure and nominally after every 6 cycles to define thermal response in terms of surface and in-depth temperatures, mass loss and surface recession, surface properties in terms of emissivity and catalycity, failure modes, and operating limits.

TABLE OF CONTENTS

LIST OF FIGURES

FIGURES (continued)

LIST OF TABLES

LIST OF SYMBOLS

A_*	throat area
C_H	heat transfer coefficient
C_p	specific heat
h	enthalpy
h_{eb}	enthalpy defined by energy balance
h_{mb}	enthalpy defined by mass balance (sonic flow)
h_{hf}	enthalpy defined by heat flux and pressure
$\dot{m}$	flow rate
p, P	pressure
q_c	convective heat flux
q_r	radiation heat flux
r, R	radius
R_b	model body radius
R_{eff}	effective model radius
T	temperature
ε	emissivity
σ	Stefan-Boltzmann constant

SUBSCRIPTS

cw	cold wall
e	edge
hw	hot wall
o	total or chamber
s	stagnation
w	surface, cooling water

SECTION 1

INTRODUCTION

The spectrum of candidate TPS material concepts and types for the NASA space shuttle orbiter vehicle is extremely broad. The evaluation of these materials requires extensive thermal testing, even for screening purposes, under cyclic convective heating conditions which simulate multiple reentries of the shuttle vehicle. Because of the broad spectrum of materials and the multiple reuse requirement, the testing to accomplish this evaluation must be performed in as efficient a manner as possible. A low cost cyclic screening test procedure for evaluating candidate TPS materials - metallics, surface insulators, carbon-carbon composites, and ablators - in an arc heater test facility was therefore developed. This procedure was then employed in an extensive cyclic screening test program in which the complete spectrum of material concepts and types was evaluated under simulated reentry convective heating conditions.

Consistent with the above requirements, the basic guidelines for the program were to:

- Provide a test stream which simulates as closely as possible the convective heating environment (heating rate, surface pressure, and total enthalpy) expected for the space shuttle orbiter vehicle
- Design and fabricate model and test sample configurations which result in maximum test results and maximum test efficiency
- Conduct cyclic tests of candidate TPS materials in this environment and with these configurations to:
  - Determine surface and in-depth temperature response characteristics
  - Define surface properties (emittance and surface catalytic activity)
  - Determine mass loss and surface recession
  - Identify the sensitivity of the above to the cyclic performance requirement

This report describes the low cost cyclic test procedure and presents the screening test results for the spectrum of space shuttle orbiter TPS materials. Note that the interpretation of the test results was outside the scope of this work and therefore is not included. Section 2 describes the test program in terms of the test facility, test samples and models, instrumentation and data reduction, test procedure, and test conditions. Section 3 presents the calibration test results which encompassed the definition of the basic test conditions, stream distributions and model distributions of properties (pressure, heat flux, and enthalpy), and surface catalycity measurements. Section 4 presents the test results on the TPS material concepts (and types) - metallics (TD nickel chrome, coated columbium, and coated tantalum), surface insulators (LI-1500, HCF, REI, silicon carbide foam), carbon-carbon composites (various oxidation inhibiting systems), and ablators (SS41). Finally, Section 5 presents the conclusions and recommendations.

SECTION 2

TEST PROGRAM

A detailed description of the test program is included in the following subsections which present the:

- Test facility
- Model and test sample configurations
- Instrumentation and data reduction
- Test procedure
- Test conditions

2.1 TEST FACILITY

The tests were performed in the Aerotherm 1.5-MW arc plasma facility described in Table 1, and the hyperthermal test stream was generated by the Aerotherm 300 kw constrictor arc heater shown schematically in Figure 1. In the arc unit, the energy is added to the primary test gas via a steady electric arc discharge, the arc striking from the tungsten cathode to the downstream diverging copper anode. The primary test gas was high purity nitrogen and was introduced at the downstream end of the cathode module. The secondary gas was high purity oxygen in the proper amount to yield the composition of air and was introduced in the plenum and mixing chamber.

The arc heater and associated hardware were cooled with high pressure, deionized water. Power was supplied by a 660 kw continuous duty, 1.5 MW overload saturable reactor controlled DC rectifier. The conical test nozzle had a throat diameter of 1.0 inch and an exit diameter of 8.0 inches. The arc heater, plenum, and nozzle assembly were mounted on the vacuum test chamber to which the nozzle exhausted. This chamber also contained the model sting mechanisms and other necessary support equipment. The vacuum chamber pressure during test was about 0.3 mm Hg for the 8-inch nozzle which closely matched the nozzle exit pressure. The continuous vacuum pumping capability was provided by a five-stage steam ejector vacuum pumping system.

The model stings were pneumatically actuated to provide a radial motion in and out of the test stream and included variable stop positions for stepwise traverse of the test stream. The stings were water cooled to provide continuous duty operation at all test conditions. Three stings were employed as follows:

Sting Position	Model Configuration	
	Sample Tests	Calibration Tests
2	Test Sample Model	Pressure Probe
3	Calibration Model	Calibration Model
4	Test Sample Model	Calorimeter

These model configurations are described below.

TABLE 1

DESCRIPTION OF TEST FACILITY

• Arc Heater	
Type	Aerotherm 1.5 Mw and 300 kw Constrictor Arc Heaters
Input Power	1.2 Mw to 50 kw DC, 300 to 10 kw DC
Chamber Pressure	0.04 to 30 atm
Enthalpy	1000 to 80,000 Btu/lb
Gas Flow Rate	0.002 to 0.15 lb/sec
Gas Compositions	N_2, O_2, Air, He, A, H_2, CO_2, CO, H_2O, HCl, BF_3, Solid particles, and mixtures of the above
Stabilization	Gas
Electrodes	Copper/Tungsten, Copper/Copper
• Power Supply	
Type	Rectifier, Saturable reactor controlled
Rating	800 kilowatts for 1 hour, 1 megawatt for 10 minutes
• Nozzles and Test Sections	
Supersonic Nozzles	
Exit Diameter	8.0 to 0.45 inch } 10 Combinations
Throat Diameter	1.0 to 0.32 inch }
Area Ratio	64 to 2
Expansion Angle	7.5° and 8.5° half angle, and contoured
Duct Flow Apparatus	
Size	0.1 to 0.5 inch high, 3.0 to 5.0 inch long, 1.0 inch wide
Model Size/Shape	0.5 to 1.0 inch thick/flat or contoured
Sonic Nozzles	
Throat Diameter	0.3 to 1.0 inch
Type	Water cooled or ablating test section
• Test Chamber	
Size	3.5 ft. diameter by 15 ft. long
Chamber Cooling	Cooled diffuser with heat exchanger
Viewing and Access	2 - 12 x 16 inch windows, 4 - 3 in. diameter quartz windows
• Vacuum System	
Type	Steam ejector, 5 stage continuous operation
Capacity	0.1 lb/sec at 10 torr, 0.02 lb/sec at 0.2 torr, 0.004 lb/sec at 0.05 torr
• Model Sting System	
Type	Pneumatic actuated, variable insertion speed
Capacity	7 stings per test maximum
• Instrumentation	
Enthalpy	Energy balance, mass balance, heat flux potential
Flow Rate	ASME orifice, rotometer
Temperature	Thermocouple, thermopile, pyrometer
Pressure	Strain gauge & reluctance transducers and Bourdon tube gauge
Recording	High speed 80-channel digital data acquisition system with magnetic tape recording, high speed 36-channel oscillograph, digital and potentiometric recorders, oscilloscopes

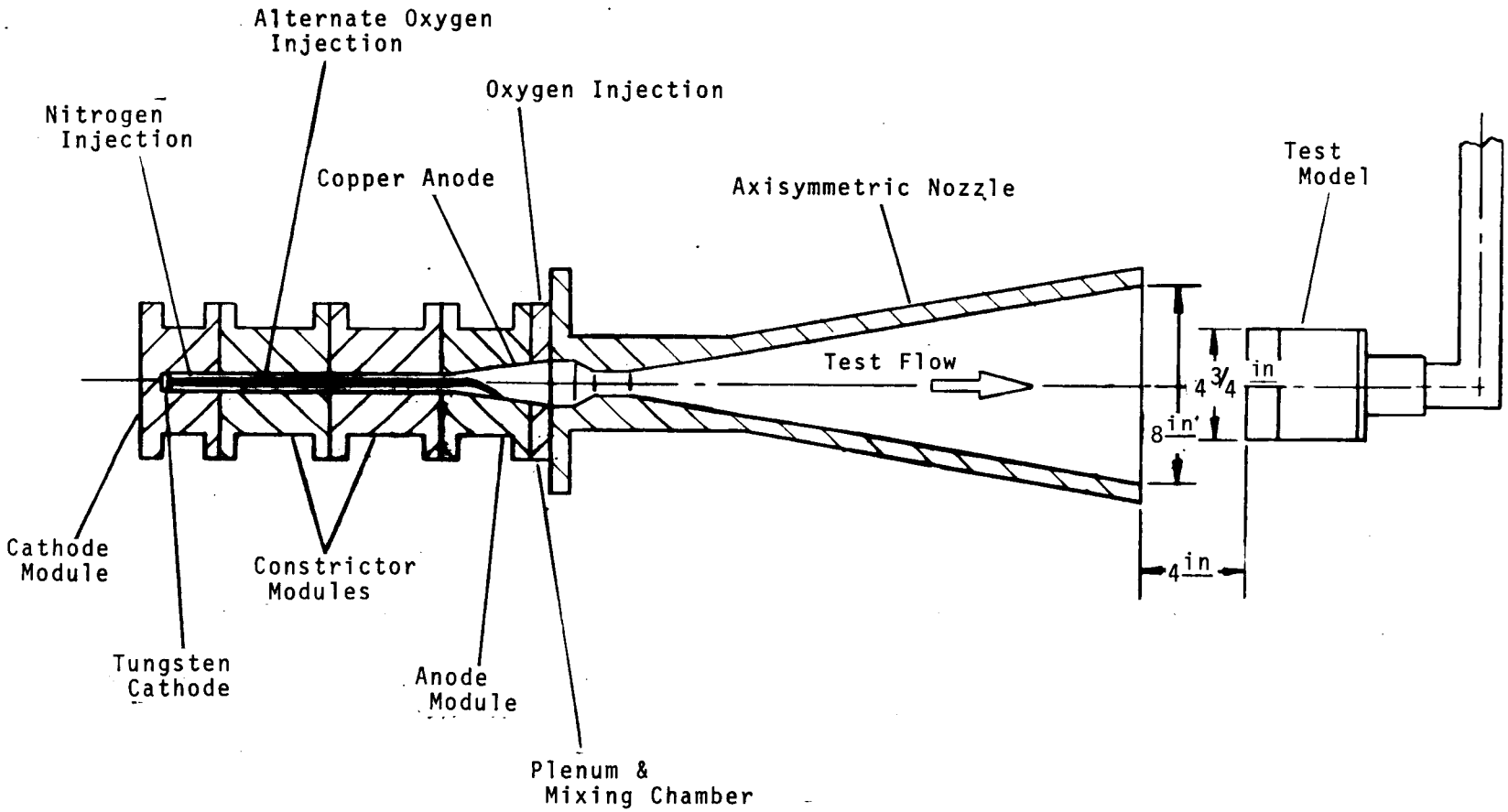

Figure 1 Aerotherm 300kw Constrictor Arc Heater and Overall Test Setup

The test data were recorded on magnetic tape with an 80-channel digital data acquisition system. The high speed, multi-channel system was required to accommodate data recording of up to 78 channels (metallics tests) every minute for at least 6-1/2 hours. The magnetic data tape was converted to an unscrambled, easily readable format on a second magnetic tape which served directly as the input to the data reduction computer code.

2.2 MODEL AND TEST SAMPLE CONFIGURATIONS

The flat-face stagnation point model and test sample configurations are presented in Figures 2 and 3 as follows:

- Figure 2 - assembly drawing of models including test samples for all four material types - metallics, surface insulators, carbon-carbon composites, and ablators
- Figure 3 - photograph of a typical model and test samples (metallics) showing model assembly, samples, and components

The flat-face model configuration was chosen for convenience in test sample fabrication, and was 4 3/4 inches in diameter with a 1/8-inch corner radius. This model body diameter allowed the maximum practical test sample size consistent with uniform property distributions across the test samples for the 8-inch diameter test stream and the projected test conditions. The test models were made of copper and were water cooled to:

- Provide a well defined backwall boundary condition
- Allow continuous operation at all test conditions
- Provide the necessary sample cooldown between cycles

For all but the ablator model, the models included a centerpost which contained a calorimeter and pressure tap for continuously monitoring the test conditions throughout each test. A peripheral copper ring was employed to insure that the test samples were not exposed to any unusual thermal or aerodynamic edge effects such as:

- The large edge heat flux for a flat-face model in a uniform stream (Figure 4)
- The large pressure gradient around the corner of the model
- Any significant drop-off in properties due to a non-uniform test stream distribution

The outside diameter of the test samples was therefore 4 1/8 inches (metallics) to 4 1/4 inches (surface insulators and carbon-carbon composites), these dimensions

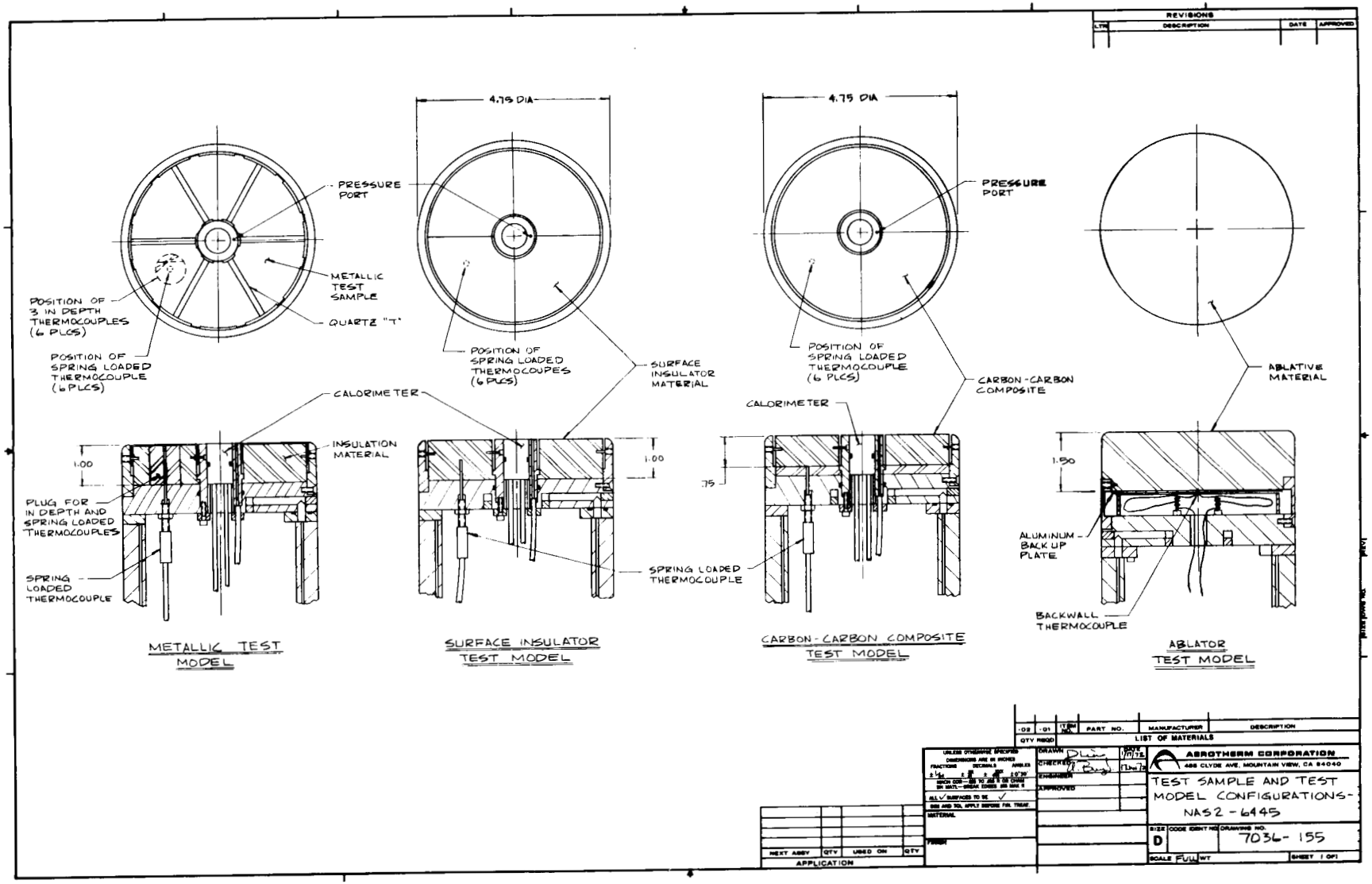

Figure 2 Test Sample and Test Model Configurations

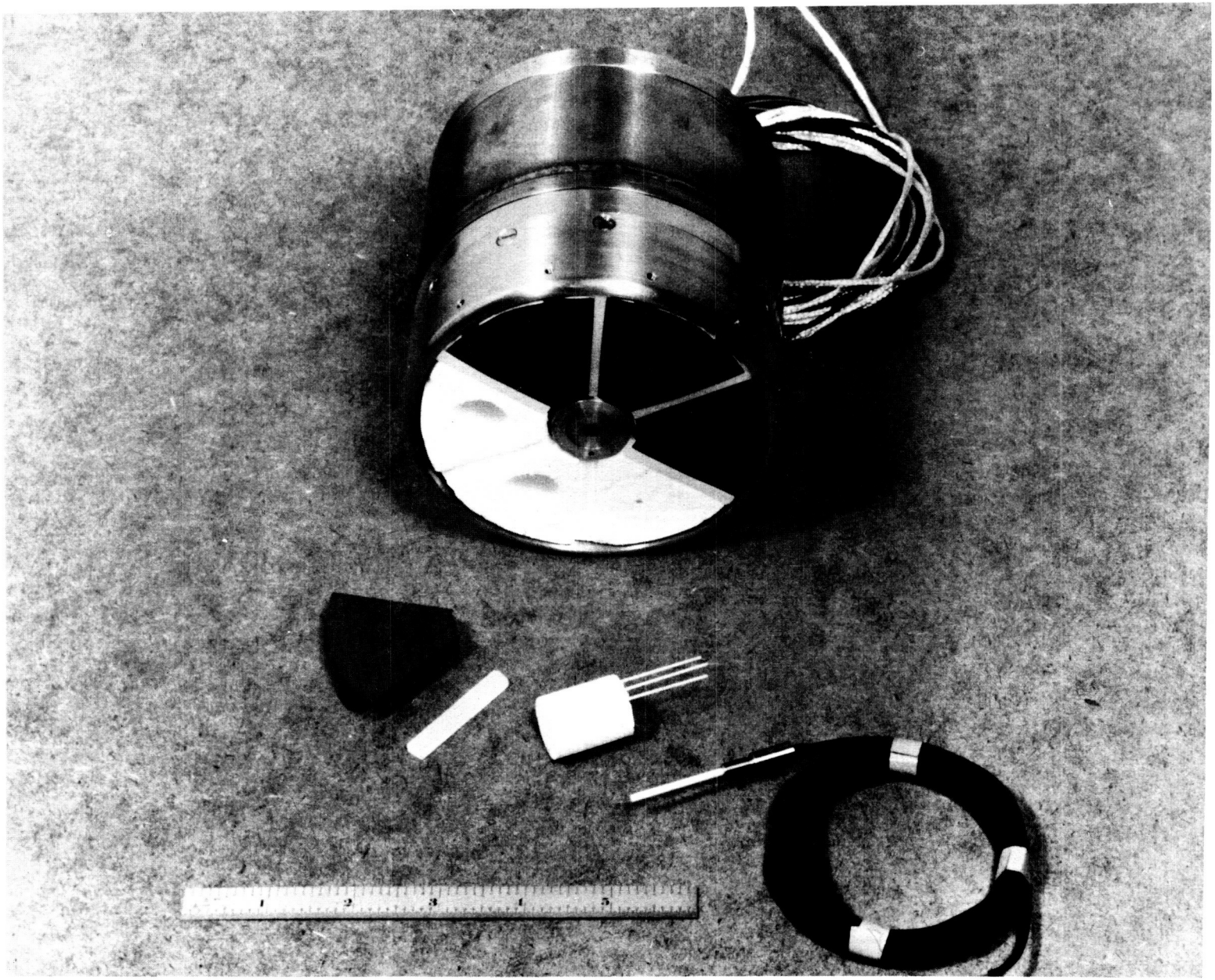

Figure 3 Typical Test Model Configuration and Test Samples (TD NiCr)

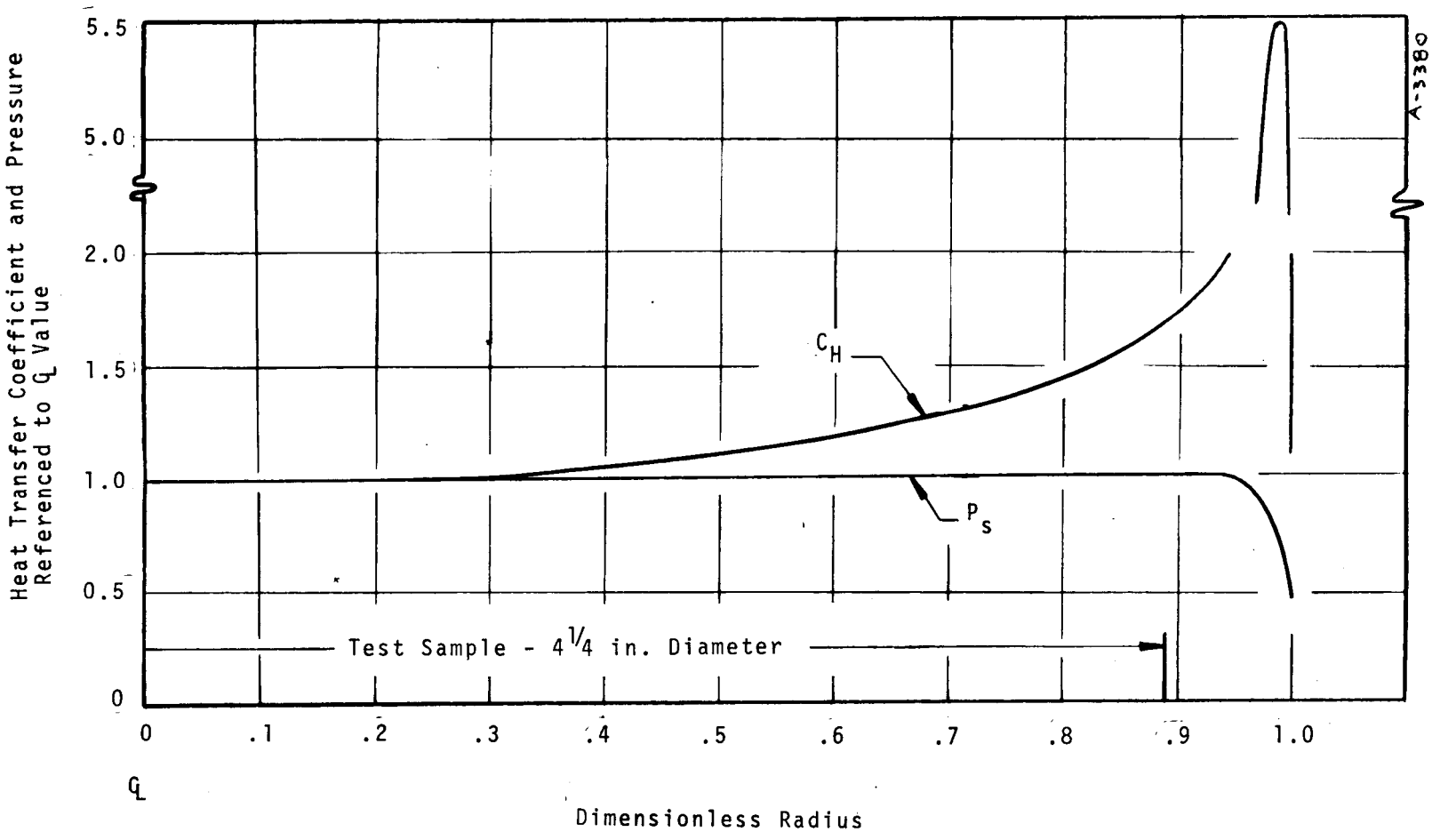

Figure 4 Calculated Distribution of Heat Transfer Coefficient and Pressure Across a Flat Face Model at Typical Test Conditions

accounting for the necessary thermal expansion allowance. The test sample or test sample plus backup insulator was 1-inch thick.

The backup insulator was Silfrax in all cases (metallics and carbon-carbon composites). This material is a pure silica foam with a nominal density of 30 lb/ft^3. Originally, a lower density mat-type insulation was to have been used; this material, however, exhibited difficult handling characteristics and structural integrity for the multiple reuse and sample change requirements of this program. A graphite foam insulation was also checked out and found to exhibit a too severe long term degradation due to oxidation.

The test model was designed to accept pie-shaped test samples of 60° or multiples thereof (see Figures 2 and 3). The actual configurations employed for the material types were as follows:

- Metallics - 60°
- Surface insulators - 180° and 120°
- Carbon-carbon composites - 180°, 360°, and 60°

The pie-shaped configuration was selected as optimum based on a design study at the start of the program; this configuration provided:

- Large surface area
- Low sensitivity to side wall losses
- Versatility in the number and size of test samples (6 at 60° each to 1 at 360°)

The alternate configuration that was rejected was an array of 6 test samples approximately 1-inch in diameter spaced 60° apart on a common model diameter. Note that none of the above advantages are achieved with this configuration.

All designs incorporated the necessary quick-change capability for optimum testing efficiency. The test samples were removed simply by removing the retention pins in the peripheral ring (Figure 2 and 3). The backup insulator where appropriate remained untouched and in place during sample removal and installation. Spring-loaded thermocouples were used throughout to eliminate the requirement for disconnecting instrumentation leads.

The metallic test samples had a single tab on the inside diameter (ID) and two tabs on the outside diameter (OD) for retention (Figures 2 and 3). The ID tab incorporated a hook detail so that it was unnecessary to remove the ID retention pin for sample removal and installation. The metallic samples were separated by quartz T sections which were higher than the metallic surface for thermal and flow

isolation. The backup insulator included instrumented thermocouple plugs every 60°. Each plug contained 3 Chromel/Alumel thermocouples for in-depth temperature measurement and definition of the metallic backwall heat loss. These thermocouples were on a line offset from but parallel to the axis of the plug; a hole on the plug centerline accomodated the spring-loaded thermocouple.

The surface insulator test samples were retained by the pins in the peripheral ring only and no separator between test samples was used. Holes to the midplane of each sample (1/2-inch depth) every 60° accomodated the spring-loaded thermocouples (Figure 2). Additional instrumentation was not practical because of the quick change requirements.

The carbon-carbon composite test samples were retained on the OD only for the 180° and 360° samples and on both the OD and ID for the 60° samples. The backup insulator had holes every 60° to accomodate the backwall spring-loaded thermocouples. The 180° and 360° test samples were of the "truss core" construction illustrated below. The triangular voids were filled

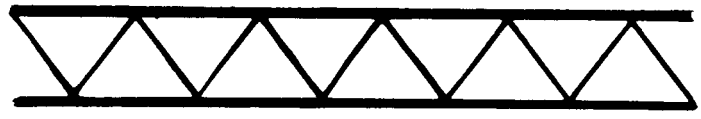

with graphite felt. Its susceptibility to oxidation required Dynaflex insulation between the sample OD and the peripheral copper ring.

The ablator model/test sample (Figure 2) was simply a monolithic slab 4 3/4 inches in diameter with a 1/8-inch corner radius and 1 1/2 inches thick. It was retained by pins around the periphery at the base of the test sample. The ablative material was backed by a 0.035-inch thick aluminum plate bonded to the ablative sample with RTV on one side and painted flat black on the other side. A backwall thermocouple was peened in place on the aluminum plate. Originally three plugs for in-depth temperature measurement and for weight loss and dimension change measurement were to have been used. However, the material was so poorly bonded together and to the honeycomb that it was impossible to successfully fabricate the required 1-inch diameter plugs.

2.3 INSTRUMENTATION AND DATA REDUCTION

Instrumentation was provided and data reduction was performed to define:

- Arc heater and facility operating conditions
- Test stream and model boundary conditions
- Test sample response

All data except for transient calorimetry were recorded on magnetic tape using the 80-channel digital data acquisition system (Section 2.1). The data acquisition system was set to trigger every minute at a scan rate of 43 channels per second. The unscrambled data tape served as the input to the data reduction code which computed all data in proper units (e.g. °F, atm, Btu/ft^2sec) and also computed the appropriate multi-variable test and operating conditions (e.g. energy and mass balance enthalpies, efficiency). The output from the transient calorimeters was recorded on a high-speed, 36-channel oscillograph. In some cases, data were recorded by hand from visual indicators, primarily as a backup to the recorded data. The instrumentation and data reduction in the above three categories is presented in the following paragraphs.

2.3.1 Operating Condition Measurements

The following basic operating condition measurements were made to characterize arc heater and facility performance:

- Voltage
- Current
- Gas mass flow rate
- Cooling water flow rate
- Cooling water temperature rise
- Arc chamber pressure
- Test cabin pressure

Table 2 summarizes the various measuring devices and the standard laboratory methods employed. The flow rates of nitrogen and oxygen were measured separately as 76.8 percent nitrogen and 23.2 percent oxygen by mass to yield the composition of air. Calibrated rotameter/pressure gauge combinations were used to set and meter the gas flow rates. Calibrated sharp edged ASME standard orifice was used to meter the cooling water flow rate. The arc heater cooling water temperature rise differential thermopile consisted of a four-pair

TABLE 2

OPERATING CONDITION MEASUREMENTS

Type of Measurement	Visual		Recorded	
	Output Device	Type of Output	Output Device	Type of Output
Arc Voltage	Voltage divider	Voltmeter	Voltage divider	0-50 millivolts
Arc current	Shunt	Ammeter	Shunt	0-50 millivolts
Gas mass flow rate	Rotameter or sharp-edge orifice	Percent of full scale or differential pressure	--	--
Cooling water flow rate	Sharp edge orifice	Differential pressure	Δp transducer	0-5 volts
Cooling water temperature rise	Dial thermometer	Deg. Fahrenheit	Differential thermopile	0-20 millivolts
Arc chamber pressure	Pressure gauge	psig or mm Hg	Absolute pressure transducer	0-10 volts
Test cabin pressure	McLeod gauge	Microns	--	--
	Thermocouple gauge	Microns	--	--
	Absolute pressure gauge	mm Hg	--	--

copper-constantan thermocouple assembly. Arc heater and test cabin pressures were measured by one of several absolute pressure strain gauge transducers depending on operating conditions. The transducer output signal was suitably amplified for recording. Test cabin pressure was also periodically checked with a McLeod gauge and was visually monitored during each test with a thermocouple gauge pressure indicator.

2.3.2 Test Condition Measurements

The boundary conditions to which the test samples were exposed were defined by:

- Enthalpy
- Pressure
- Heat Flux
- Surface catalycity effect

Three enthalpy measurement methods were employed:

- Energy balance
- Mass balance (sonic flow)
- Heat flux

The first two methods provided the average stream enthalpy and the last method provided local enthalpy. Energy balance enthalpy was determined from measurements of input power, total energy loss to the cooling water, and gas flow rate from the relation

$$h_{eb} = \frac{Q_{in} - Q_{loss}}{\dot{m}} = \frac{0.948 \times 10^{-3} VI - \dot{m}_w C_{pw} \Delta T_w}{\dot{m}} \qquad (1)$$

where the measurement of the necessary operating conditions ($V, I, \dot{m}, \dot{m}_w, \Delta T_w$) was presented above. The mass balance enthalpy was determined from the relation

$$\frac{\dot{m}}{p_o A_*} = f(h_{mb}) \qquad (2)$$

where this sonic flow parameter (left term) is essentially a function of enthalpy only. This function has been determined in Reference 1 to enthalpies of 10,000 Btu/lb and extended to higher enthalpies in References 2 and 3. The measurement of the necessary operating conditions ($\dot{m}$ and p_o) was presented above and A_* is the throat area. The heat flux enthalpy was determined from

calorimeter measurement of heating rate and the calculation of heat transfer coefficient. This enthalpy is given by

$$h_{hf} = \frac{q_c}{C_H} + h_w \tag{3}$$

where q_c is the stagnation convective heat flux measured by a catalytic surface calorimeter, C_H is the calculated heat transfer coefficient, and h_w is the enthalpy corresponding to the calorimeter surface temperature. The heat transfer coefficient was calculated from the relation (References 4 and 3).

$$C_H = 0.042 \sqrt{\frac{p_s}{R_{eff}}} \tag{4}$$

where p_s is the measured stagnation pressure and

$$R_{eff} = 3.78\ R_b \tag{5}$$

for a flat face model at moderate to high Mach number (Reference 5).

Heat flux and pressure measurements were made as follows:

- Calibration model of identical geometry to the test models of Figure 2 for model property distributions - 6 Gardon-type calorimeters and 6 pressure taps
- 1 1/4-inch diameter flat-face calorimeter model for stream property surveys - Gardon-type calorimeter
- 3/8-inch diameter pitot probe for stream property surveys
- 1 1/4-inch diameter flat-face calorimeter model for surface catalycity measurements - slug calorimeter

The calibration model is shown in Figures 5 and 6 in the form of an assembly drawing and a photograph, respectively. The model body was copper and water cooled and the calorimeters were also individually water cooled. The calorimeter assemblies were held in place with set screws. The configuration and the assembly details of the calorimeters used for surface catalycity measurements are presented in Figure 7. The surface treatments employed on these calorimeters were:

- Catalytic - clean, polished copper
- Noncatalytic - teflon coated or silicon monoxide coated copper

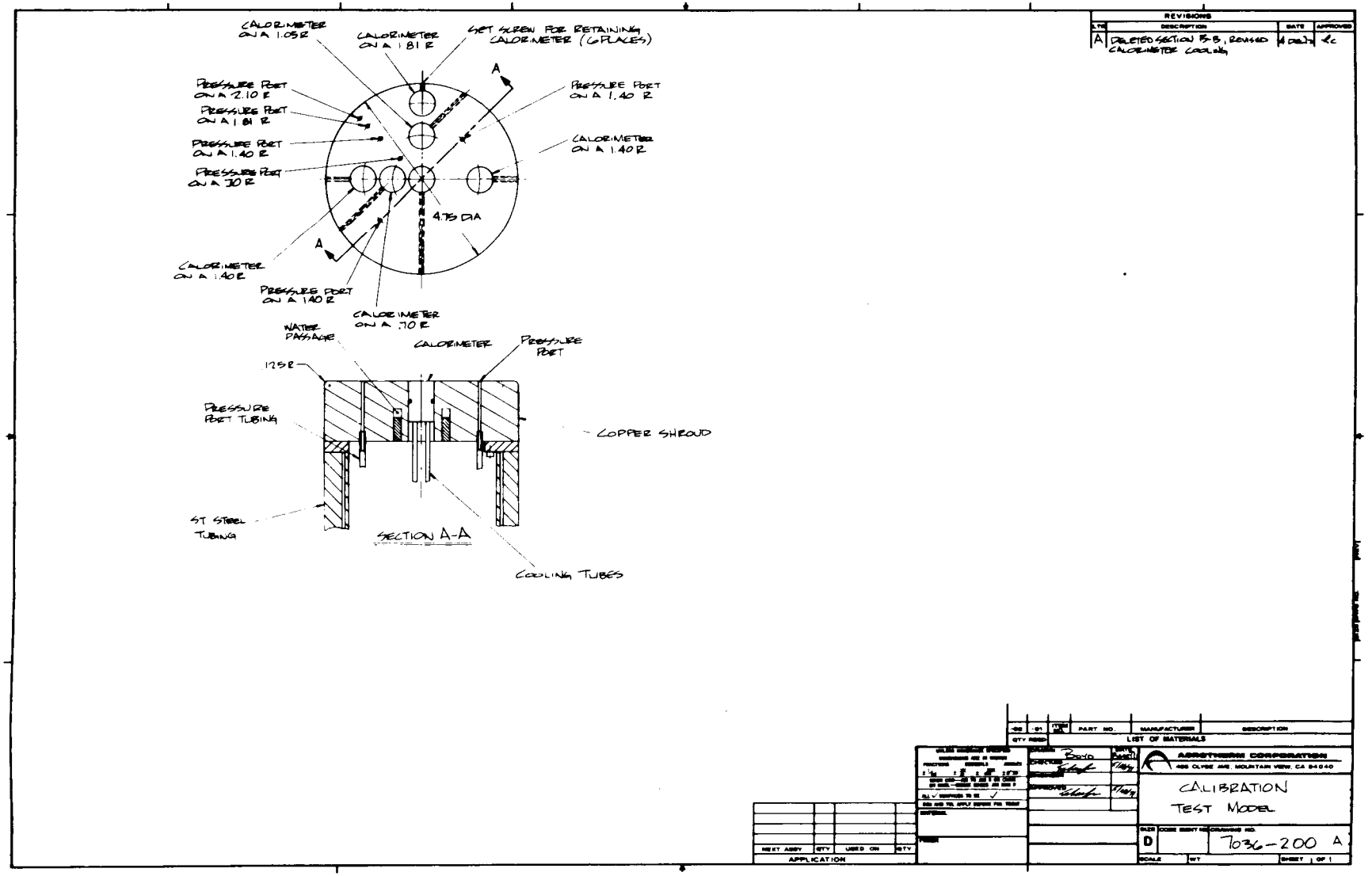

Figure 5. Calibration Model Configuration

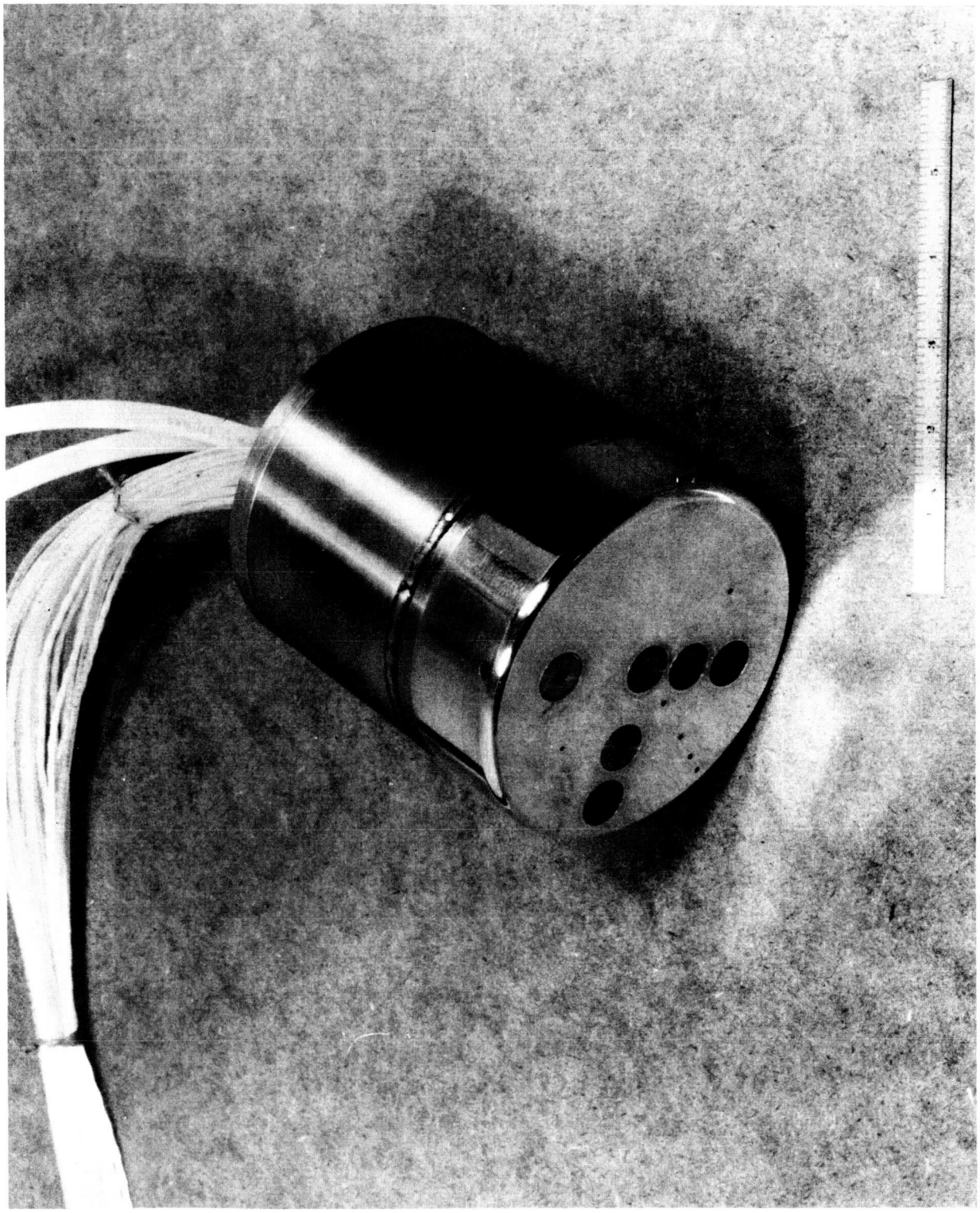

Figure 6 Calibration Model

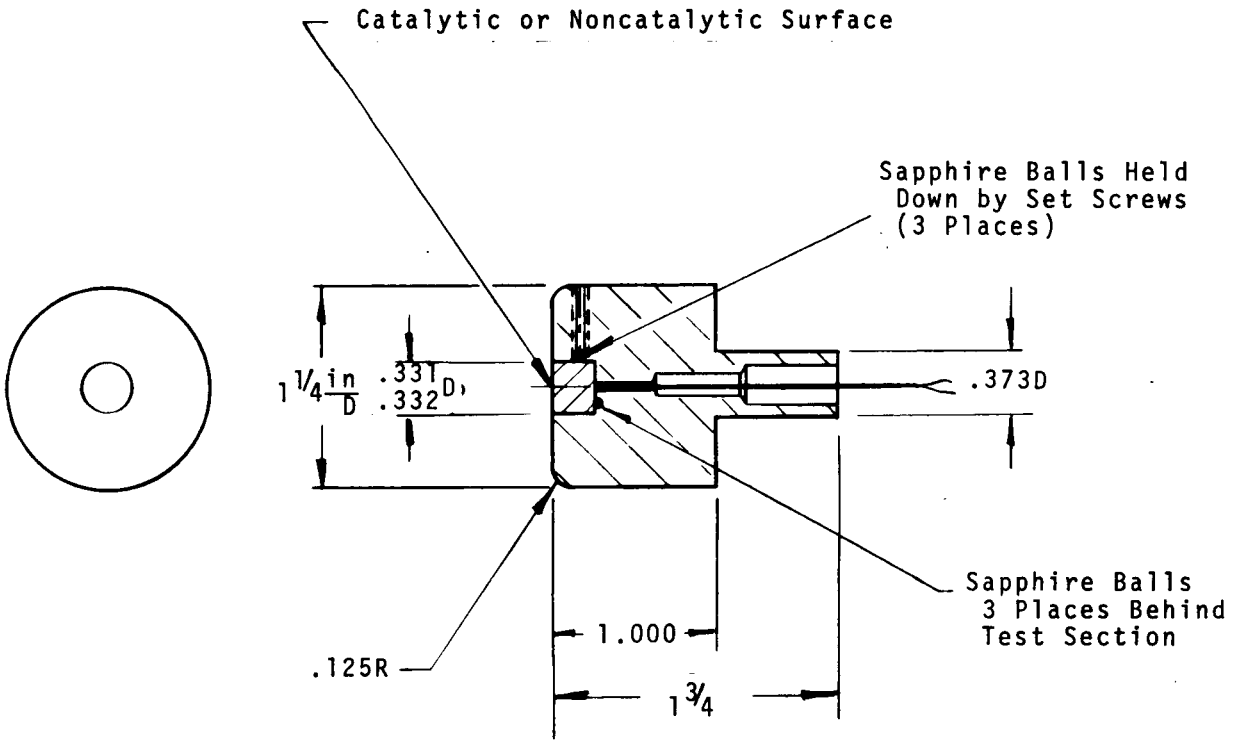

Figure 7 Calorimeter Configuration for Surface Catalycity Measurements

The calorimeter model employed for stream surveys had the identical geometry to that of Figure 7 but used a Gardon-type sensor identical to those of the calorimeter model (but with double the heat flux capacity).

2.3.3 Test Sample Response

The test sample response was defined quantitatively by measurements of surface and in-depth temperatures, surface recession, and weight loss, and qualitatively by photography as presented in Table 3. The surface temperature was measured pyrometrically with 2 or 3 different pyrometers:

- Infrared Industries Thermodot TD-7 Pyrometer - Sensing wavelength range from 1.7 to 2.6 microns, low to moderate temperatures, requires accurate knowledge of emissivity
- Infrared Industries Thermodot TD-9 Pyrometer - Sensing wavelength of 0.8 microns, moderate to high temperatures, relatively insensitive to emissivity
- Thermogage Miniature Optical Pyrometer - Peak sensing wavelength of 0.9 microns, low to high temperatures

The primary pyrometer (TD-7 or TD-9) was mounted on an oscillating mechanism which indexed the pyrometer 60° every minute and which described a circle through the central region of the test samples. This unit is shown schematically in Figure 8. The drive unit was an automatic stepping motor, and the drive mechanism pivot and adjustable swing radius allowed the motion to describe an ellipse (including a circle) with any major and minor axis required. Note that an elliptical pattern was required when viewing the test model at an angle. The secondary pyrometer(s) typically viewed one of the test samples throughout a cycle.

Backwall temperatures for the metallic and carbon-carbon composite test samples and midplane temperatures for the surface insulator test samples were measured with platinum/platinum 13 percent rhodium or Platinel spring-loaded thermocouples. For the metallic test samples, the original spring-loaded thermocouple configuration apparently represented a noticeable heat sink. This configuration with a 0.093-inch diameter insulator and 5 mil thermocouple wire was modified to a 0.031-inch diameter insulator and 3 mil thermocouple wire, and the problem was eliminated. Also for the metallics, the Silfrax backup insulator was instrumented at each of the six sample locations with three Chromel/Alumel thermocouples as discussed previously.

TABLE 3

TEST SAMPLE RESPONSE INSTRUMENTATION

Variable \ Sample Type	Metallic	Surface Insulator	Ablator	Carbon-Carbon Composite
Surface Temperature Primary	TD-7 Pyrometer	TD-7 or TD-9 Pyrometer	TD-9 Pyrometer	TD-9 Pyrometer
Secondary	Thermogage Pyrometer	Thermogage and/or TD-7 or TD-9 Pyrometers	Thermogage and TD-7 Pyrometers	Thermogage and TD-7 Pyrometers
Backwall Temperatures	Pt/Pt 13% Rh Spring-Loaded TC	--	C/A TC	Platinel Spring-Loaded TC
Midplane Temperatures	--	Platinel Spring-Loaded TC	--	--
Backup Insulator In-Depth Temperatures	C/A TC	--	--	--
Surface Recession	Microscope Micrometer	Microscope Micrometer	Micrometer	Microscope Micrometer
Weight Loss	Semi-Micro Analytic Balance	Semi-Micro Analytic Balance	Semi-Micro Analytic Balance	Semi-Micro Analytic Balance
Qualitative Response	35 mm Slides	35 mm Slides	35 mm Slides	35 mm Slides

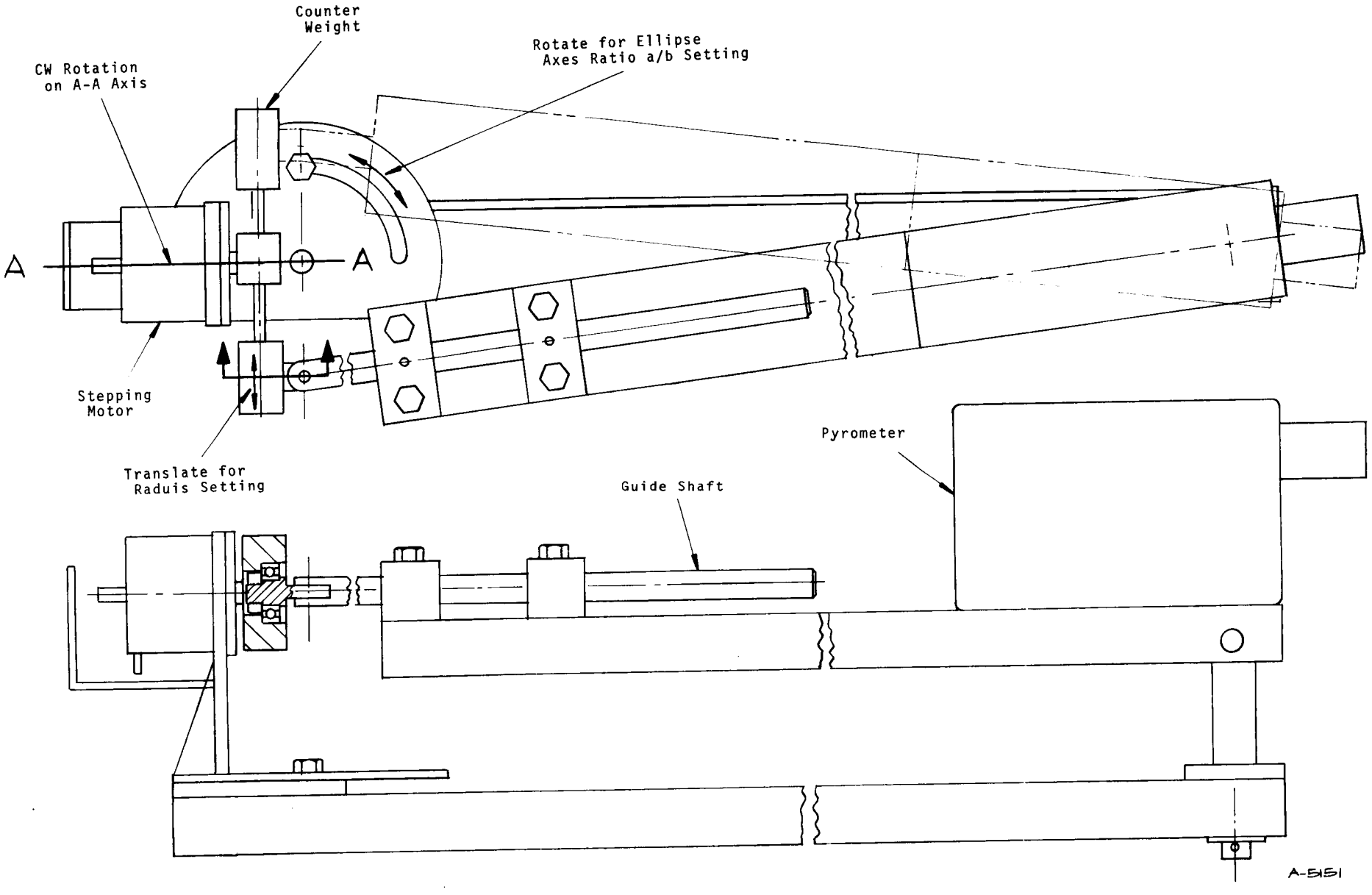

Figure 8 Pyrometer Indexing Mechanism

Surface recession was measured by a special microscope micrometer shown in Figure 9. This device employed the microscope focus as the surface position indicator. This non-contact technique was necessary to insure no disturbance of the typically delicate surface coatings or oxide films. Weight loss was measured with a conventional semi-micro analytic balance and the qualitative test sample response was defined by pre- and post-test 35 mm color still photography. Surface recession and weight loss measurements and color photography were performed nominally after every six cycles or after a sample was changed for any reason.

2.4 TEST PROCEDURE

Testing on the metallics, surface insulators, and carbon-carbon composites was nominally performed in blocks of six cycles on each of the two test models as shown in Figure 10. For a typical 8-hour shift, testing was performed during a continuous 6-1/2 hours of facility operation and the remaining 1-1/2 hours was occupied by test sample changes and measurements. As shown in Figure 10, the calibration model was exposed to the test stream before and after each cycle (accounting for the extra 1/2 hour). The data acquisition system operated continuously during the 6-1/2 hour period. The nominal test procedure (Figure 10) was typically repeated 5 times to achieve the required 30 cycles of exposure. The model identification (2 and 4) of Figure 10 corresponds to the two sting positions employed; the calibration model was in sting position 3. Test sample failures and off-nominal cycling in some test series resulted in a modification to the number of cycles between facility shutdowns. The same cycle variables of Figure 10 were maintained throughout the program, however. Two-model operation as illustrated was nominally employed throughout the program for optimum efficiency. Sample failures, however, necessitated single model operation in 9 3/4 of the 271 1/3 facility hours of the program. In these cases the cooldown period was either the nominal 30 minutes or the time for the backwall to reach 100°F.

The tests were performed by controlling the predetermined surface temperature for the metallics and about half the surface insulators. The one location of the six viewed by the primary pyrometer that was hottest was used as the reference location for this temperature control. In all cases once the desired temperature was achieved, this temperature was held with only minor changes in test conditions, these changes being accomplished simply by changing arc heater current. Part way through the surface insulator test series, the surface temperature control approach was reassessed in the light of the unknown or questionable values of emissivity and surface catalycity. Based on this reassessment, all subsequent tests were performed by controlling the predetermined convective heat flux (see Section 4). This was accomplished simply by operating at constant arc heater current.

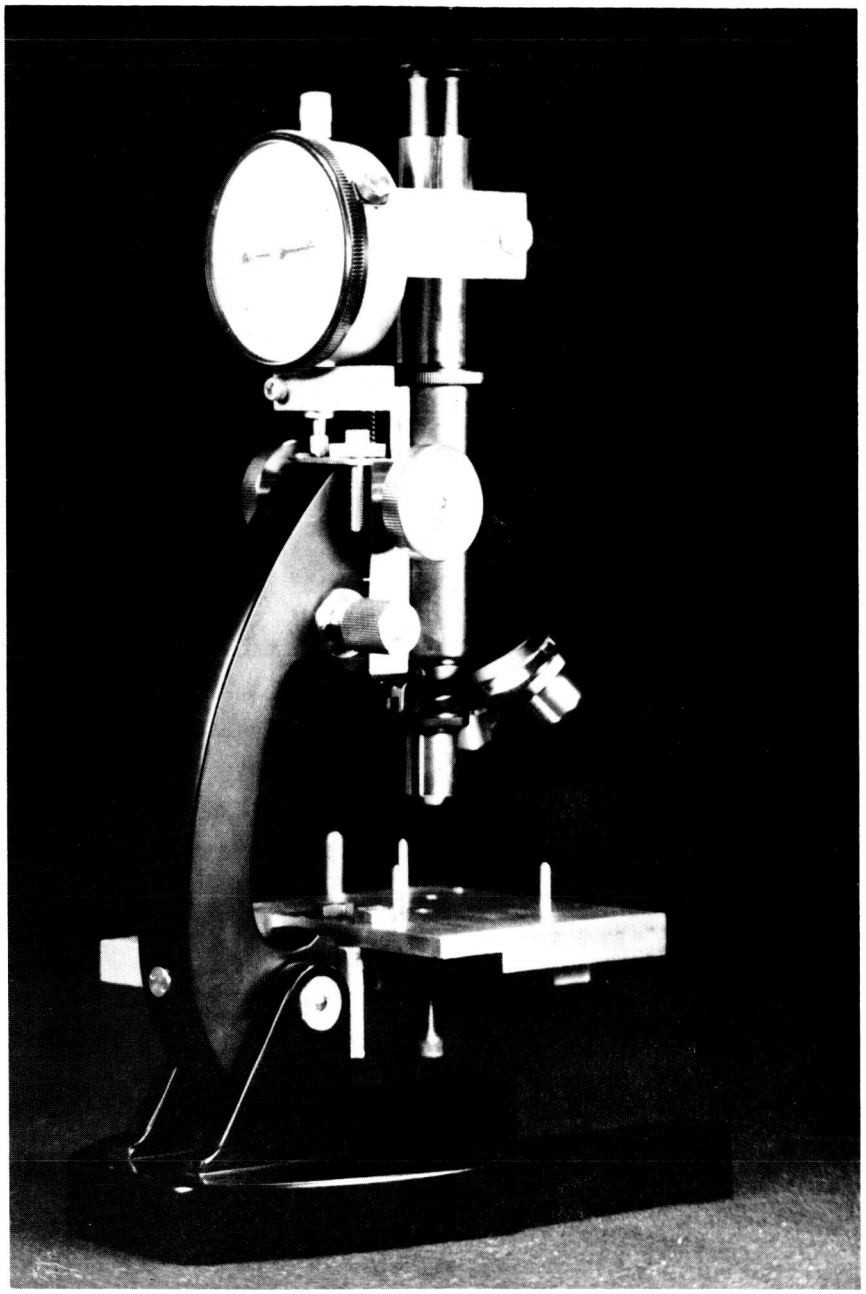

Figure 9 Microscope Micrometer for Surface Recession Measurement

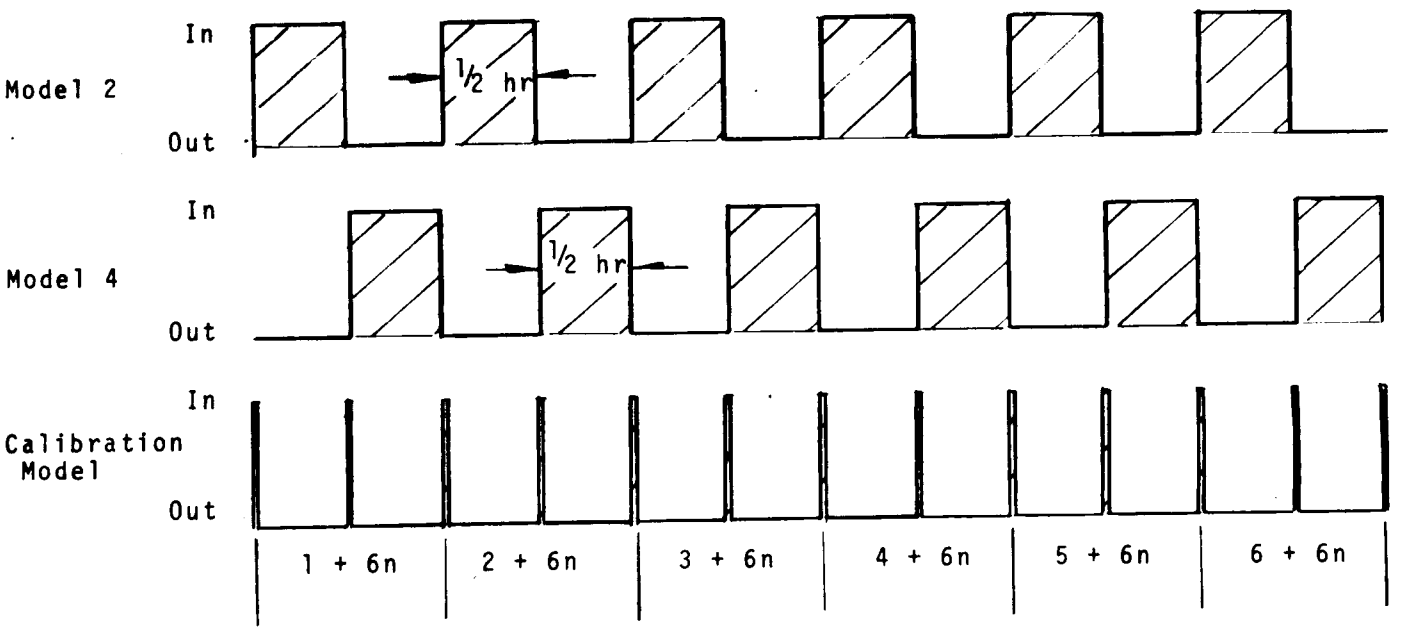

Figure 10 Nominal Test Procedure

The ablator model/test samples were tested at constant heat flux conditions for single exposures of 1000 or 2000 seconds duration.

A detailed log of the test sample status and of the test parameter identification was necessarily maintained continuously throughout the program. Contingency plans in case of failure were also continuously maintained and updated to eliminate any delays in the test operations.

2.5 TEST CONDITIONS

The nominal test conditions are presented in Figure 11 and Table 4 The indicated heat flux - surface temperature correspondence applies for a fully catalytic surface with a surface emissivity of 0.85. The baseline test parameters were a nominal heat transfer coefficient of 0.0038 lb/ft^2sec and a nominal stagnation pressure of 0.006 atm with heat flux variation accomplished by enthalpy variation. These test conditions were typical of the shuttle vehicle reentry heating (e.g., see Reference 6), and eliminated heat transfer coefficient and pressure as a variable in interpreting the test results. In order to study surface catalycity effects on surface insulators, one test series was performed at higher values of heat transfer coefficient and pressure, and a broad range of heat flux was achieved over one cycle for each of two test models. Originally, the maximum heat flux was to have been 56 Btu/ft^2sec (ablators), and the above baseline values of heat transfer coefficient and stagnation pressure were selected on this basis. After the test program had started, the maximum heat flux value was raised to 100 Btu/ft^2sec (ablators and carbon-carbon composites) to provide more representative test results.

For the tests performed at predetermined surface temperatures, variations in the nominal conditions shown in Figure 11 and Table 4 were necessary due to variations in surface emissivity and surface catalycity.

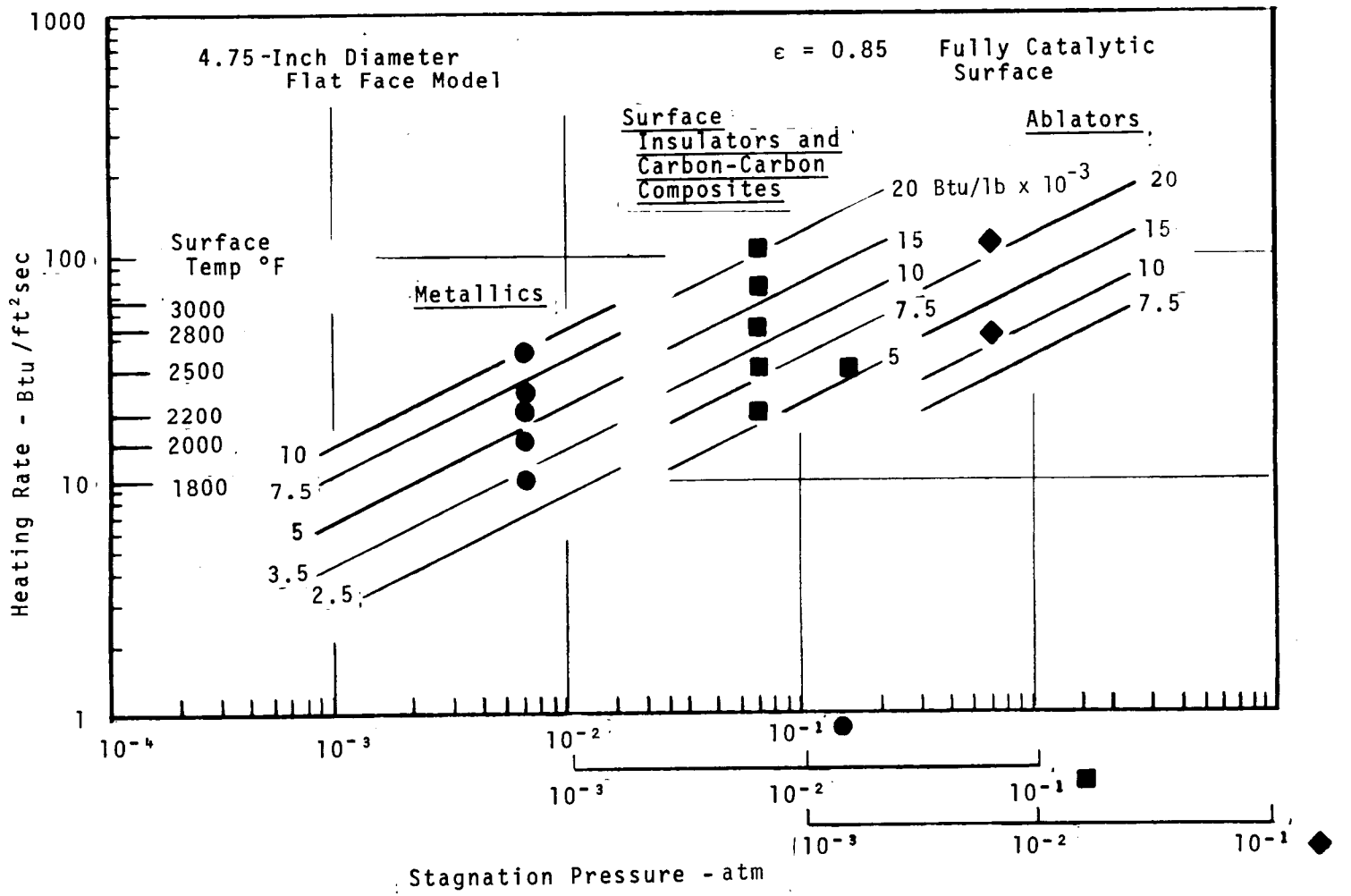

Figure 11 Nominal Test Conditions

TABLE 4

NOMINAL TEST CONDITIONS

Material Type	Surface Temperature (°F)	Convective Heat Flux (Btu/ft^{2}sec)	Heat Transfer Coefficient (lb/ft^{2}sec)	Enthalpy (Btu/lb)	Stagnation Pressure (atm)
Metallics	2000	14.0	0.0038	4300	0.006
	1800	9.9	|	3200	|
	2200	19.0	|	5600	|
	2300	22.0	|	6400	|
	2600	33.2	|	9400	|
Surface Insulators	2500	29.3	0.0038	8300	0.006
	2200	19.0	|	5600	|
	2800	43.0	|	11900	|
	2500	29.3	0.0059	5600	0.014
Carbon-Carbon Composites	-	75.0*	0.0038	18500	0.006
	-	95.0*	|	22000	|
Ablators	-	40.0*	0.0038	11200	0.006
	-	100.0*	|	23000	|

* Revised conditions; changed to indicated values after start of test program

4.75"D flatface stagnation point model surface temperature corresponds to $\varepsilon = 0.85$ and fully catalytic wall

SECTION 3

CALIBRATION TEST RESULTS

Calibration tests were performed at the original nominal test conditions to define the:

- Centerline and bulk average properties
- Distribution of properties across the test stream
- Distribution of properties across the test model
- Catalytic and noncatalytic surface heat flux

The results of the calibration tests are presented in the following subsections.

3.1 Centerline and Average Properties

The basic test conditions were defined by measurements of the centerline and average properties as follows:

- Enthalpy
  - Energy balance (average)
  - Mass balance (average)
  - Heat flux (centerline)
- Stagnation (pitot) pressure (centerline)
- Cold wall heat flux (centerline)

These results for the original nominal test conditions are presented in Table 5.* The test conditions are presented in order of ascending enthalpy. The test condition number primarily identifies the air flow rate at which the tests were run; current was then varied to achieve the desired surface temperature or heat flux. All measurements but heat flux enthalpy and model heat flux were obtained directly from the data for the indicated test number. Heat flux enthalpy was defined from Equations (3) through (5) and the

*No sample tests were performed for test conditions 4 and 8 but they are included since surface catalycity results were obtained and presented later. Preliminary calibration results were also obtained for test conditions 1, 2, 3 and 5, but they are not included since no sample tests were performed and no surface catalycity results were obtained.

TABLE 5

CALIBRATION RESULTS FOR THE BASIC TEST CONDITIONS

Condition Number	Test Number	Enthalpy (Btu/lb)			Stagnation Pressure (atm)	Heat Flux (Btu/ft^{2}sec)		Air Flow Rate (lb/sec)	Arc Heater Current (amps)
		Energy Balance	Mass Balance	Heat Flux		$1\frac{1}{4}$-inch Dia. Calorimeter	Model		
6	1939-1	2280	2200	3,750	.0055	32.4	13.7	.0134	224
	1928-9	2310	1990	3,760	.0058	--	14.1	.0134	225
	1928-1	2270	--	3,740	.0058	--	14.0	.0134	223
	1927-1	2320	--	3,675	.0056	25.8	13.5	.0134	220
7	1939-2	3220	3400	6,025	.0057	49.0	22.4	.0107	304
	1928-10	3310	2950	6,125	.0060	--	23.4	.0107	309
	1928-6	3350	2990	6,125	.0060	--	23.4	.0107	309
	1927-2	3410	--	6,175	.0059	41.0	23.3	.0107	312
9	1940-1	3440	3400	6,350	.0062	--	24.6	.0107	326
	1938-1	3300	3400	6,250	.0060	51.2	23.8	.0107	320
	1937-1	3420	3400	6,250	.0059	49.7	23.6	.0107	320
4	1939-3	3690	4000	7,400	.0060	57.3	28.2	.0090	345
8	1939-4	4680	5000	9,580	.0067	77.7	38.6	.0090	441
10	1940-2	4320	4500	9,770	.0060	--	37.2	.0082	392
	1938-2	4280	4600	9,770	.0058	65.8	36.6	.0082	392
	1937-2	4360	4500	9,760	.0060	66.1	37.2	.0082	391
11	1940-3	5720	6000	16,400	.0061	--	63.0	.0071	489
	1938-3	5640	6100	16,400	.0059	80.8	62.0	.0071	488
	1937-3	5600	6100	16,400	.0061	86.2	63.0	.0071	491
12	1940-4	6790	7500	19,150	.0061	--	73.6	.0065	577
	1938-4	6670	7600	19,150	.0057	104.0	71.1	.0065	578
	1937-4	6990	7700	19,450	.0063	103.0	76.0	.0065	587
13	1989-3	4220	5100	5,000	.0137	--	28.8	.0280	568

calibration model results obtained during both the calibration and sample test series. This enthalpy was plotted as a function of current, as shown for example in Figure 12 for test condition 9, and the best-fit line then used to define the enthalpy value for the measured current. The model cold wall heat flux presented in the table was calculated from the relation (References 2 and 3)

$$q_c = 0.042 \sqrt{\frac{p_s}{R_{eff}}}\, h_{hf} \qquad (6)$$

As seen from the table and presented in Section 2.6, the nominal stagnation pressures were 0.006 and 0.014 atm.

The basic test conditions seen by the test model were defined by the centerline values (Table 5):

- Heat flux enthalpy
- Stagnation pressure
- Model heat flux

Note that the heat flux enthalpy was significantly higher than the two average enthalpies. In most cases this enthalpy and the indicated model heat flux were representative of that for the test stream seen by the model and the complete model surface (as presented in Section 3.2 and 3.3). For some conditions at heat fluxes above the originally anticipated maximum 56 Btu/ft^{2}sec, the heat fluxes dropped off considerably with radial distance from the centerline, however.

3.2 Stream Distributions

The measured distributions of stagnation pressure, heat flux, and enthalpy across the test stream are presented in Figure 13 for all test conditions.* The complete set of test conditions corresponding to each plot is presented in Table 5 by test condition and test number. The enthalpy was calculated from Equations (3) through (5) applied to the local measurements of heat flux and stagnation pressure (Reference 2).

*All except test condition 13 which was added to the program after the calibration tests were completed.

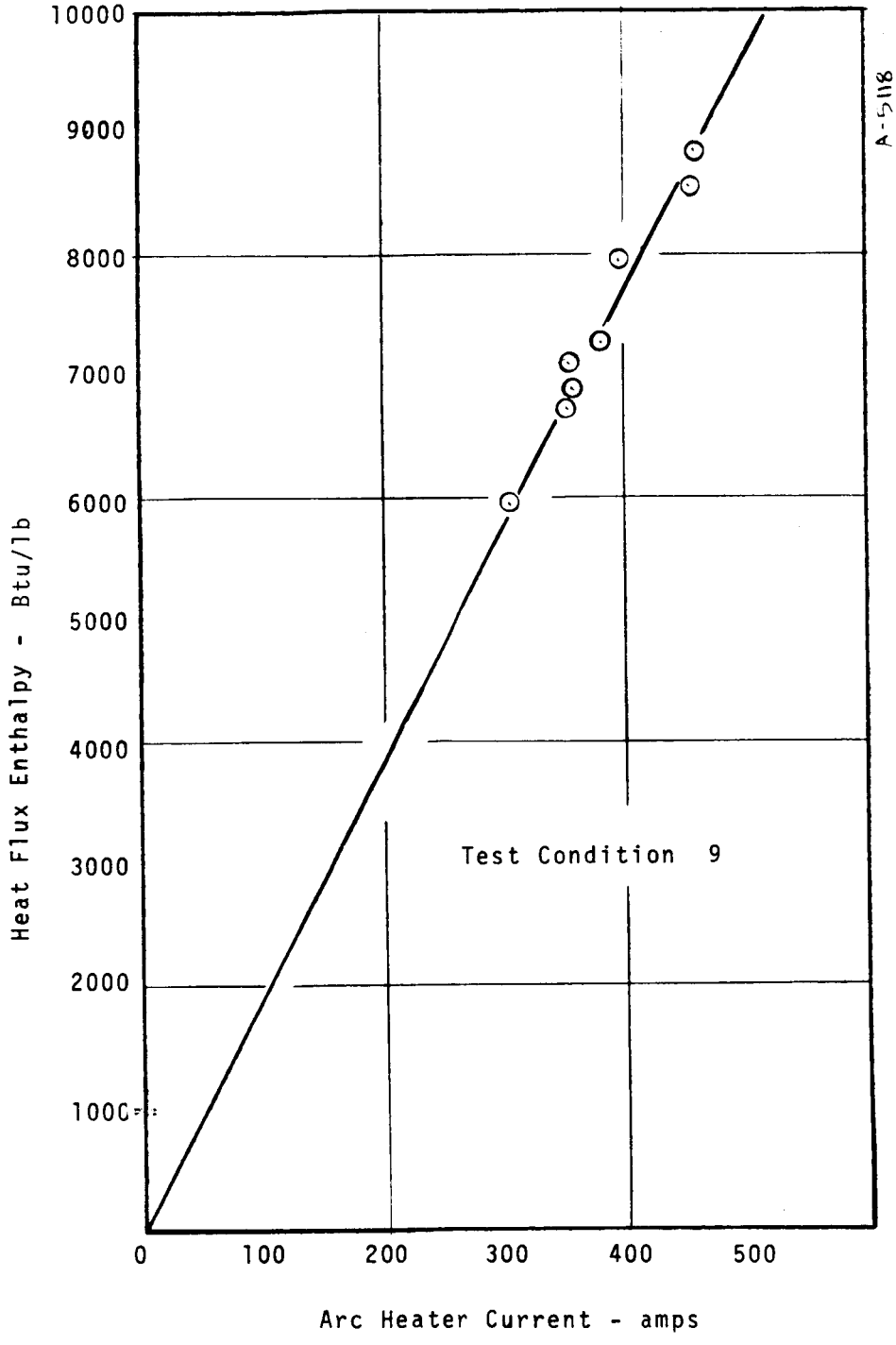

Figure 12 Typical Heat Flux Enthalpy Results

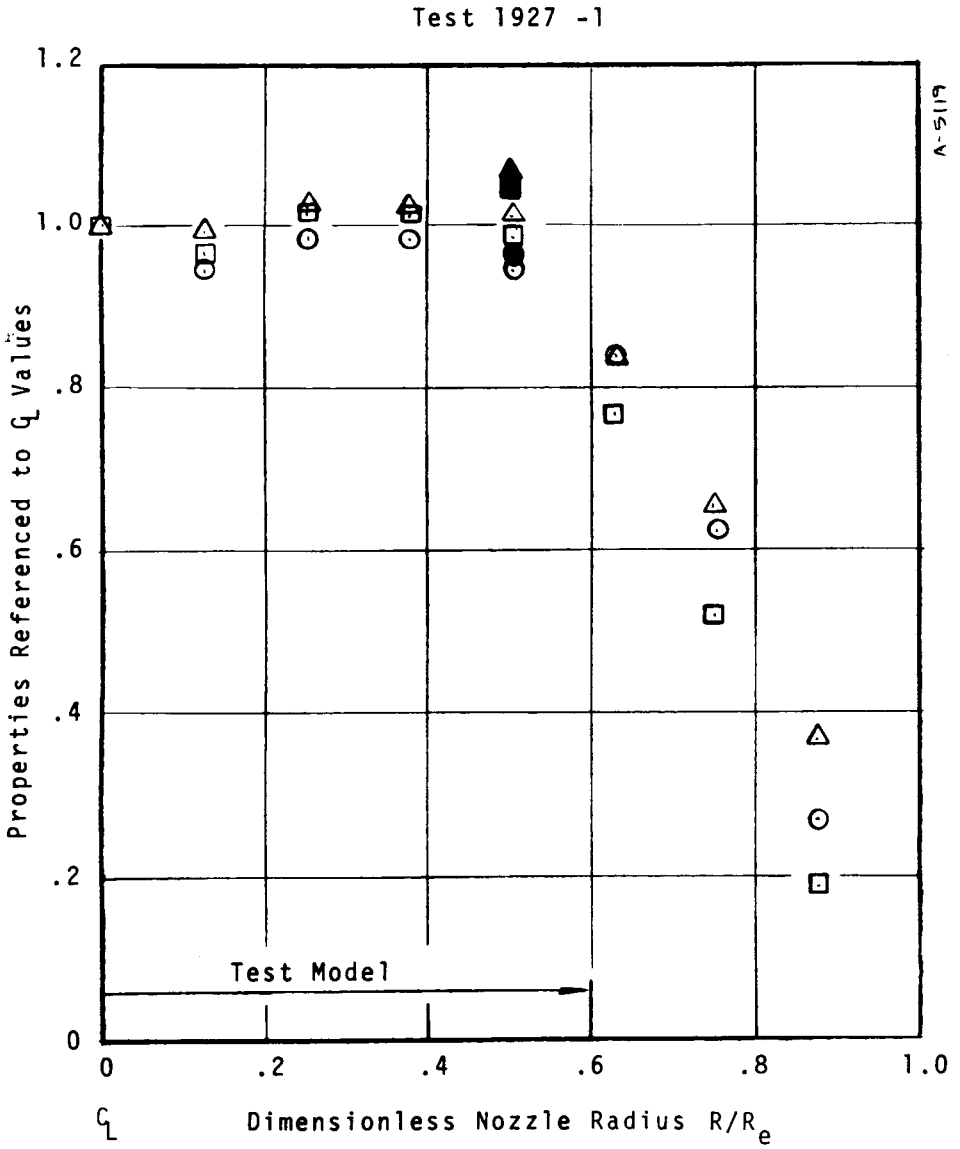

NOTES:

Filled Symbols Indicate Location on Opposite Side of Nozzle q_L From Primary Traverse

R_e = 4.0 inches

Figure 13 Test Stream Distribution Results

a) Test Condition 6

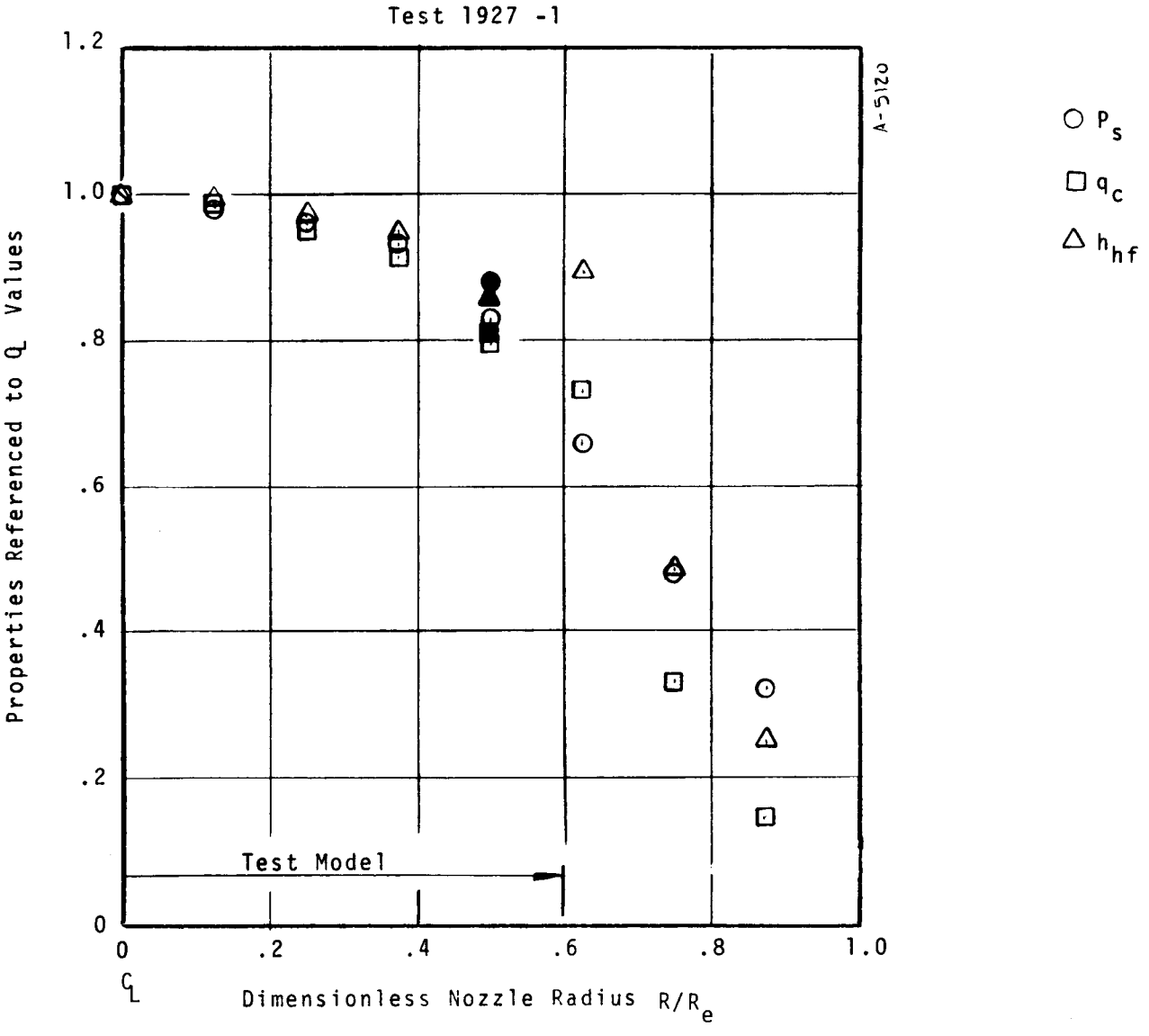

Figure 13 Continued
b) Test Condition 7

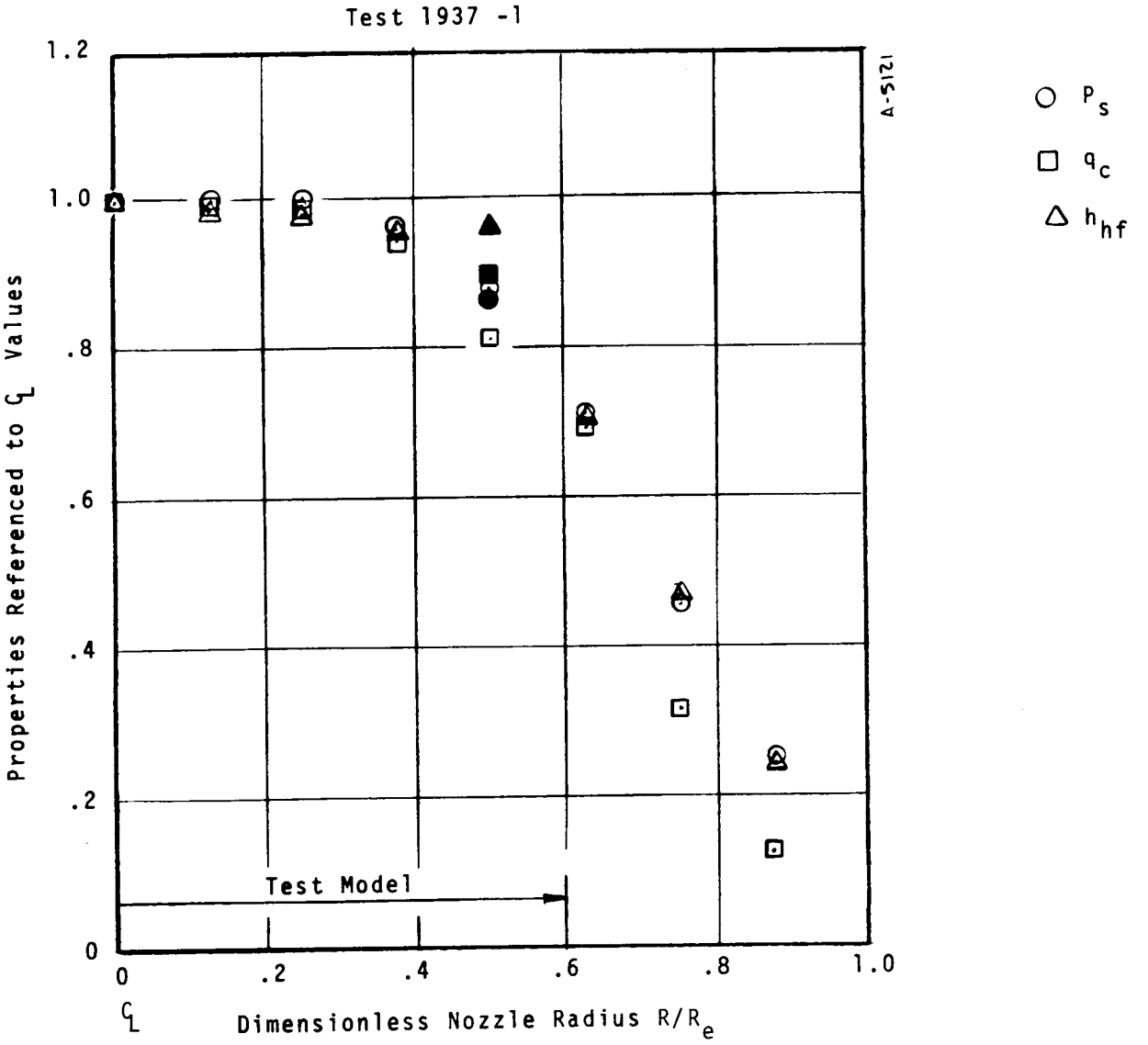

Figure 13 Continued

c) Test Condition 9

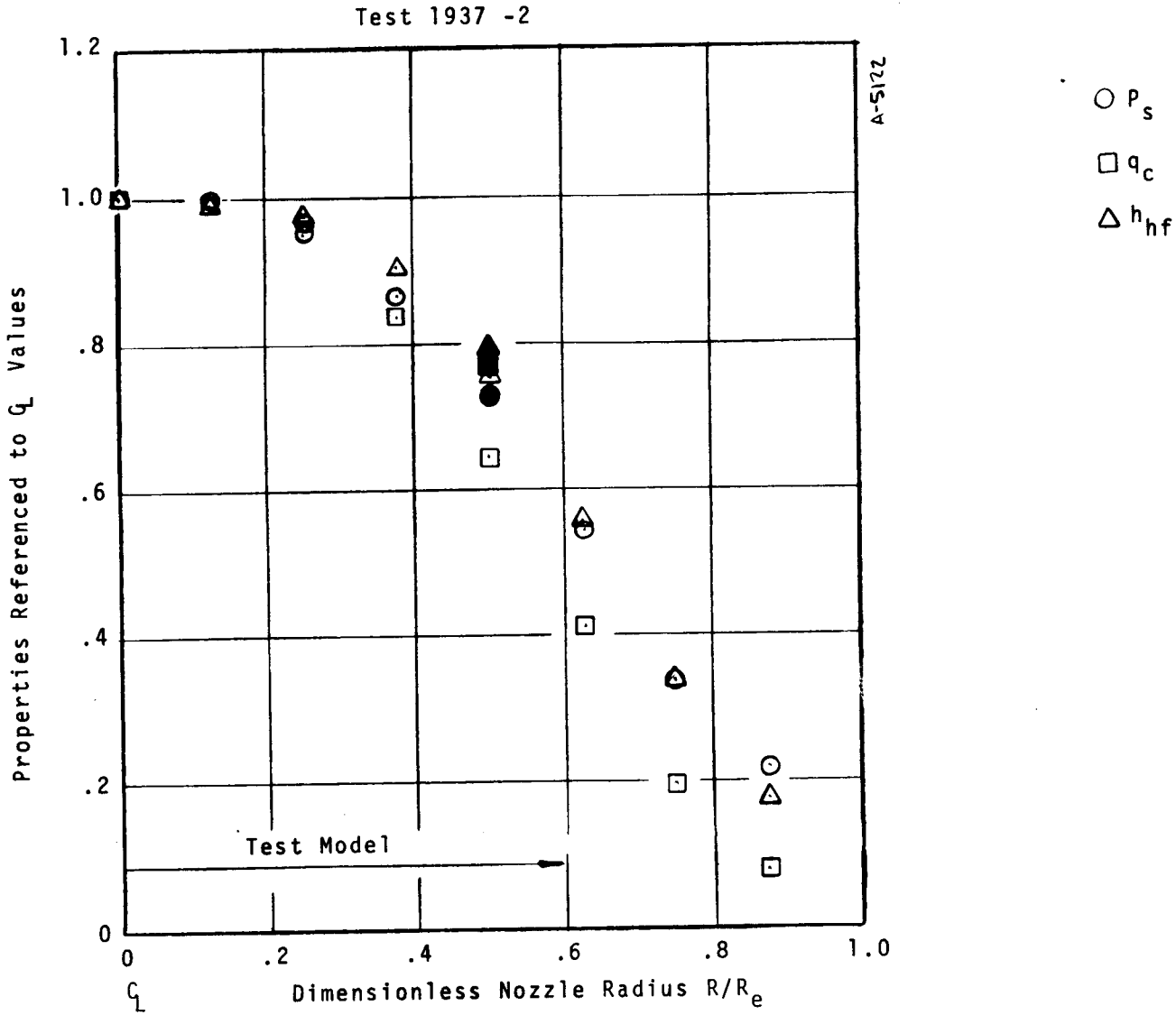

Figure 13 Continued
d) Test Condition 10

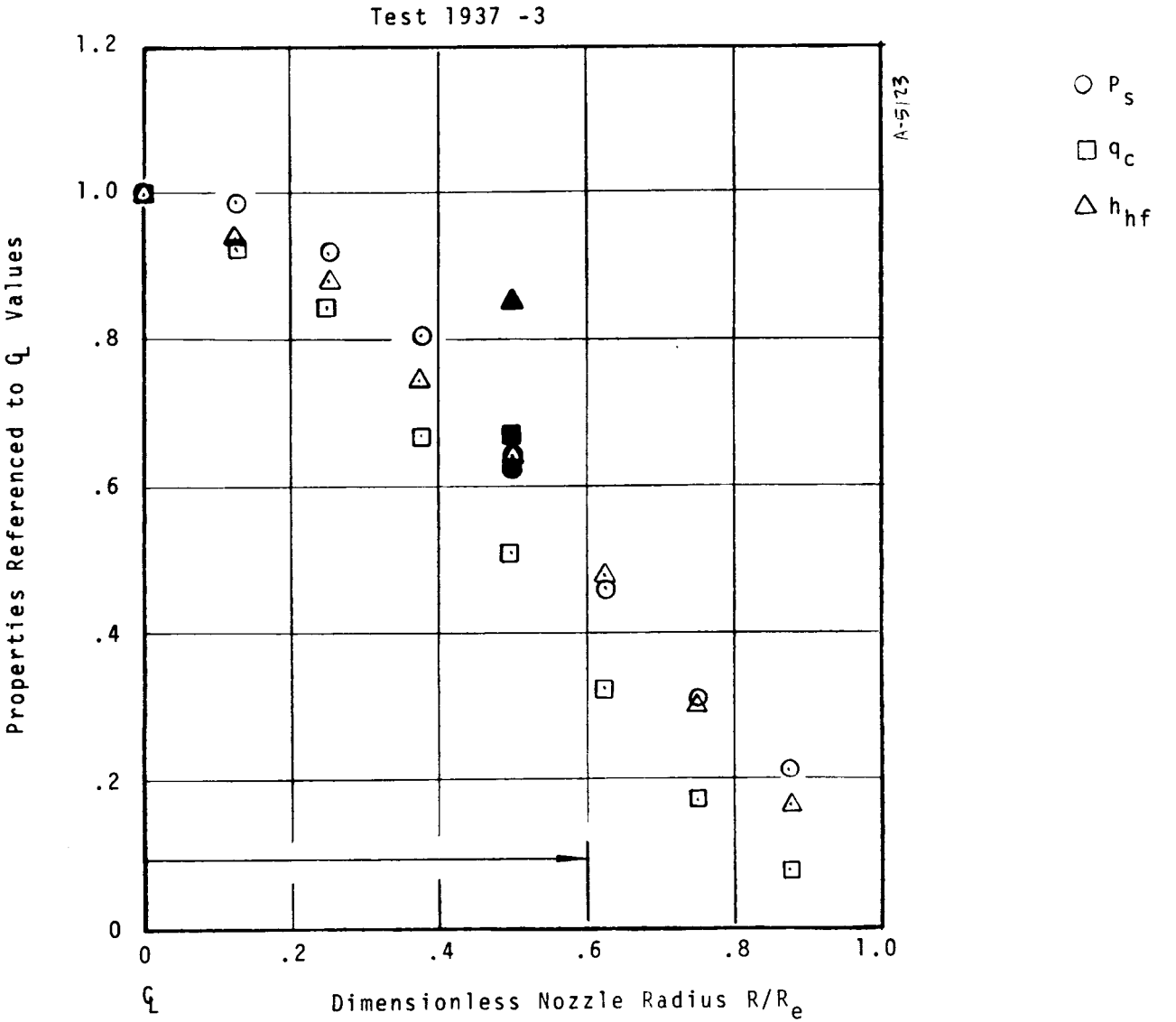

Figure 13 Continued

e) Test Condition 11

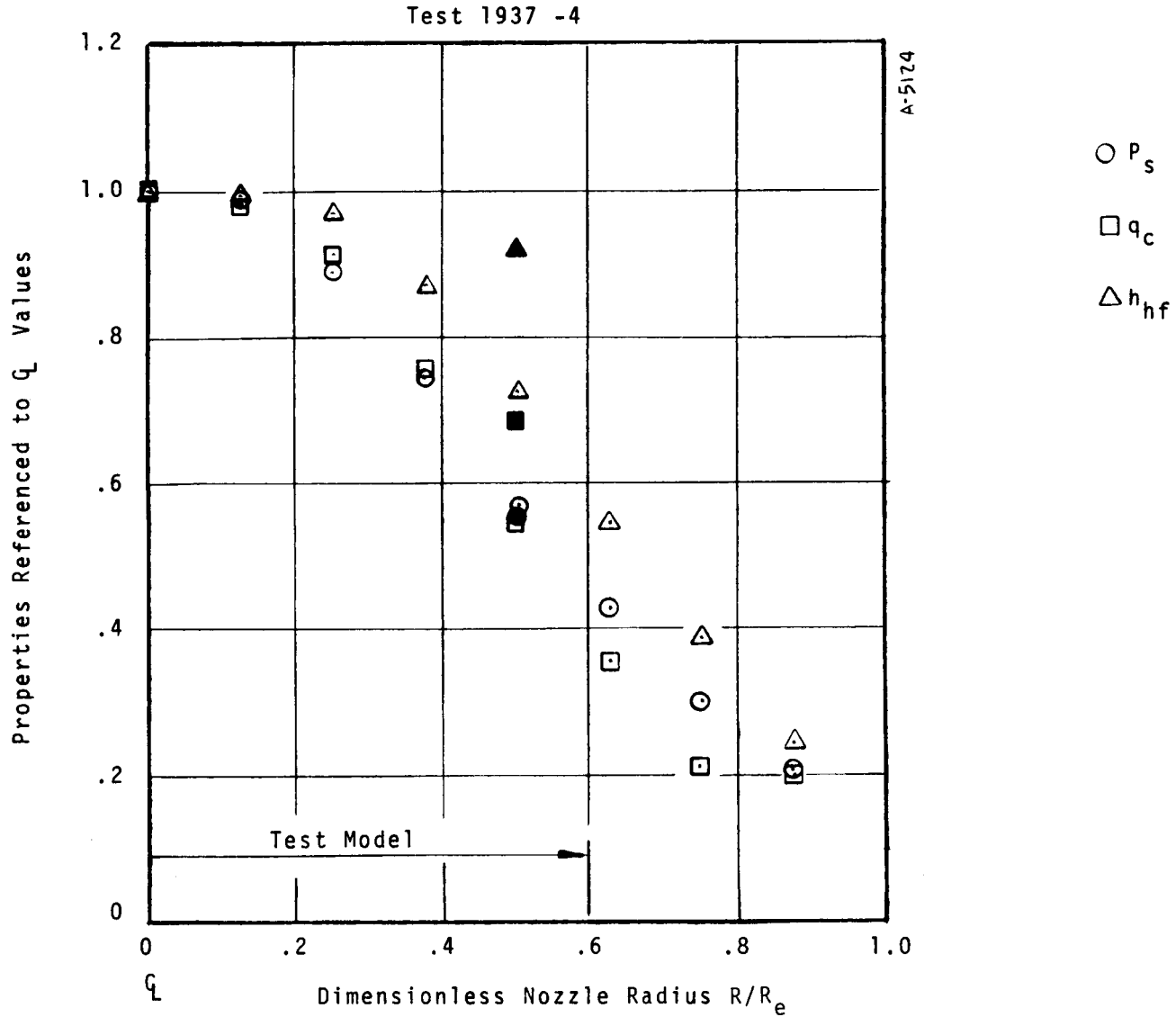

Figure 13 Concluded

f) Test Condition 12

The distributions are essentially flat across the model region for the low and moderate enthalpy conditions but drop off at the high enthalpy conditions. This nonuniformity is not as apparent in the model distributions (Section 3.3) since the stream tube that the model sees is smaller than the model diameter. The measurements on the opposite side of the stream centerline indicate that the test stream is symmetric about the centerline except for some nonuniformities at high enthalpy.

3.3 Model Distributions

The measured distributions of heat flux and stagnation pressure across the model face are presented in Figure 14 for all test conditions.* The complete set of test conditions corresponding to each plot is presented in Table 5 by test condition and test number. The tails on the symbols denote calorimeter locations 90^{o} either side of the primary calorimeter locations. The scatter in the heat flux measurements is felt to be due to scatter in the calorimeter performance and not an indication of the actual distribution on the model. Irregularities in the sensor surface and in the surface at its attachment to the calorimeter body and the resultant disturbance to the convective heating are the probable cause. Note that the pressure distributions are uniform.

The distributions are relatively flat for the low and moderate enthalpy conditions, and drop off for the high enthalpy conditions. This drop-off was more severe for some tests at higher heat fluxes than achieved in these calibration tests as discussed in Section 4. The circumferential uniformity (as defined by the pressure measurements) is seen to be excellent at all conditions.

3.4 Surface Catalycity

The surface catalycity test results are presented in Table 6 for all test conditions.* The catalytic surface was polished copper and the non-catalytic surface was a teflon coating. Tests were also performed with a silicon monoxide coating but it exhibited only a slight non-catalytic effect due apparently to an improper coating process. The average value of noncatalytic-to-catalytic surface heat flux was 0.61 and no consistent trend with enthalpy was apparent.

*See footnote p. 30

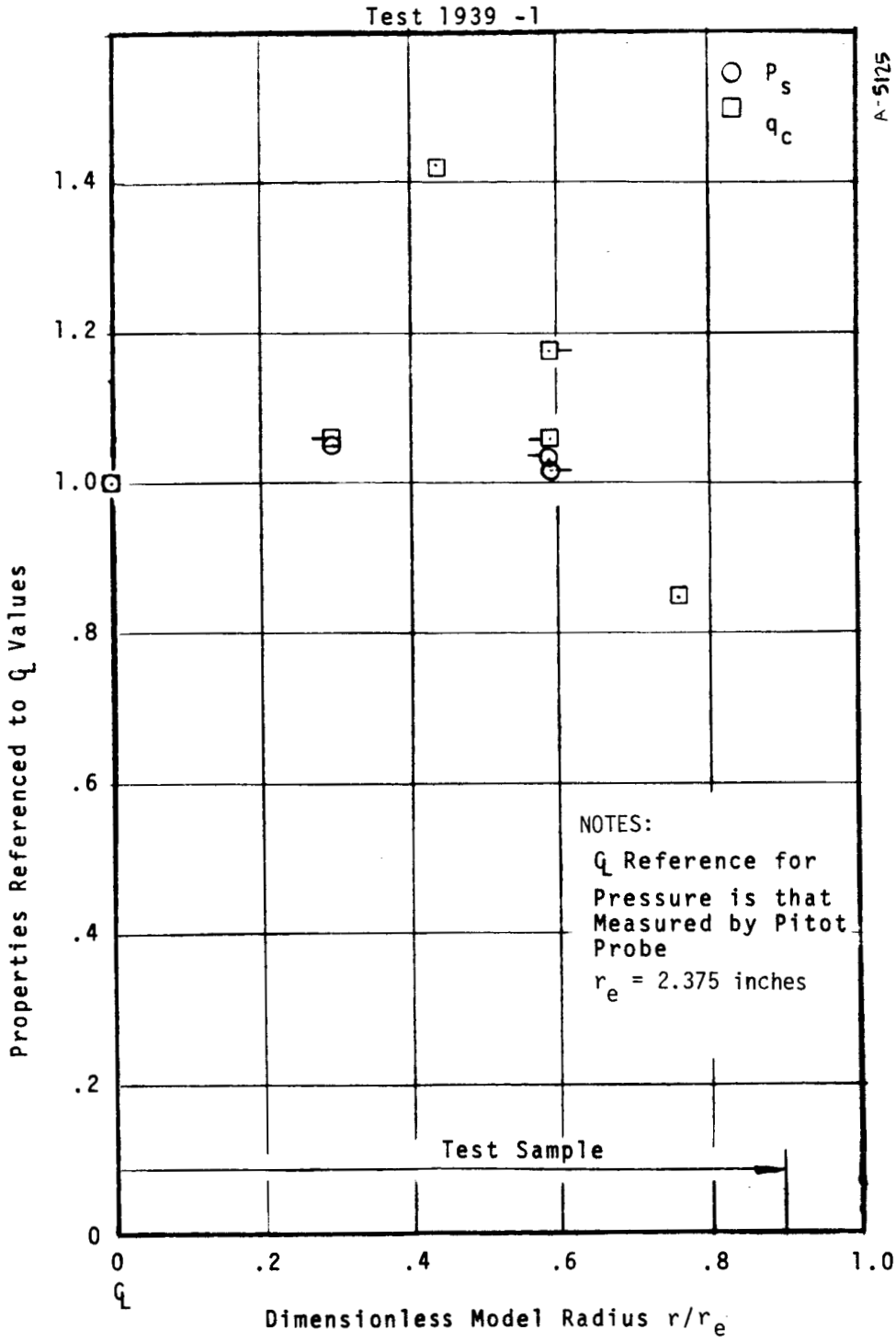

Figure 14 Model Distribution Results

a) Test Condition 6

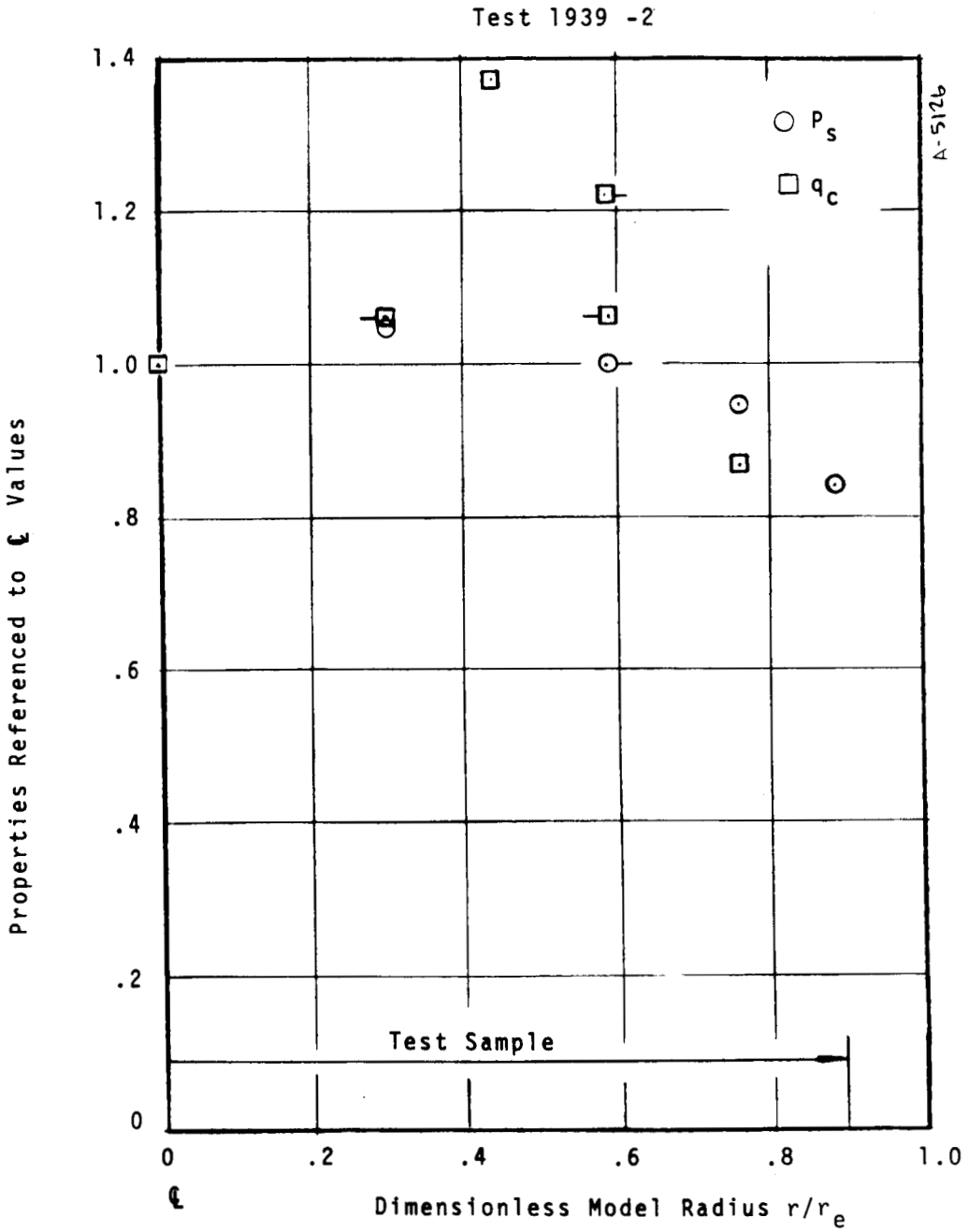

Figure 14 Continued
b) Test Condition 7

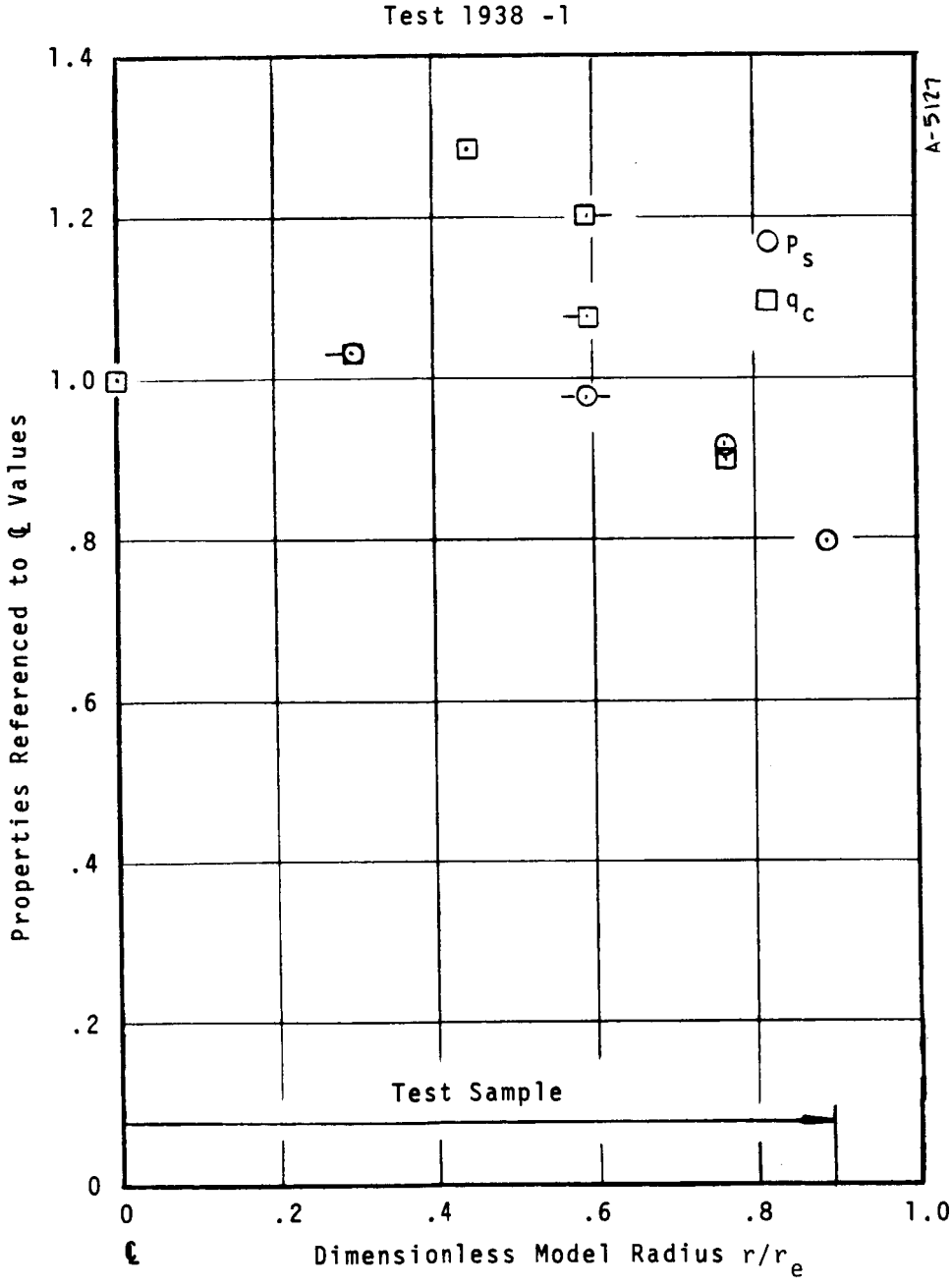

Figure 14 Continued

c) Test Condition 9

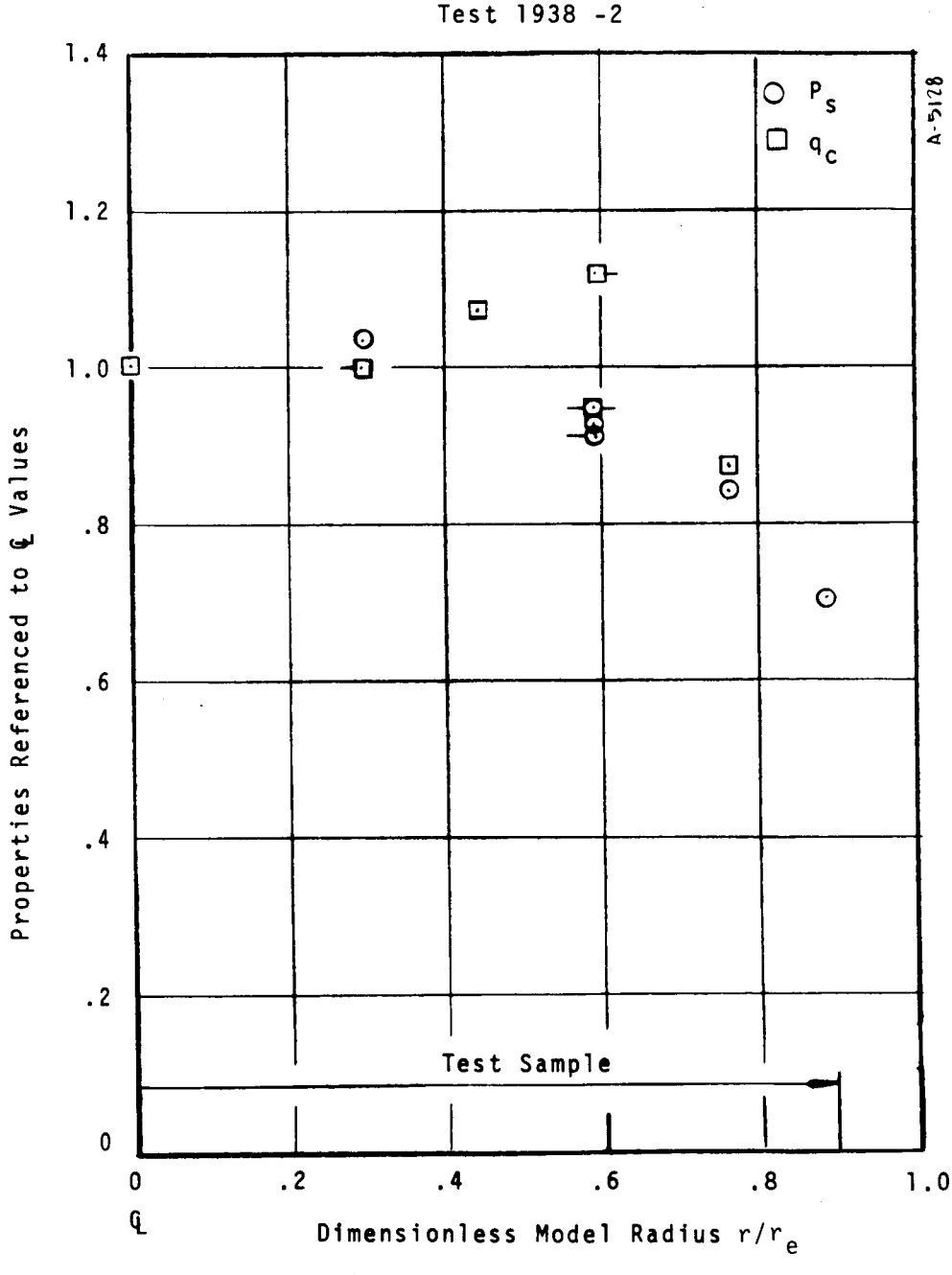

Figure 14 Continued
d) Test Condition 10

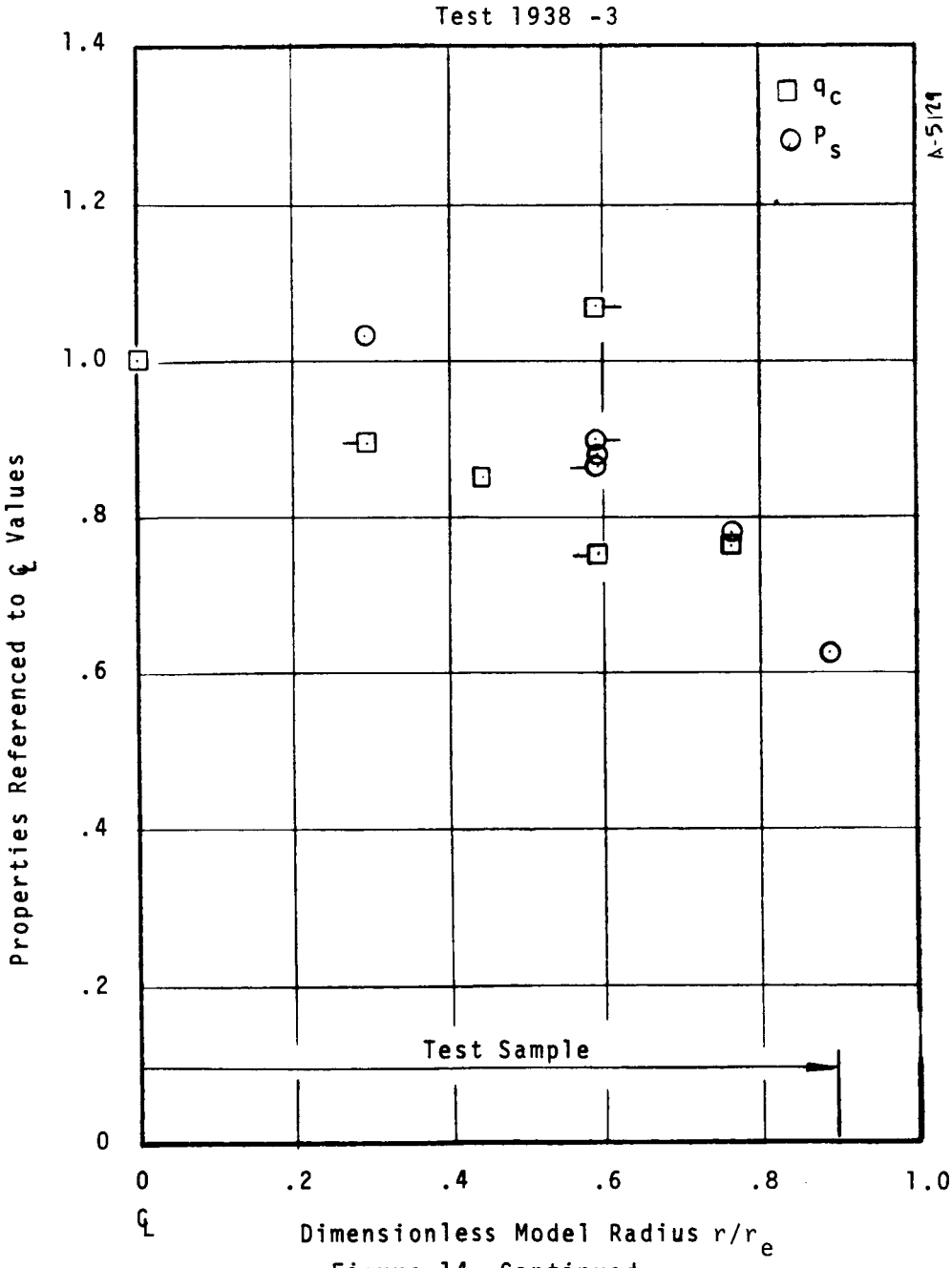

Figure 14 Continued

e) Test Condition 11

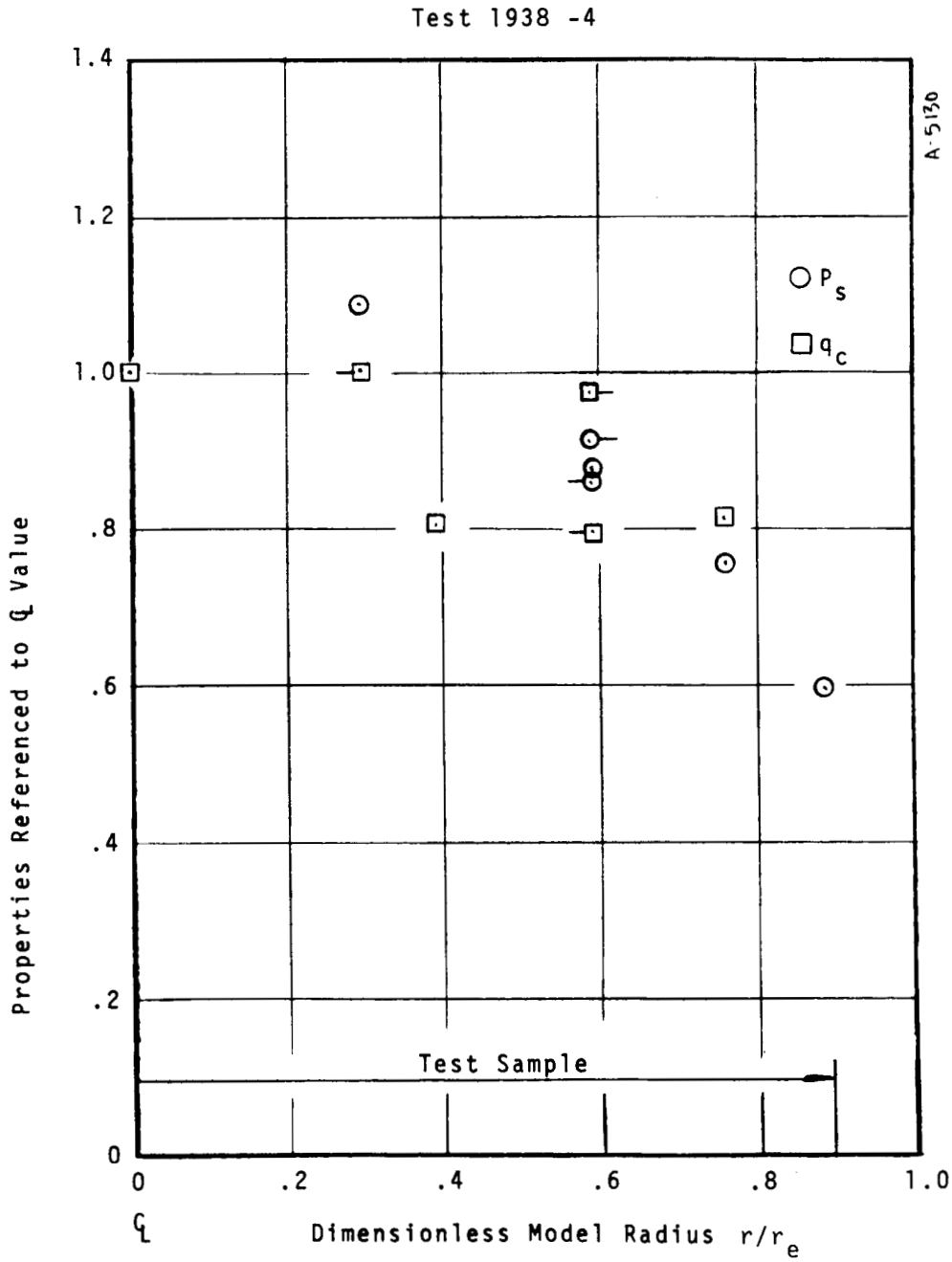

Figure 14 Concluded

f) Test Condition 12

TABLE 6

SURFACE CATALYCITY CALIBRATION RESULTS

Condition Number	Test Number	Catalytic Wall Heat Flux (Btu/ft^2sec)	Heat Flux Ratio Noncat/Cat Wall	Stagnation Pressure (atm)	Heat Flux Enthalpy (Btu/lb)
6	1928-9	14.1	0.65	.0058	3,760
7	1928-10	23.4	0.63	.0060	6,125
9	1940-1	24.6	0.55	.0062	6,350
4	1928-11	28.2	0.61	.0059	7,400
10	1940-2	37.2	0.58	.0060	9,770
8	1928-12	38.6	0.59	.0066	9,580
11	1940-3	63.0	0.62	.0061	16,400
12	1940-4	73.6	0.65	.0061	19,150
Average		--	0.61	--	--

SECTION 4

TEST RESULTS

Detailed test results in terms of:

- Surface and in-depth temperature response
- Mass loss and surface recession response
- Surface properties of emissivity and catalycity
- Failure modes and operating limits

were obtained for all candidate shuttle TPS concepts - metallics, surface insulators, carbon-carbon composites, and ablators. Typical results are presented in the following subsections according to the above material categories. Prior to this presentation, an overview of all results is also presented.

4.1 OVERVIEW

The types of materials tested in each material category were as follows:

- Metallics

  TD nickel chrome (TD NiCr)
  Coated columbium (Cb)
  Coated tantalum (Ta)

- Surface insulators

  LI-1500
  HCF
  REI
  Silicon carbide foam (SiC)

- Carbon-carbon composites

  Various coating systems (including none)

- Ablators

  SS41

A complete tabulation of all test results for all the above materials is presented in Appendix A. These tables describe in detail the:

- Test samples
- Test conditions
- Test sample response
- Test sample performance

and include tabulations for each continuous testing period (nominally 6 cycles) of:

- Enthalpy
- Heat flux
- Stagnation pressure
- Heat transfer coefficient
- Exposure time
- Surface temperature
- Surface emissivity
- Backwall and in-depth temperature
- Mass loss
- Dimension change
- Qualitative description of sample performance

Because of the great quantity of results, the variations of the above parameters through each cycle are not included. These results are available at Aerotherm, and typical results are presented in the following subsections. The 35 mm color slides of the test sample before test and after each continuous testing period also are not included here. These are available at the Ames Research Center,* and typical results are also included (in black-and-white) in the following subsections.

The range of test conditions and material response for the metallics is presented in the table below where the primary test conditions resulted in approximate surface temperatures as follows:

- TD NiCr - 1950°F, 2175°F, 2400°F
- Coated Cb - 2500°F
- Coated Ta - 2700°F

*Nick S. Vojvodich, 415 965-6108

Metallic Type	Surface Temperature (°F)	Heat Flux (Btu/ft^{2}sec)	Total Enthalpy (Btu/lb)	Stagnation Pressure (atm)
TD NiCr	1800 to 2400	10 to 25	3200 to 6500	0.006
Coated Cb	2500	42	11,000	0.006
Coated Ta	2300 to 2700	42 to (90)	11,000 to (20,000)	0.006

Typical results for the metallics are presented in Section 4.2.

All surface insulator types were exposed to the same test conditions. This range of conditions and the corresponding range of response for the surface insulators (LI-1500, HCF, REI, and SiC foam) is presented below:

- Surface temperature - 2000 to 3000°F
- Heat flux - 25 to 85 Btu/ft^{2}sec
- Total enthalpy - 5000 to 24,000 Btu/lb
- Stagnation pressure - 0.006 to 0.007 atm

Typical results for the surface insulators are presented in Section 4.3.

The carbon-carbon composites were exposed to a single nominal test condition which was

- Heat flux - 75 Btu/ft^{2}sec
- Total enthalpy - 19,000 Btu/lb
- Stagnation pressure - 0.007 atm

The measured surface temperature at this condition for the several coating systems tested covered the range 2100 to 2900°F. Typical results for the carbon-carbon composites are presented in Section 4.4.

The ablator models were tested at two nominal test conditions as follows:

- Heat flux - 40 and 100 Btu/ft^{2}sec
- Total enthalpy - 9500 and 19,000 Btu/lb
- Stagnation pressure - 0.006 and 0.007 atm

and the resultant surface temperatures were approximately 2000 and 2600°F, respectively, for the SS41 material tested. Typical results for the ablators are presented in Section 4.5.

4.2 METALLICS

4.2.1 Test Matrix

The types of metallics tested were TD nickel chrome, coated columbium, and coated tantalum. The TD NiCr samples were pre-conditioned to yield high initial emissivity, the coated Cb samples all had R512E coatings but three different substrates were used (Cb-752, FS-85, and C129Y), and the coated Ta samples were fabricated by two different suppliers (LMSC and Solar). A more detailed description of the test samples is presented in Appendix A.

The nominal and actual test matrices for these materials are presented in Figure 15. The lines ⟷ indicate the nominal test program, and in the absence of any other symbols the actual test program as well. The symbol ▲ indicates termination of testing on the particular sample due to a sample failure and the symbol ● indicates termination of testing on the particular sample due to insufficient companion samples. In the case of a sample failure, testing was continued whenever possible by replacing the failed sample with another to-be-tested sample or with a spare sample. Note that the open block on the right side of the coated Cb test matrix (Figure 15b) accommodates the coated Ta test matrix (Figure 15c).

The TD NiCr test program (Figure 15a) was performed as projected - no sample failures occurred. The nominal surface temperatures at which tests were performed were 1800°F, 2000°F, and 2200°F, which when corrected as discussed below were actually about 1950°F, 2175°F, and 2400°F.

The coated Cb test program (Figure 15b) included some failures as noted. The necessary 6 sample set required to continue testing was maintained by:

- Performing some of the 1 and 5 cycle tests as part of the long term test series (50 and 25 cycles)
- Replacement of the failed samples with spare coated Ta samples*

The nominal surface temperature was 2300°F which when corrected as discussed below was actually about 2500°F. The 1 and 5 cycle samples all contained intentional flaws in the form of holes, coating removal, notches, and impressions.

The coated Ta test program (Figure 15c) was rather abbreviated due to sample failures. A maximum of 5 cycles was achieved at the nominal test condition; however, one coated Ta sample went 33 cycles total - 32 at the coated Cb test condition and 1 at the coated Ta test condition (see Appendix A). The nominal

*These samples are not included in the test matrices of Figure 15 but the results are included in Appendix A.

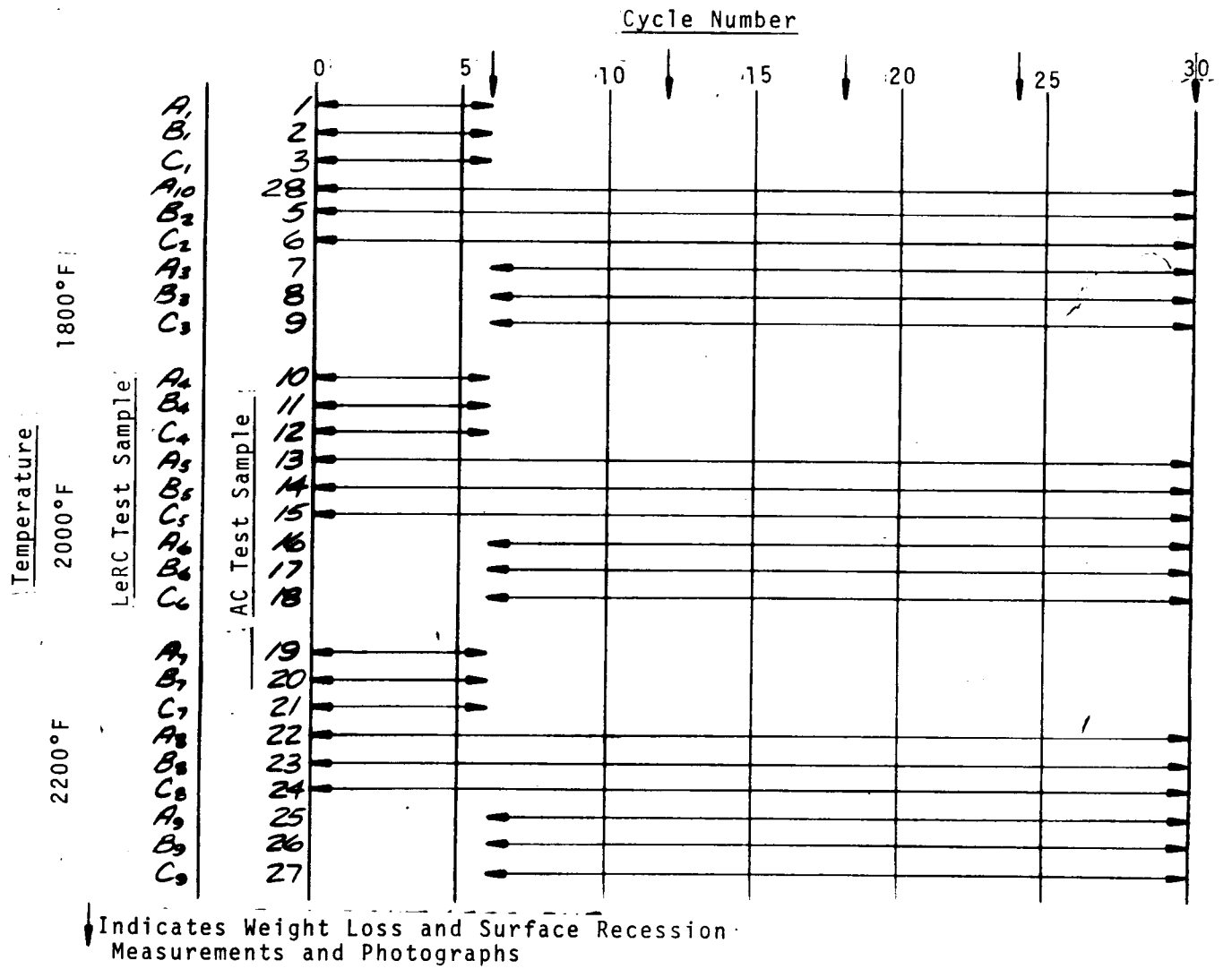

Figure 15 Metallics Test Matrix
a) TD NiCr

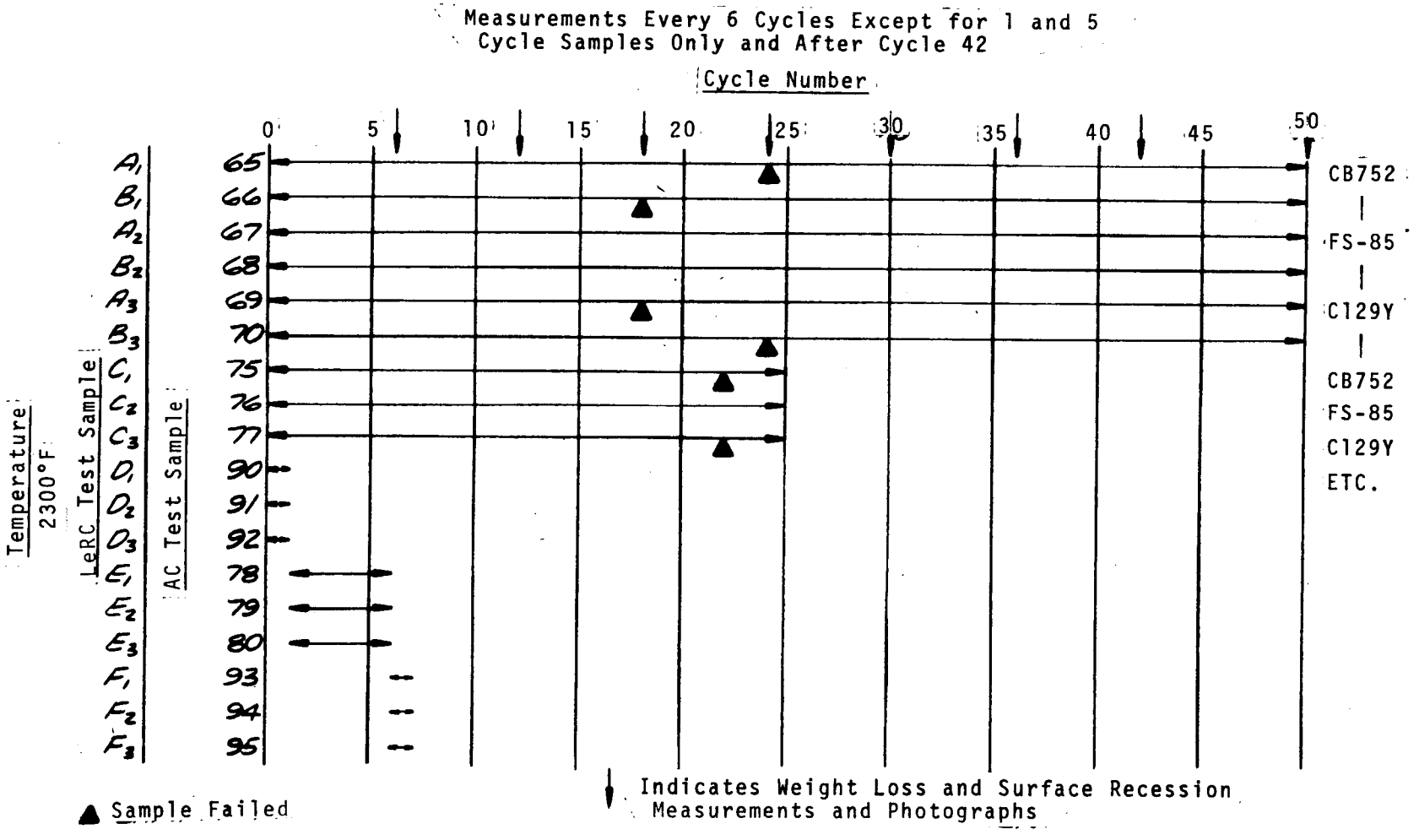

Figure 15 Continued
b) Coated Columbium

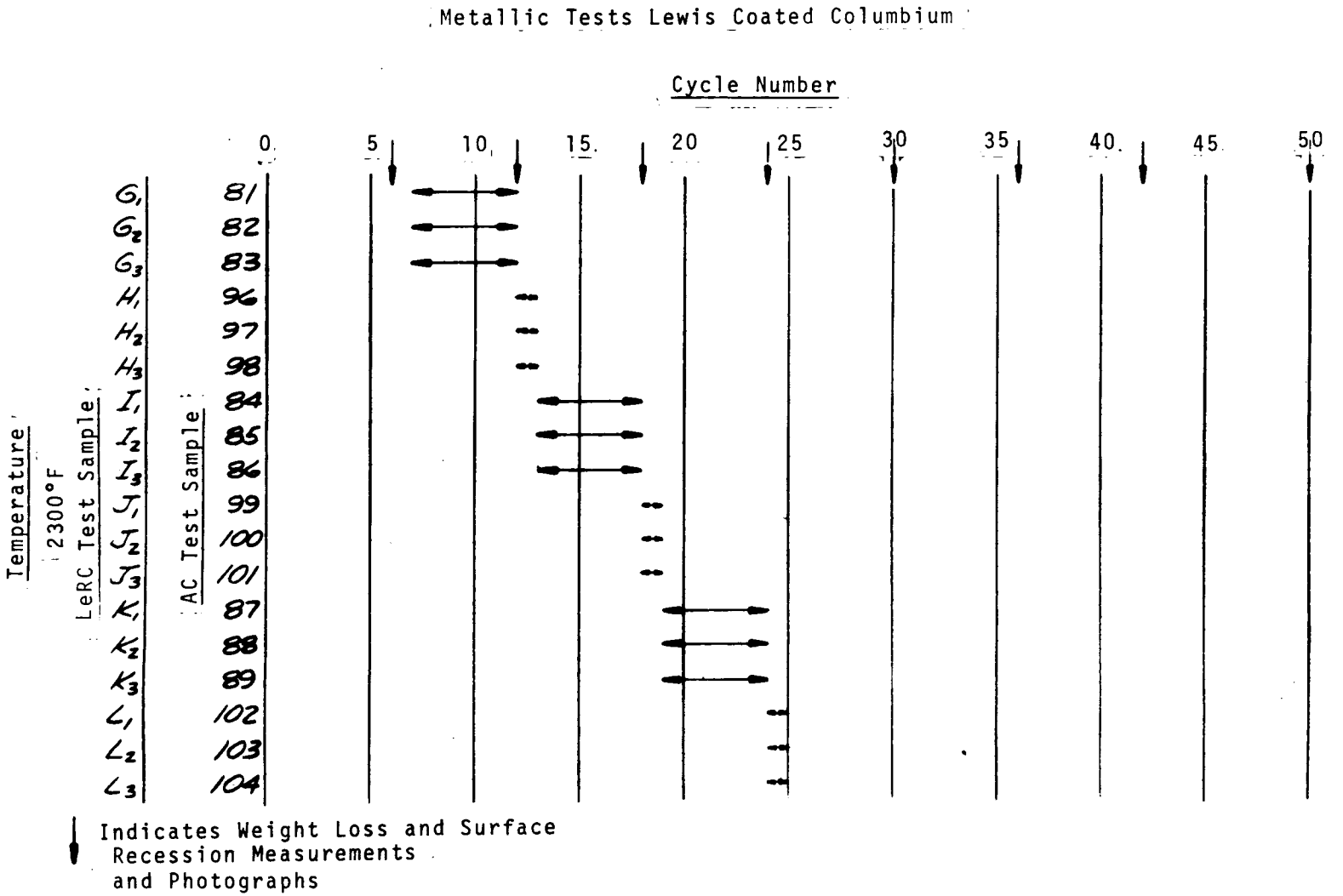

Figure 15 Continued
b) Concluded

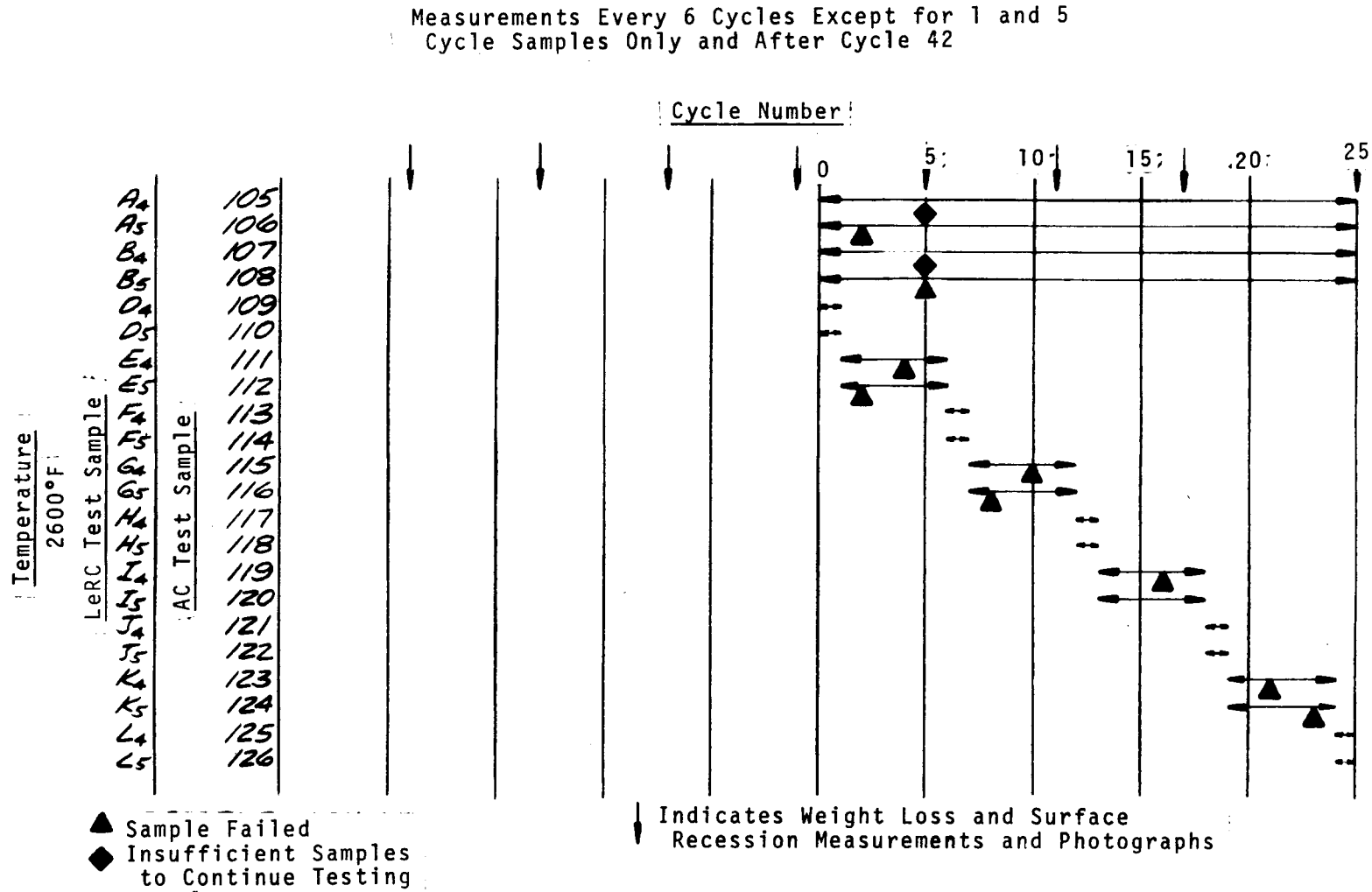

Figure 15 Concluded

c) Coated Tantalum

surface temperature for the coated Ta test series was 2600°F which when corrected as discussed below was actually about 2700°F. The 1 and 5 cycle samples all contained intentional flaws in the same form as the coated Cb samples.

4.2.2 Typical Results

Typical test results for the metallics are presented below in terms of surface temperature and mass loss response, emissivity and surface catalycity, and failure modes and operating limits. Emphasis is placed on TD NiCr because of the quantity and quality of the results. In the cases where results for TD NiCr only are presented, similar results for coated Cb and coated Ta are available in Appendix A.

Typical surface temperature results for the metallics are presented in Table 7. The significant disparity in the results for the different measurement techniques used is apparent. Because of this disparity, all results were subjected to detailed scrutiny during and after the test program. This study indicated that:

- The metallics exhibit a decreased emissivity in the sensing wavelength band of the primary TD-7 pyrometer. The actual surface temperatures were therefore higher than measured.
- The spring-loaded thermocouples exhibited at least a small error due to contact resistance and conduction losses. The actual surface temperatures were therefore higher than measured.
- The Thermogage pyrometer indicated more realistic temperatures but was somewhat erratic for unexplained reasons.

These conclusions are amplified in the following paragraphs.

During the metallics test series, detailed information on the spectral emissivity of the oxide coating on TD NiCr and the coated Cb and coated Ta surfaces was not available. Total emissivity values of 0.85 were felt reasonable for all surfaces and in the absence of better data were used for pyrometer measurements and surface temperature control. After test, emissivity measurements on the TD NiCr samples were made (Reference 7)* and some preliminary results are presented in Figure 16. These results show a minimum emissivity of about 0.56 near a wavelength of 2 microns. Note that this region of lower emissivity falls in the wavelength band of the TD-7 pyrometer, and that the average emissivity in this band is about 0.61. Also note that a reasonable total emissivity in the temperature range around 2000°F (half the radiant energy below about 3 microns, peak radiant energy at 2.1 microns) is about 0.75.

*These measurements are currently in progress on the actual samples tested and therefore final results are not available at this writing.

TABLE 7

COMPARISON OF SURFACE TEMPERATURE MEASUREMENT RESULTS FOR METALLICS

	TD-7 Pyrometer		Thermogage Pyrometer	Spring-Loaded Thermocouple
	Measured (ε = .85)	Corrected (ε = .61)		
• TD NiCr				
	1790°F	1940°F	1980°F	--
	1990°F	2160°F	2300°F	1950°F
	2160°F	2360°F	2370°F	--
	2160°F	2360°F	--	2130°F
• Coated Cb				
	2280°F		2510°F	2390°F
	2290°F		2530°F	2420°F
	2310°F		2360°F	2410°F
• Coated Ta				
	2510°F		2770°F	--
	2520°F		--	2670°F
	2520°F		2550°F	2570°F

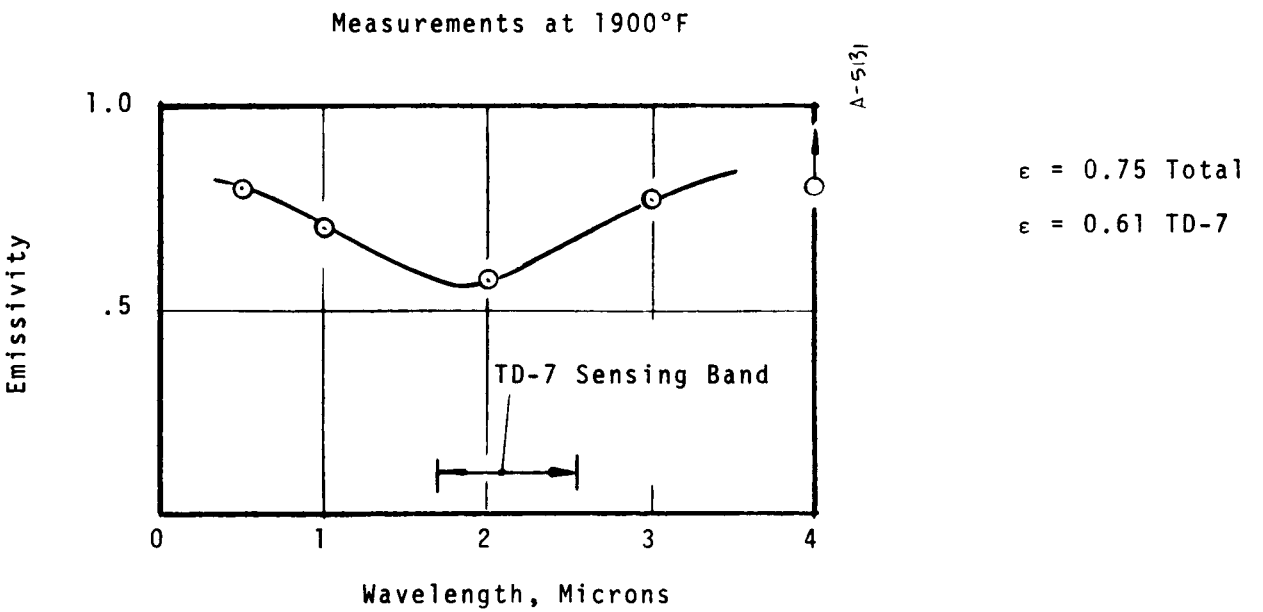

Figure 16 Preliminary Emissivity Results for TD NiCr Test Samples

Based on the results of Figure 16, the TD-7 pyrometer output should be corrected for an emissivity of 0.61 for TD NiCr, and this correction is shown in Figure 17. The resultant typical temperatures are also included in Table 7. Actual temperatures for TD NiCr were therefore about 150°F to 200°F higher than originally measured with the TD-7 pyrometer. Note from Table 7 that the Thermogage pyrometer, which is relatively insensitive to emissivity, provided results which agreed quite well with the corrected TD-7 pyrometer results.

No emissivity data were available for coated Cb and coated Ta, and therefore the similar analysis for these materials was not performed. The comparison of the TD-7 and Thermogage pyrometer results indicate a similar emissivity depression in the wavelength region around 2 microns for these materials however.

The corrected TD-7 pyrometer results for TD NiCr indicate that the spring-loaded thermocouples measured a temperature about 200°F lower than actual (Table 7). An approximate error analysis considering conduction losses and contact resistance accounted, at the maximum, for about 50°F of the apparent 200°F error. The remaining contribution, except for the possibility of unusually poor contact, is presently unexplained. The 200°F error for TD NiCr has also been determined in the program of Reference 8 however. These results for TD NiCr indicated that, although the Aerotherm spring-loaded probes used herein exhibited the best accuracy of those evaluated, the indicated temperature was about 200°F lower than the actual surface temperature. On the basis of this analysis, all spring-loaded thermocouple results for TD NiCr should be corrected by about +200°F.

Based on the above discussion of the pyrometer results for coated Cb and coated Ta, the spring-loaded thermocouple measurements are also in error for these materials but not by as large an amount. The approximate corrections are:

- Coated Cb + 100°F
- Coated Ta + 50°F

The reason for the improved accuracy of the spring-loaded thermocouples for the coated samples is not obvious. Possibly the roughness and compliance of the coatings allowed a more intimate contact with the sample.

Based on the above presentation, the surface and backwall temperatures for metallics presented in the tables of Appendix A and unless otherwise noted in the presentation below should be corrected approximately as follows:

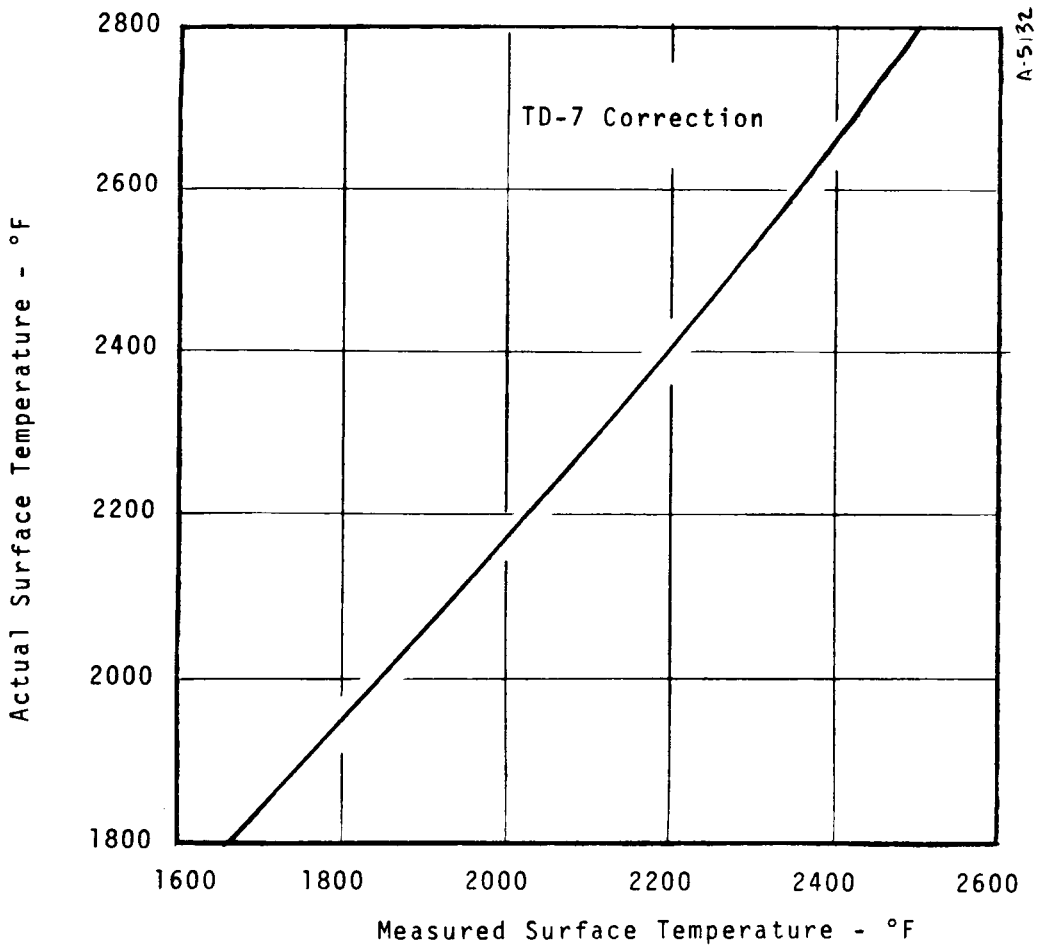

Figure 17 Correction to TD-7 Pyrometer Measurements for TD NiCr Test Samples

- TD NiCr

TD-7 Pyrometer	Spring-Loaded Thermocouple
+ 150 to 200°F (Figure 17)	+ 200°F

- Coated Cb

+ 200°F	+ 100°F

- Coated Ta

+ 150°F	+ 50°F

The nominal surface temperautres at which these materials were tested were therefore:

- TD NiCr - 1950°F, 2175°F, 2400°F
- Coated Cb - 2500°F
- Coated Ta - 2700°F

Typical surface and backwall temperature history results for a single TD NiCr test sample over six cycles are presented in Figure 18. These temperatures are uncorrected relative to the analysis above. The spring-loaded thermocouple agrees very well with the pyrometer measurement throughout the test, which is of course due to the similar magnitude of the errors in these two measurement techniques (see above).

Typical temperature distributions through the Silfrax backup insulator for the metallics tests are shown in Figure 19. At 5 minutes into the cycle the response is still transient; however, steady state is achieved within 15 minutes. The heat loss defined from these distributions is less than 5 percent of the incident flux - 0.44 Btu/ft^{2}sec loss versus approximately 10 Btu/ft^{2}sec incident. Note that the corrected backwall temperature on the metallic test sample (point at zero distance below the surface) is of the order of 50°F higher than the extrapolated surface temperature of the Silfrax backup insulator. An approximate analysis indicated that this difference is consistant with minimal contact and radiation interchange between the metallic sample and the backup insulator.

Mass loss results for each set of 3 TD NiCr samples that were tested for 30 cycles are presented in Figure 20. The effect of temperature is significant both in the magnitudes of the weight loss and in the rates of change with time. The average loss rates over 30 cycles and the trends in loss rates at 30 cycles are presented in the table below.

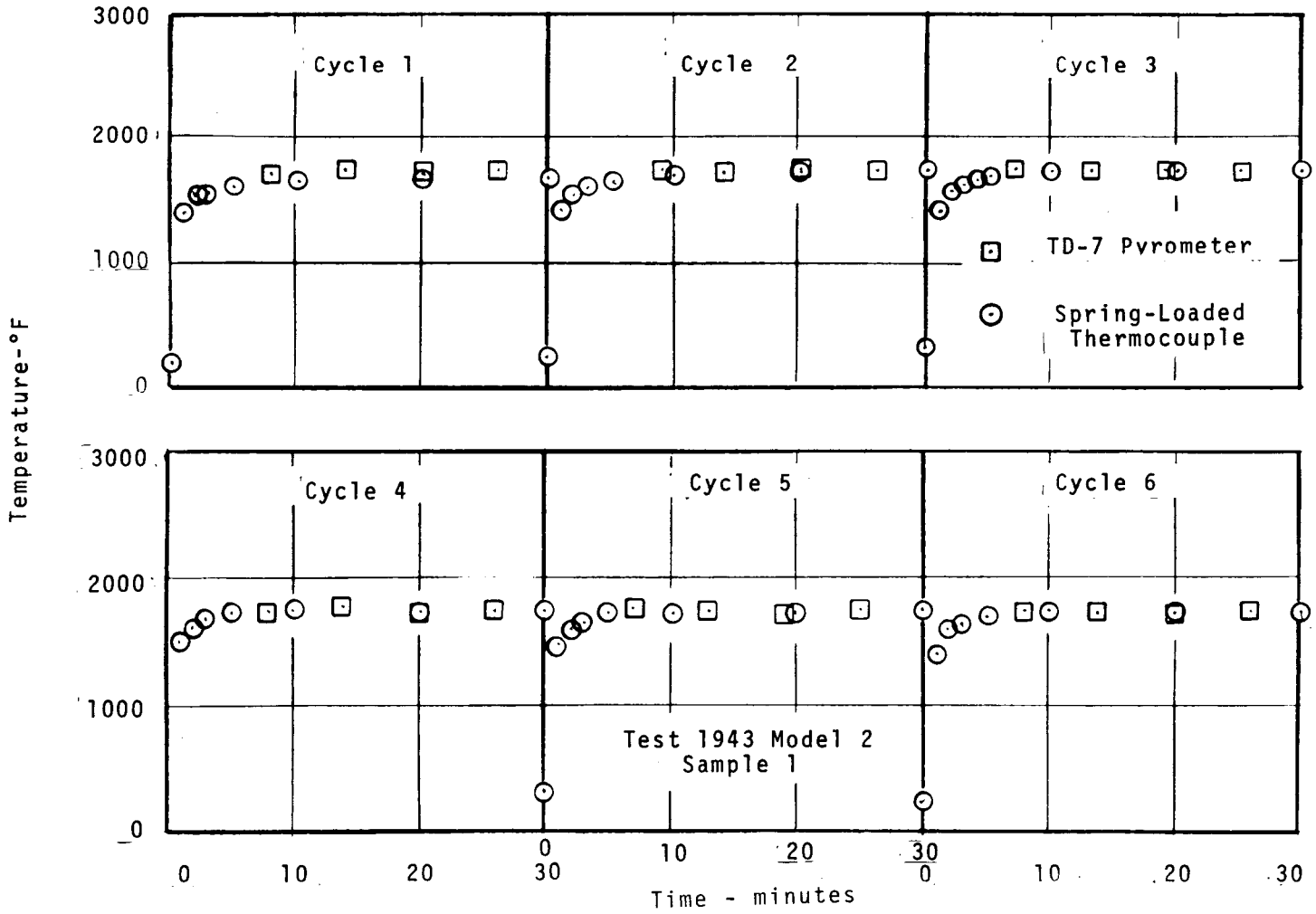

Figure 18 Typical Cyclic Temperature - Time Results for TD NiCr

Run 1943 Cycle 3 Model 2 Sample 1

ρ = 30 lb/ft^3 (Silfrax)

$\frac{q_{loss}}{q_c} \doteq .05$

○ In-Depth Thermocouples
□ Corrected Spring-Loaded Backwall Thermocouples

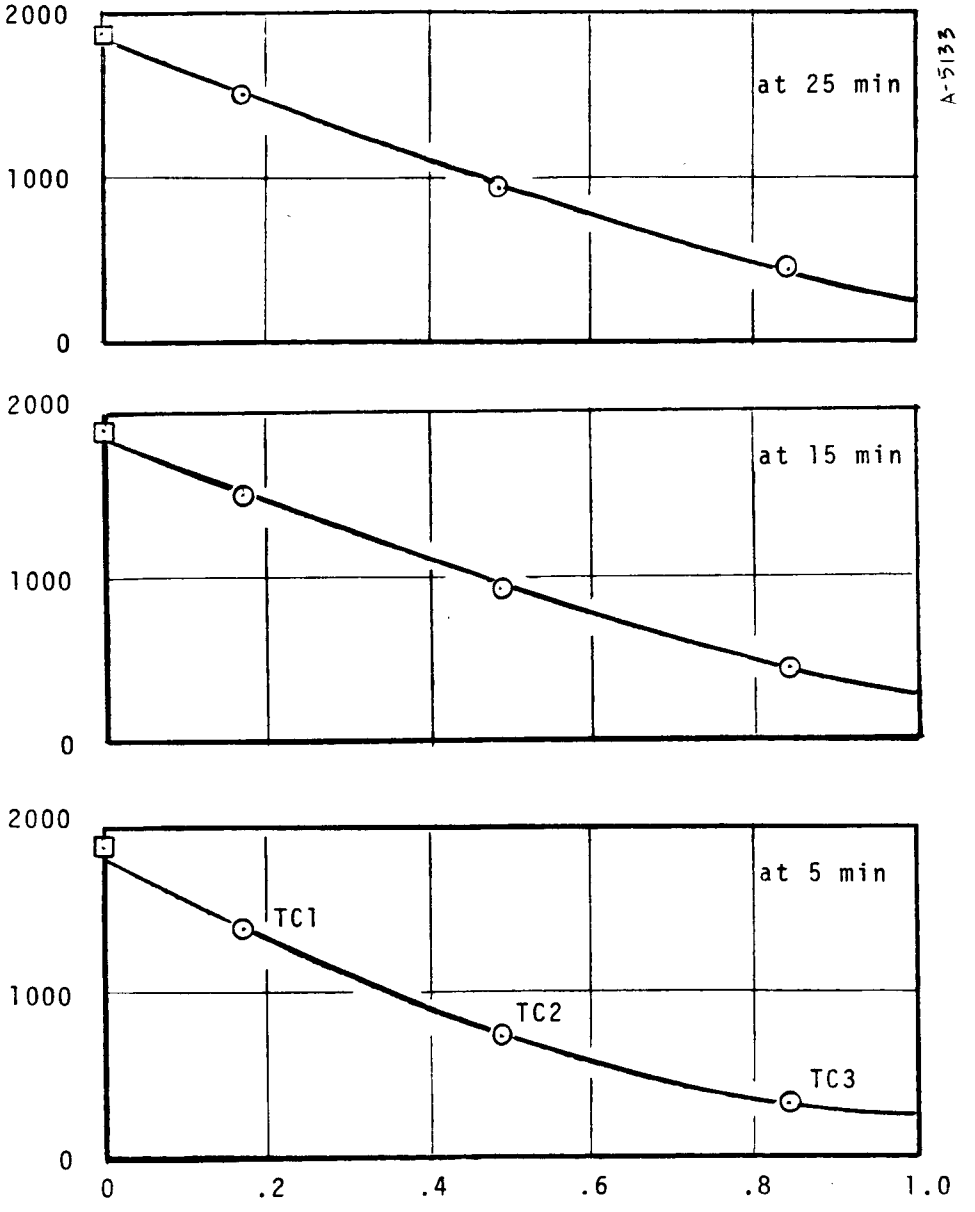

Figure 19 Typical Silfrax Backup Insulator Temperature Distributions

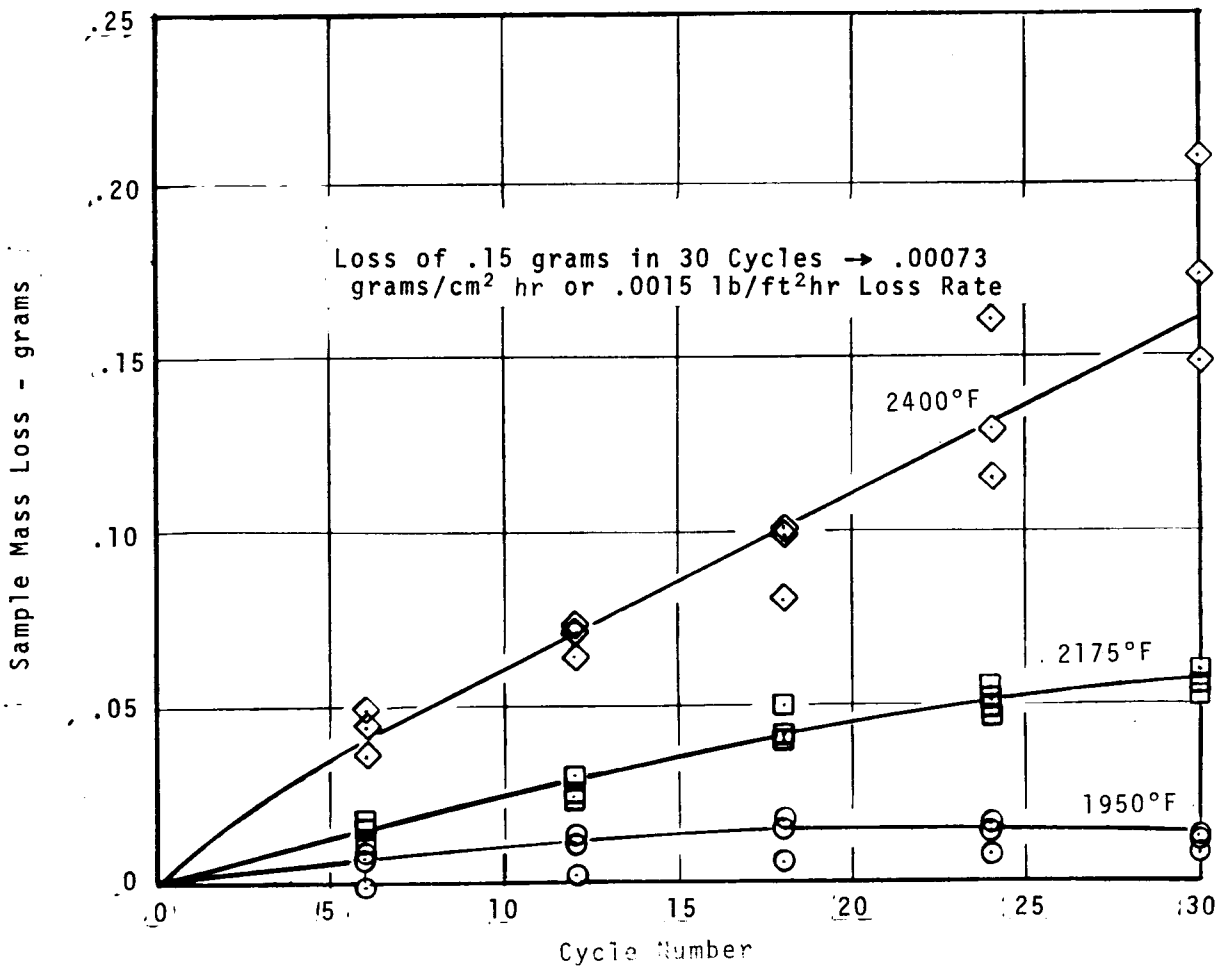

Figure 20 Typical Mass Loss Results for TD NiCr

Corrected Temperature	Loss Rates	
	Average Over 30 Cycles	Trend at 30 Cycles
1950°F	0.00014 lb/ft^{2}hr	Zero
2175°F	0.00057 lb/ft^{2}hr	Decreasing
2400°F	0.00160 lb/ft^{2}hr	Constant or increasing

Typical surface catalycity results for all metallic types are presented in Table 8. The surface catalycity ratio (SCR) is the ratio of the radiation equilibrium heat flux to the calculated hot wall heat flux (based on the measured cold wall heat flux)

$$SCR = \frac{q_r}{q_{hw}} = \frac{\varepsilon \sigma T_w^4}{q_{hw}} \qquad (7)$$

These results indicate that the oxide film formed on TD NiCr is nearly fully catalytic and that the coated metallics surfaces are partially noncatalytic with typical surface catalycity ratios of approximately:

- Coated Cb - 0.70
- Coated Ta - 0.60

At the three nominal temperatures studied (1950°F, 2175°F, and 2400°F) for the TD NiCr test samples, consistent results were obtained and no failures occurred. In the coated Cb tests at a nominal temperature of 2500°F, one of the coating/substrate systems (R512E/FS-85) exhibited superior performance with a capability to survive approximately 50 cycles. The other two coating/substrate systems (R512E/Cb-752 and R512E/C129Y) exhibited about equal performance with a capability to survive approximately 20 cycles. The sample failures were the significant loss of material, this loss typically starting at the edge of the sample.

Some of both the coated Cb and coated Ta samples contained deliberate flaws in the form of holes, removed coating, notches, and impressions. In general, the flaws in the coated Cb samples (2500°F) healed with exposure to the simulated reentry heating conditions, whereas the flaws in the coated Ta samples (2700°F) grew and in some cases caused catastrophic failure.

An overview of the response characteristics of TD NiCr, coated Cb, and coated Ta is presented in Figure 21. The representative photographs presented are from the 35 mm color slides taken of each sample through its exposure history and illustrate the performance capabilities presented above.

TABLE 8

SURFACE CATALYCITY AND SURFACE EMISSIVITY FOR METALLICS

Sample	Sample Description	Test	Cycle	Cumulative Exposure Time (Min.)	Measured Surface Temperature (°F)	Corrected Surface Temperature (°F)	Probable Emissivity (-)	Cold Wall Heat Flux (Btu/ft²sec)	Total Enthalpy (Btu/lb)	Hot Wall Heat Flux (Btu/ft²sec)	Probable Net Heat Flux (Btu/ft²sec)	Surface Catalycity Ratio (-)
5	TDNiCr 60° B2	1943	6	180	1770	1920	.75	12.5	3500	10.7	11.4	(1.0)
		1944	12	360	1730	1880		11.9	3340	10.2	10.7		
		1945	18	540	(1660)	-		12.4	3430	10.7	-	--
		1946	24	720	1780	1930		12.5	3390	10.6	11.6	(1.0)
		1947	30	900	1780	1930		12.4	3290	10.5	11.6	
13	TDNiCr 60° A5	1943	6	180	1970	2140		17.7	5150	15.8	16.3	
		1944	12	360	1970	2140		18.4	4950	16.3	16.3	0.91
		1945	18	540	1960	2130		19.6	5350	17.6	16.1	(1.0)
		1946	24	720	1990	2160		18.6	4950	16.5	16.8	
		1947	30	900	1990	2160		16.8	4800	14.8	16.8	
14	TDNiCr 60° B5	1943	6	180	1990	2160		17.7	5150	15.8	16.8	
		1944	12	360	1980	2150		18.4	4950	16.3	16.6	0.82
		1945	18	540	1900	2060		19.6	5350	17.6	14.4	0.99
		1946	24	720	1970	2140		18.6	4950	16.5	16.3	(1.0)
		1947	30	900	1990	2160		16.8	4800	14.8	16.8	0.99
15	TDNiCr 60° C5	1943	6	180	1940	2110		17.7	5150	15.8	15.6	
		1944	12	360	1960	2130		18.4	4950	16.3	16.1	-
		1945	18	540	(1840)	-		19.6	5350	17.6	-	0.96
		1946	24	720	1950	2120		18.6	4950	16.5	15.8	-
		1947	30	900	1980	2150		-	4800	-	16.6	-
23	TDNiCr 60° B3	1948	6	180	2200	2410		-	6080	-	24.2	-
		1949	12	360	2180	2390		-	6200	-	23.6	(1.0)
		1950	18	540	2170	2380		23.4	6290	21.1	23.2	
		1951	24	720	2180	2390		25.1	6340	22.6	23.6	
		1952	30	900	2160	2360		25.2	6320	22.7	22.6	
65	Coated Cb 60° A1	1948	6	180	2230	2430	.85	44.1	10,910	41.5	28.2	0.68
		1949	12	360	2230	2430		43.0	11,330	40.6	28.2	0.69
		1950	18	540	2270	2470		42.0	11,400	39.5	29.8	0.75
		1951	24	720	2310	2510		43.7	11,670	41.2	31.5	0.76
67	Coated Cb 60° A2	1948	6	180	2280	2480		44.1	10,910	41.5	30.2	0.73
		1949	12	360	2290	2490		43.0	11,330	40.5	30.6	0.76
		1950	18	540	2300	2500		42.0	11,400	39.6	31.1	0.78
		1951	24	720	2270	2470		43.7	11,670	41.3	29.8	0.72
		1952	30	900	2240	2470		42.8	11,330	40.3	29.8	0.74
		1953	36	1080	2210	2410		41.8	10,640	39.3	27.4	0.70
		1954	42	1260	2230	2430		40.3	11,020	38.0	28.2	0.74
		1955	44	1320	2210	2410		37.3	10,910	35.1	27.4	0.78
		1956	46	1380	2200	2400		37.0	10,910	34.9	27.1	0.78
		1958	49	1470	2280	2480		55.6	12,830	52.8	30.2	0.57
		1959	50	1500	(2300)	-		-	-	-	-	-

TABLE 8 (CONCLUDED)

Sample	Sample Description	Test	Cycle	Cumulative Exposure Time (Min.)	Measured Surface Temperature (°F)	Probable Surface Temperature (°F)	Probable Emissivity (-)	Cold Wall Heat Flux (Btu/ft²sec)	Total Enthalpy (Btu/lb)	Hot Wall Heat Flux (Btu/ft²sec)	Probable Net Heat Flux (Btu/ft²sec)	Surface Catalycity Ratio (-)
68	Coated Cb 60° B2	1948	6	180	2170	2370	.85	44.1	10,910	41.6	26.0	0.62
		1949	12	360	2190	2370		43.0	11,330	40.6	26.0	0.64
		1950	18	540	2180	2380		42.0	11,400	39.7	26.3	0.66
		1951	24	720	2190	2390		43.7	11,670	41.4	26.7	0.64
		1952	30	900	2160	2360		42.8	11,300	40.5	25.6	0.63
		1953	36	1080	2140	2340		41.8	10,640	39.4	25.2	0.64
		1954	42	1260	2140	2340		40.3	11,020	38.1	25.2	0.66
		1955	44	1320	2130	2330		37.3	10,910	35.2	24.5	0.70
		1956	46	1380	2130	2330		37.0	10,910	34.9	24.5	0.70
		1958	49	1470	2190	2390		55.6	12,830	52.9	26.7	0.50
		1959	50	1500	(2220)	(2420)		-	---	-	(14.2)	-
69	Coated Cb 60° A3	1948	6	180	2280	2480		44.1	10,910	41.5	30.2	0.73
		1949	12	360	2290	2490		43.0	11,330	40.5	30.6	0.76
		1950	18	540	2270	2470		42.0	11,400	39.6	29.8	0.75
71	Coated Ta 60° N4	1951	6	180	2120	2270		43.7	11,670	41.5	22.5	0.54
		1952	12	360	2100	2250		42.8	11,330	40.6	21.8	0.54
		1953	18	540	2060	2210		41.8	10,640	39.6	20.6	0.52
		1954	24	720	2120	2270		40.3	11,020	38.1	22.5	0.59
		1955	26	780	2130	2280		37.3	10,910	35.3	22.8	0.65
		1956	28	840	2100	2250		37.0	10,910	35.0	21.8	0.62
		1958	31	930	2180	2230		55.6	12,830	53.1	21.2	0.40
		1959	32	960	(2200)	(2350)		-	---	-	(25.2)	-
72	Coated Ta 60° M4	1951	6	180	2280	2430		43.7	11,670	41.5	28.2	0.68

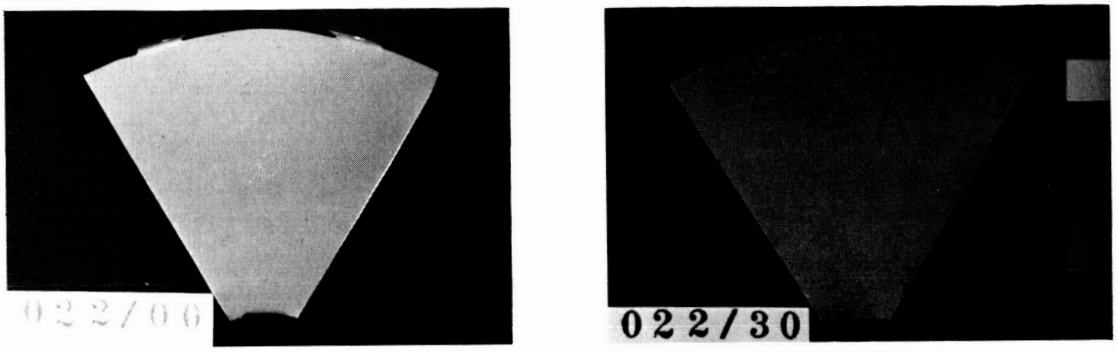

2400°F

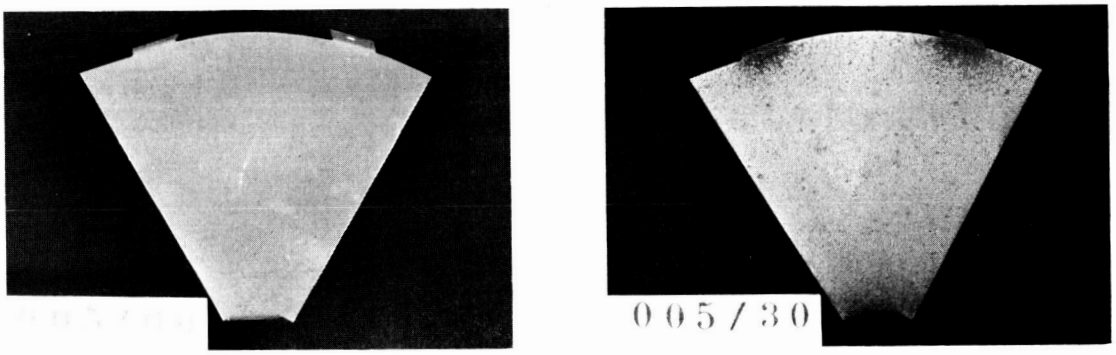

1950°F

000/00 → Sample/Cycle

Figure 21 Response Characteristics of Metallics

a) TD NiCr

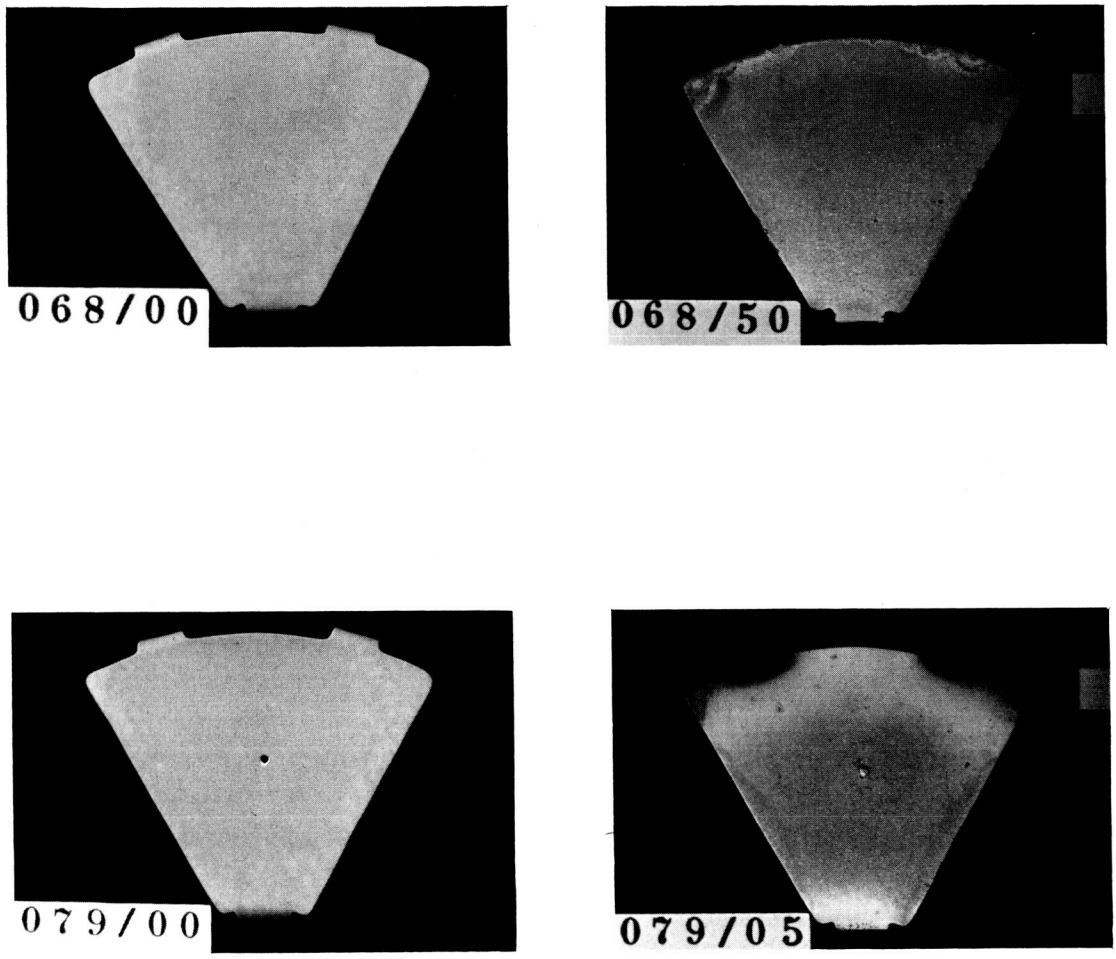

Hole

2500°F

000/00 → Sample/Cycle

Figure 21 (Continued)

b) Coated Cb

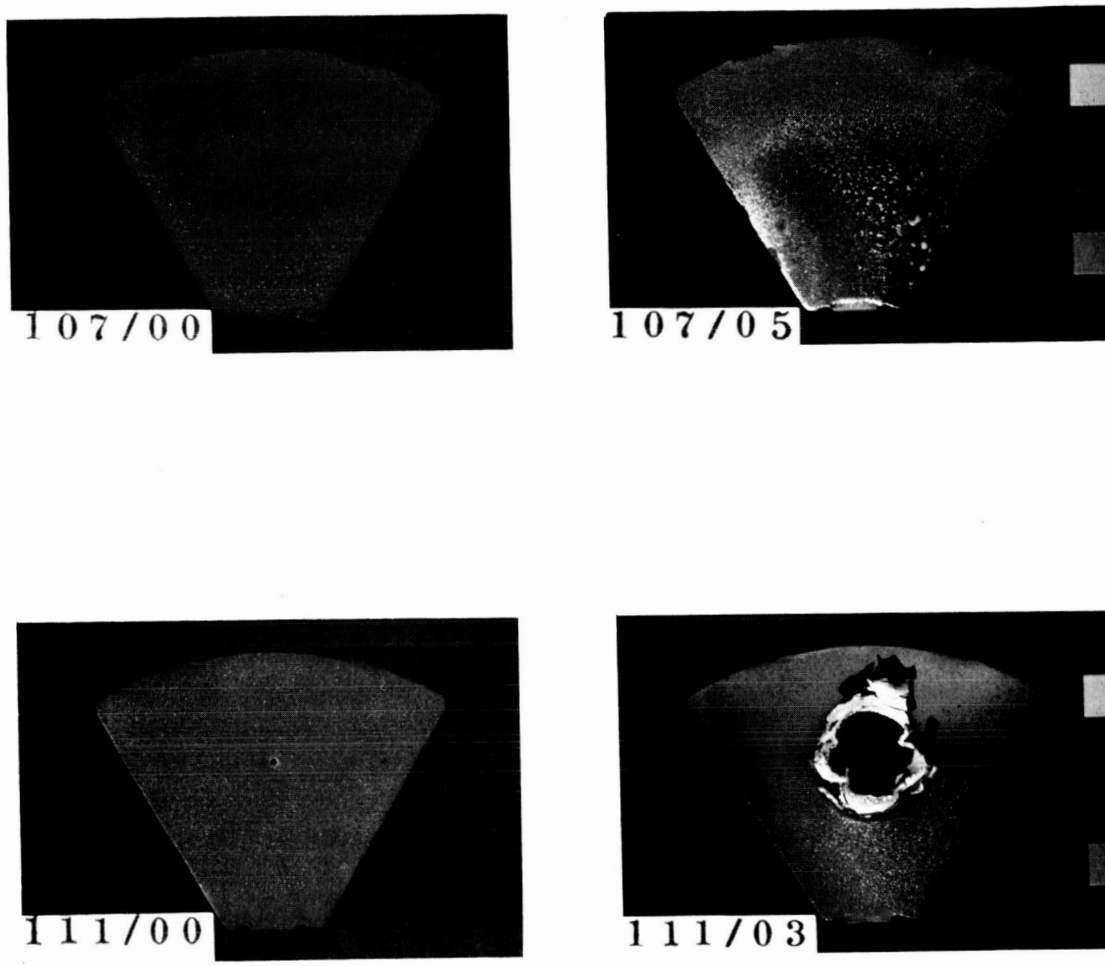

Hole

000/00 → Sample/Cycle

2700°F

Figure 21 (Concluded)

c) Coated Ta

4.3 SURFACE INSULATORS

4.3.1 Test Matrix

The types of surface insulators tested were LI-1500, HCF, REI, and SIC foam. For the first two types, 5 and 3 different surface coating variations, respectively, were tested. For the last two types, there were no material variations. The detailed description of the test samples is presented in Appendix A.

The nominal and actual test matrix for the surface insulators is presented in Figure 22. The symbology is the same as for the metallics. Note that the test matrix includes some replacement samples used in place of samples which failed. A single test series was run at the same heat flux but with approximately twice the stagnation pressure and reduced enthalpy (see Equation (6)) to investigate the affect of these variables. Another test series included 120° test samples of REI, HCF, and LI-1500 in each of the two test models.

The sample failures indicated in the test matrix were not necessarily indicative of the material performance capabilities. The initial emissivity data available and used for LI-1500 was incorrect and resulted in high surface temperatures, the radial split line between samples resulted in a singularity region which promoted failure, and the retention pins could have promoted the SiC foam failure (cracks). The specific failures are defined below:

Sample	Reason for Failure
139	Actual emissivity lower than used for surface temperature control
146	Same as sample 139
133	Severe cracking
127	Subsurface removal along radial split line
128	Same as sample 127
129	Same as sample 127
147	Severe coating cracking
148	Same as sample 147
149	Same as sample 147
150	Same as sample 147
152	Same as sample 147

4.3.2 Typical Results

Typical test results for the surface insulators are presented below in terms of temperature and mass loss response, emissivity and surface catalycity, and failure modes and operating limits. Emphasis is placed on the test series

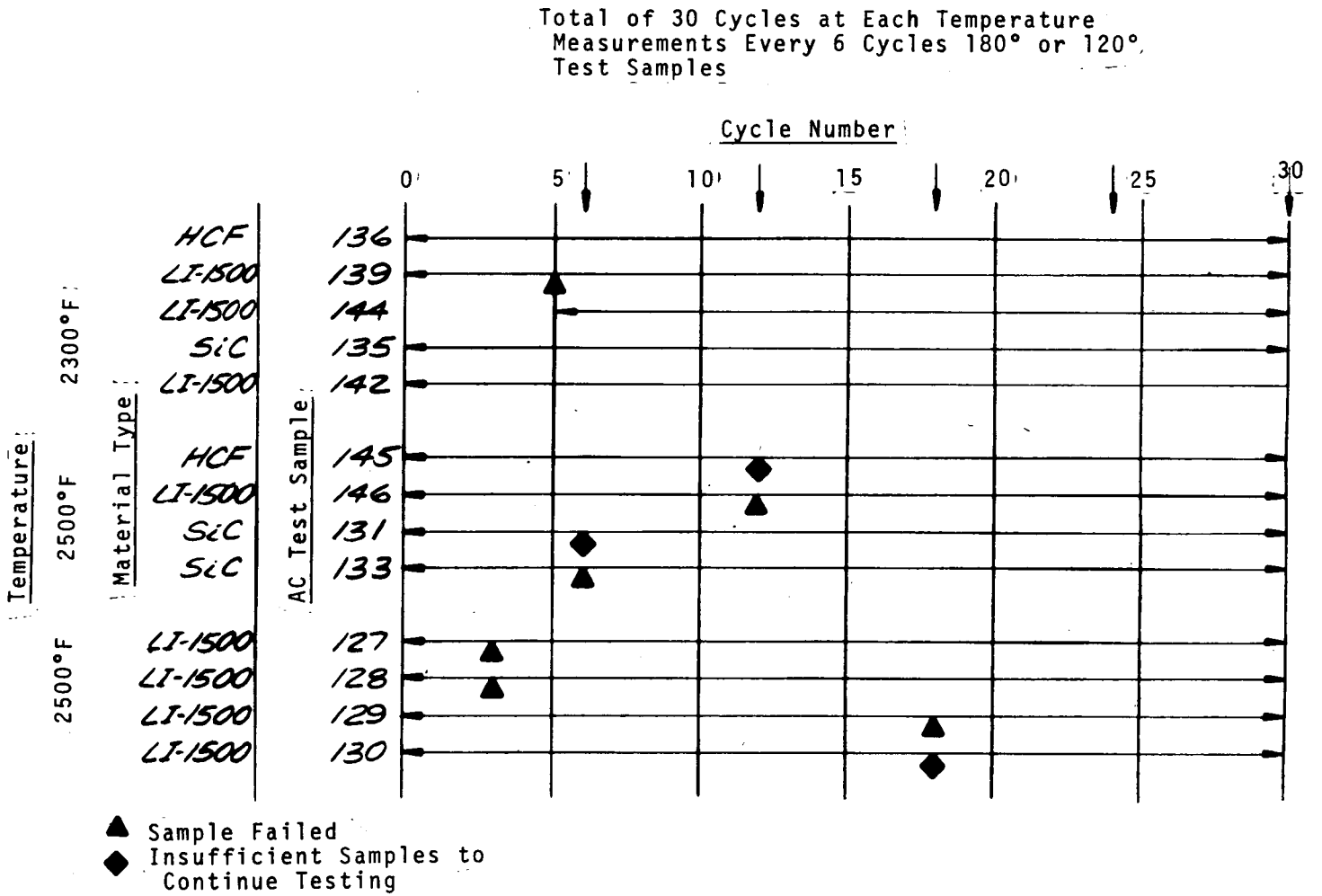

Figure 22 Surface Insulator Test Matrix

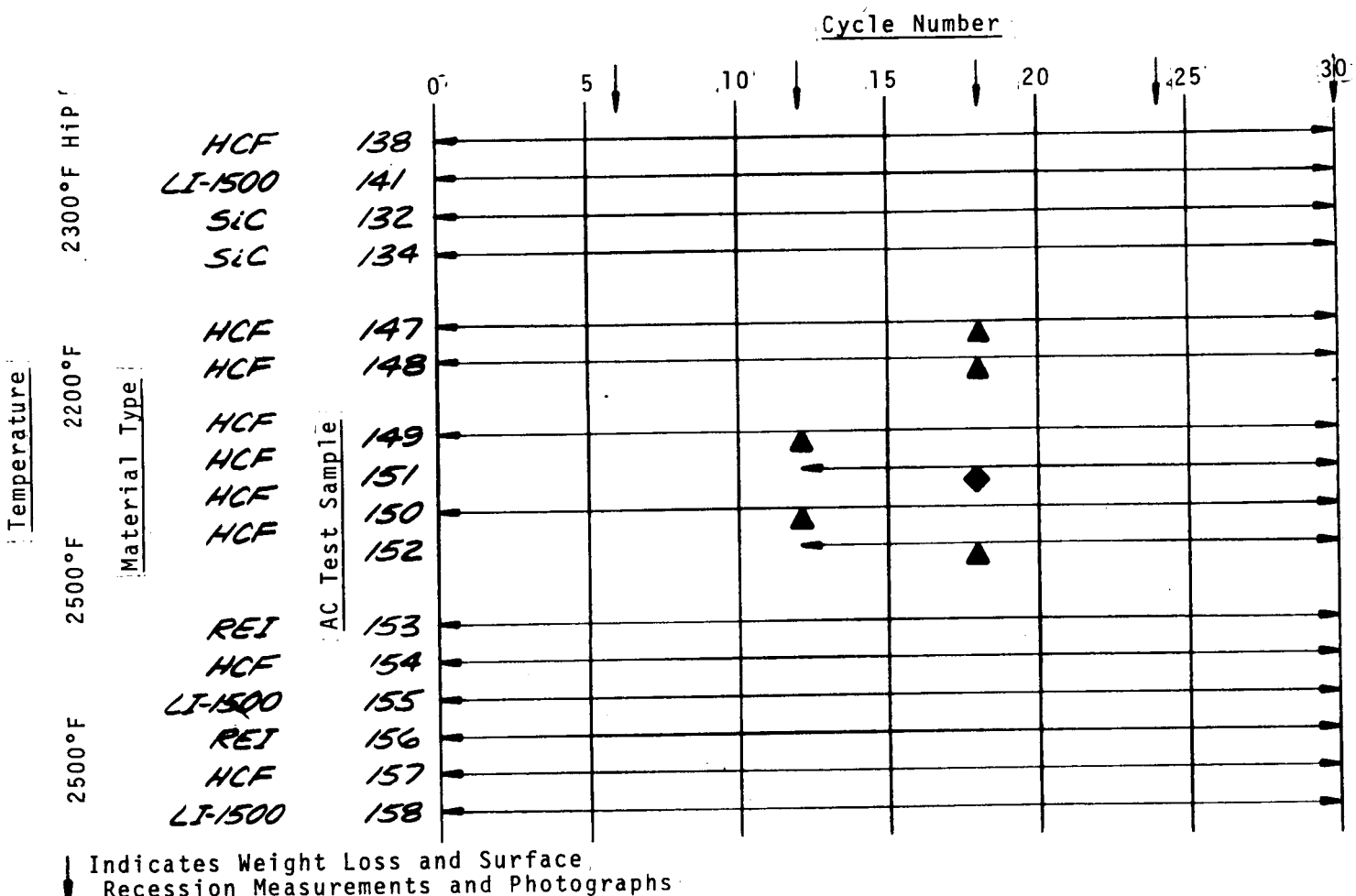

Figure 22 Concluded

which employed 120° test samples of REI, HCF, and LI-1500 since it provides complete comparative data and since the TD-9 pyrometer was used which provides a high confidence level in the surface temperature results because of its relative insensitivity to emissivity (Section 2.3.3). Results not presented are included in Appendix A.

Typical surface and in-depth temperature results over a single cycle for all three 120° test samples in one test model (REI, HCF, and LI-1500) are presented in Figure 23. The in-depth spring-loaded thermocouple is at the midplane of the test samples (1/2 inch below the surface). The different insulative performance of these materials is apparent from these measurements. The heat flux level for these tests was approximately 30 Btu/ft^{2}sec.

Typical mass loss results for the same set of 3 RSI test samples (REI, HCF, and LI-1500) exposed at constant heat flux are shown in Figure 24. The average loss rates over 30 cycles are:

RSI Type	Average Loss Rate Over 30 Cycles
REI	0.00085 lb/ft^{2}hr
HCF	0.00250 lb/ft^{2}hr
LI-1500	0.00050 lb/ft^{2}hr

Note that the high average rate for HCF is due to the very high rate during the first few cycles (during which the surface temperature was also high due to the catalytic surface condition discussed below).

During one cycle on each of 2 models (cycle 1 for one and cycle 2 for the other), the test conditions were varied in steps to define the surface catalycity effect over a flux range from about 25 to 50 Btu/ft^{2}sec. These results, obtained on one of the HCF versions, are presented in Figure 25. The solid line is the calculated fully catalytic wall variation of heat flux with surface temperature. The dotted line is a fit of the catalycity calibration results presented in Section 3 (q_{noncat}/q_{cat} = 0.61). This version of HCF is seen to have a noncatalytic surface at approximately the above heat flux ratio defined from the calibration tests.

The surface insulator types, and the coating variations within each type where appropriate, exhibited a wide range of surface emissivity and surface catalycity - from about 0.3 to 0.9 emissivity and from nearly fully catalytic to essentially fully noncatalytic. These properties varied with the material and the coating and also varied with exposure time. The low emissivity corresponded to LI-1500 in the sensing wavelength of the TD-7 pyrometer, and the high emissivity corresponded to the SiC foam. All coatings and the SiC foam exhibited essentially fully noncatalytic surfaces (based on the calibration

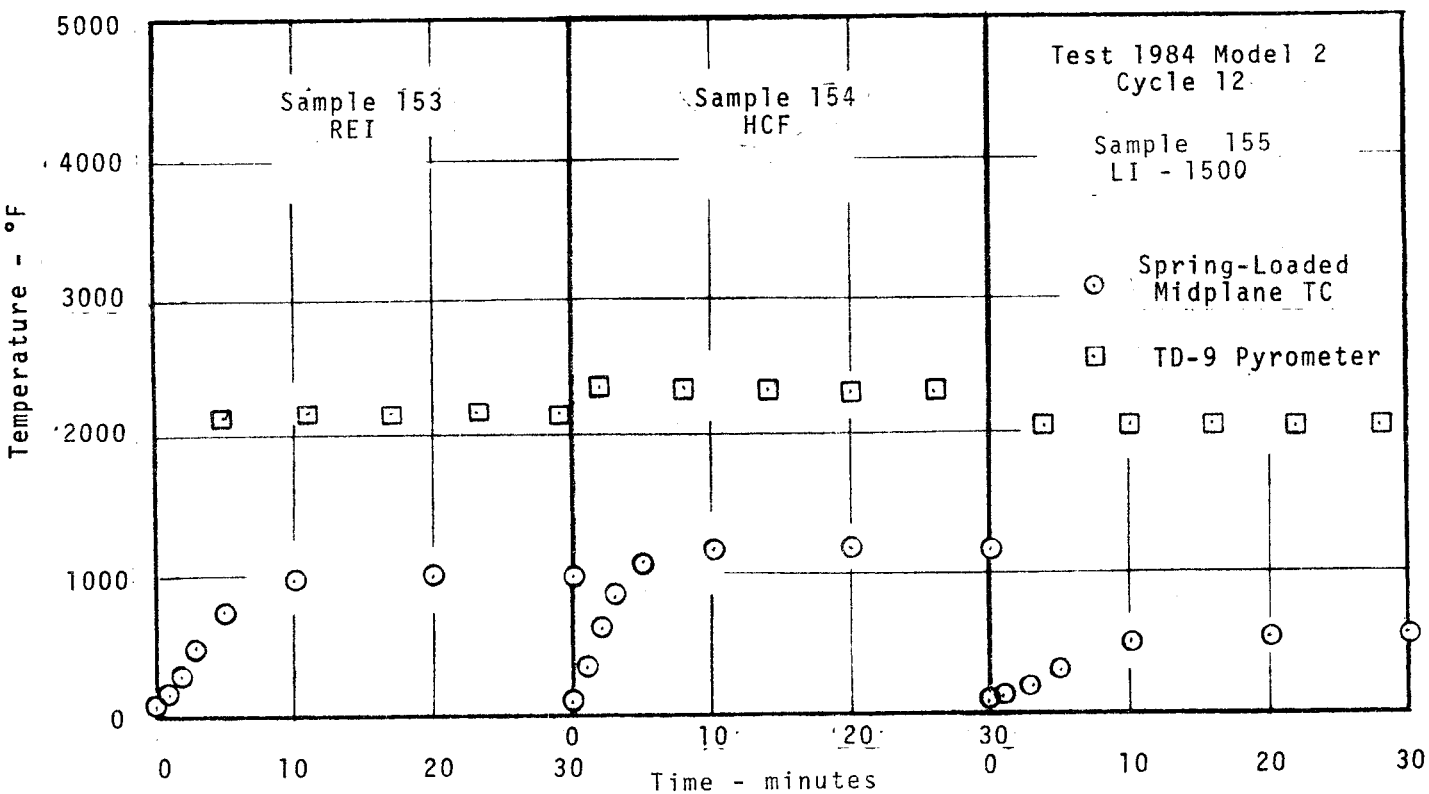

Figure 23 Typical Sample Temperature - Time Results for Surface Insulators

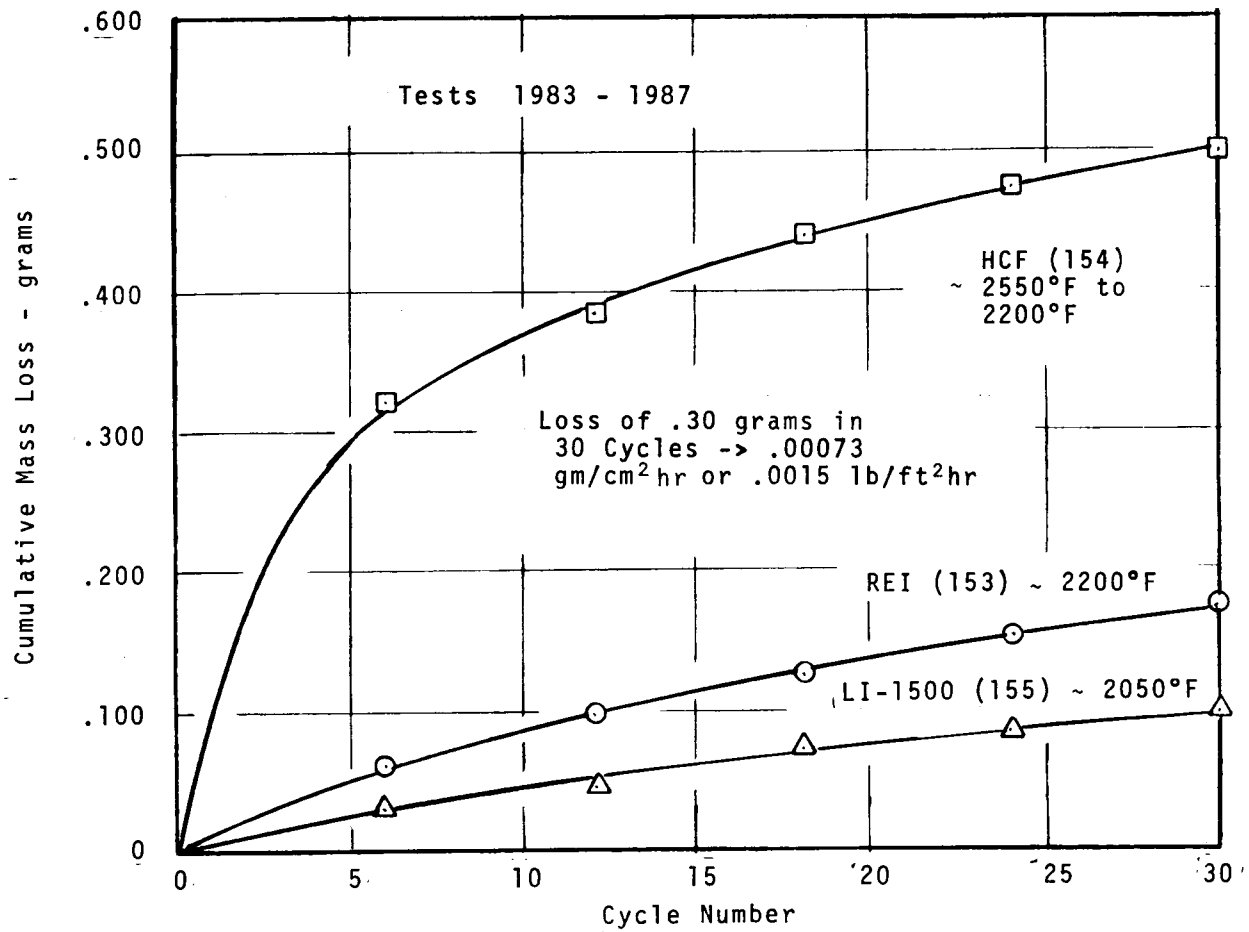

Figure 24 Typical Mass Loss Results for Surface Insulators

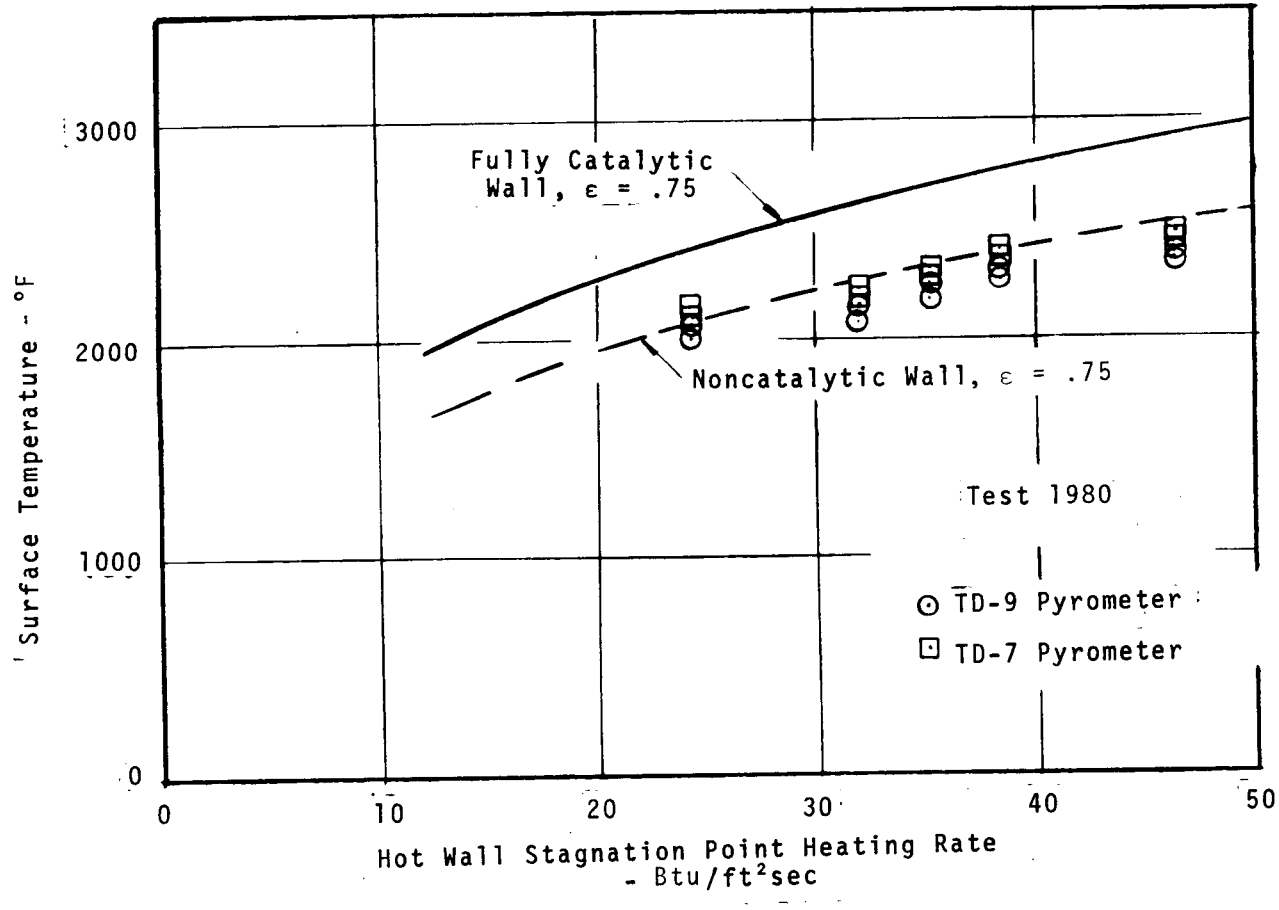

Figure 25 Surface Catalycity Results for HCF Surface Insulator

test results) except for one version of the HCF coating which transisted from essentially fully catalytic to fully noncatalytic by about the fifteenth exposure cycle. Typical surface catalycity results for all surface insulator types are presented in Table 9 and bear out the above discussion.

A comparison of typical pyrometer measurements for the surface insulators is presented in Table 10. These results indicate an emissivity depression for all coatings in the wavelength band of the TD-7 pyrometer (around 2 microns) similar to that for the metallics. The results for SiC foam however do not indicate any such emissivity depression.

In general, the surface insulators were quite sensitive to singularities such as the radial split line between test samples, the joint between the model centerpost and the sample, and the test sample retention points (Figure 2). Unexpected surface emissivities (lower than anticipated) and variations in surface catalycities resulted in some unusual and sometimes catastrophic test sample response early in the test series when test conditions were controlled according to the desired surface temperature. Because of these results, all subsequent tests throughout the program were performed at constant heat flux rather than constant surface temperature.

The primary failure mode for all materials, in addition to the singularity failures mentioned above, was surface and in-depth cracking. In addition, LI-1500 at very high heat flux exhibited melting. All coatings also appeared to be moisture absorbant after exposure.

Typical qualitative response characteristics of the surface insulator test samples are presented in Figure 26 which was taken from the 35mm color slides of the test sample response.

4.4 CARBON-CARBON COMPOSITES

4.4.1 Test Matrix

The major portion of the carbon-carbon composite tests were performed on 180° and 360° truss core* test samples with a wide variety of unspecified coating systems. A more detailed description of the test samples is presented in Appendix A.

*See Section 2.2.

TABLE 9

SURFACE CATALYCITY AND SURFACE EMISSIVITY FOR SURFACE INSULATOR

Sample	Sample Description	Test	Cycle	Cumulative Exposure Time (min.)	Measured Surface Temperature (°F)	Emissivity (-)	Cold Wall Heat Flux (Btu/ft^2 sec)	Total Enthalpy (Btu/lb)	Hot Wall Heat Flux (Btu/ft^2 sec)	Probable Net Heat Flux (Btu/ft^2 sec)	Surface Catalycity Ratio (-)
155	LI-1500G 120° 12-9	1983	6	180	2060	.83	32.4	9800	30.6	15.9	0.52
		1984	12	360	2050		35.1	9760	33.2	15.7	0.47
		1985	18	540	2070		32.0	6850	29.5	16.2	0.55
		1986	24	720	2080		30.3	9770	28.6	16.4	0.57
		1987	30	900	2090		28.8	9790	27.2	16.7	0.61
158	LI-1500G 120° 12-9	1983	6	180	2070		(26.3)	9760	(24.9)	16.2	(0.65)
		1984	12	360	1980		26.4	9770	25.0	14.0	0.56
		1985	18	540	2000		25.9	7300	24.1	14.5	0.60
		1986	24	720	1990		24.5	7030	22.7	14.2	0.63
		1987	30	900	2020		24.3	7050	22.5	14.9	0.66
154	HCF 120° 12-9	1983	6	180	2530	.75	32.4	9800	30.2	28.5	0.94
		1984	12	360	2500		35.1	9760	32.7	27.4	0.84
		1985	18	540	2230		32.0	6850	29.3	18.7	0.64
		1986	24	720	2180		30.3	9770	28.6	17.3	0.60
		1987	30	900	2170		28.8	9790	27.2	17.1	0.63
157	HCF 120° 12-9	1983	6	180	2540		(26.3)	9760	(24.5)	28.9	(1.0)
		1984	12	360	2490		26.4	9770	24.6	27.0	|
		1985	18	540	2420		25.9	7300	23.6	24.6	
		1986	24	720	2230		24.5	7030	22.5	18.7	0.83
		1987	30	900	2180		24.3	7050	22.4	17.3	0.77
153	REI 120° 12-9	1983	6	180	2160		32.4	9800	30.5	16.8	0.55
		1984	12	360	2160		35.1	9760	33.1	16.8	0.51
		1985	18	540	2180		32.0	6850	29.4	17.3	0.59
		1986	24	720	2170		30.3	9770	28.6	17.1	0.60
		1987	30	900	2170		28.8	9790	27.2	17.1	0.63
156	REI 120° 12-9	1983	6	180	2160		(26.3)	9760	(24.8)	16.8	(0.68)
		1984	12	360	2060		26.4	9770	25.0	14.4	0.58
		1985	18	540	2110		25.9	7300	24.0	15.6	0.65
		1986	24	720	2070		24.5	7030	22.7	14.6	0.64
		1987	30	900	2090		24.3	7050	22.5	15.1	0.67
135	SiC Foam 180° 8-24	1970	6	180	2200	.85	47.7	10,770	45.2	20.3	0.45
		1973	12	360	2060		34.1	6930	31.5	16.3	0.52
		1975	18	540	2040		31.9	6700	29.4	15.8	0.54
		1976	24	720	2050		28.3	7200	26.2	16.1	0.61
		1977	30	900	2060		25.3	7300	23.5	15.8	0.67

TABLE 10

COMPARISON OF SURFACE TEMPERATURE
MEASUREMENT RESULTS FOR SURFACE INSULATOR

	TD-9 Pyrometer	Thermogage Pyrometer	TD-7 Pyrometer
• LI-1500			
	2070°F	2080°F	--
	2000°F	1980°F	--
	2080°F	--	1900°F
	1990°F	--	1790°F
• HCF			
	2230°F	--	1950°F
	2420°F	--	2160°F
	2180°F	2180°F	--
	2230°F	2290°F	--
• REI			
	2160°F	2050°F	1760°F
	2160°F	2040°F	1770°F
	2170°F	1910°F	--
• SiC Foam			
	--	2050°F	2060°F
	2140°F	2190°F	2170°F
	--	2190°F	2200°F
	2120°F	--	2140°F
	--	2370°F	2180°F

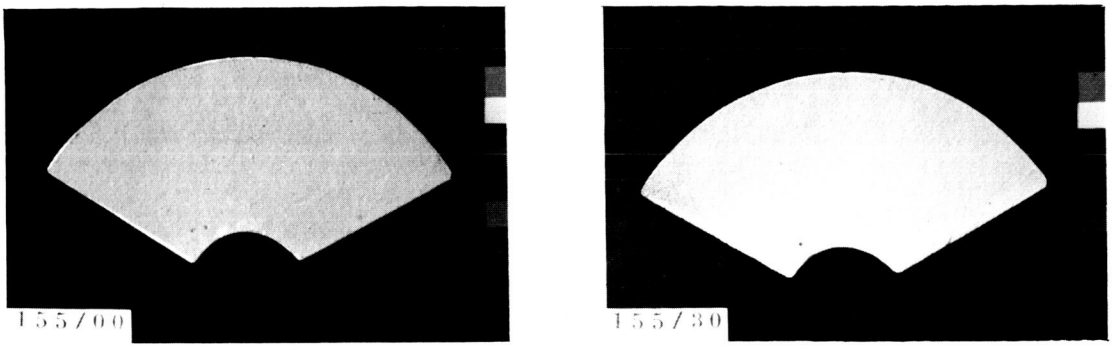

LI-1500 2100°F

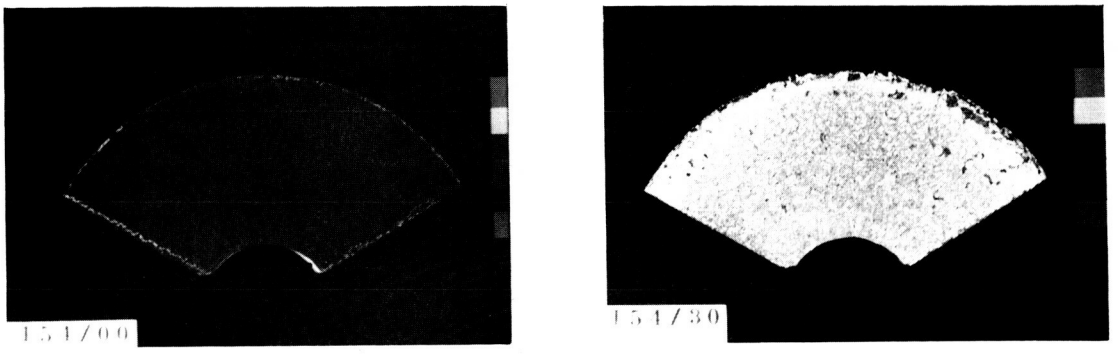

HCF 2500-2200°F

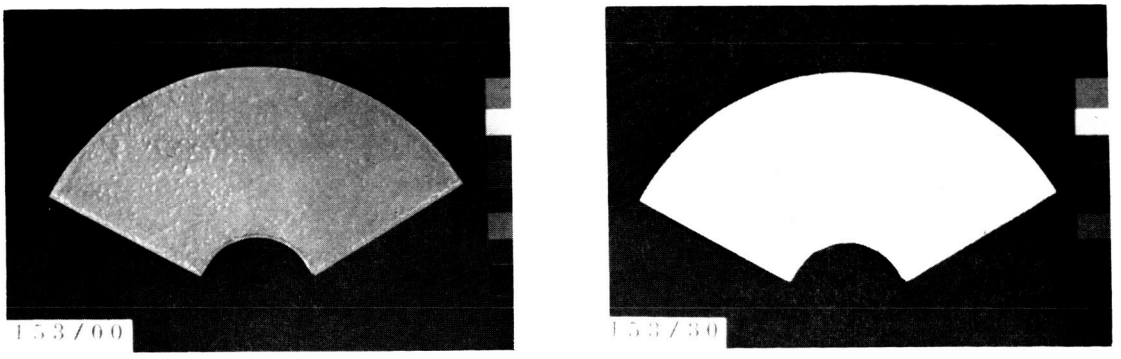

REI 2200°F

30 Btu/ft^{2}sec 000/00 → Sample/Cycle

Figure 26 Response Characteristics of Surface Insulators

The nominal and actual test matrix for the carbon-carbon composites is presented in Figure 27. The symbology is the same as for the metallics. The first four samples were tested at a nominal heat flux of 95 Btu/ft^{2}sec and all other samples were tested at a nominal flux of 75 Btu/ft^{2}sec. All but the last eleven samples were 180° or 360° truss core samples; the last eleven were 60° conventional samples. The coating systems were unspecified but included no coating at all. Only one sample (48) survived 30 cycles; the sample failures are discussed below.

4.4.2 Typical Results

Typical test results for the carbon-carbon composites are presented below in terms of temperature and mass loss response, emissivity and surface catalycity, and failure modes and operating limits. Results not presented are included in Appendix A.

Surface and backwall temperature results for a single typical truss core model for three of the twelve cycles of exposure are presented in Figure 28. The cross-hatching indicates the range in temperature over the six positions for which the pyrometer viewed the test sample. The surface temperature remained essentially constant throughout the entire cyclic exposure. The backwall temperature dropped continuously throughout this exposure, however. The explanation is not obvious but two possibilities are:

- Degradation of the thermocouple performance
- The internal oxidation of the truss core reduced the conduction path to the backwall and therefore the temperature at the backwall

Typical mass loss results for two samples with large variations in surface catalycity (see below) are shown in Figures 29. Note that this loss includes the effects of internal oxidation (see below) and therefore the results reflect a loss which is greater than that of the surface alone.

Specific emissivity data were not available for the test samples and therefore the value of 0.85 suggested by the supplier was assumed for all samples. Within this assumption, the surface catalycity exhibited the spectrum from nearly fully catalytic to fully noncatalytic depending on the coating type. At a heat flux of about 75 Btu/ft^{2}sec, this range in catalycity resulted in a measured surface temperature range from 2900°F to 2100°F. This corresponds to a net flux to the surface for the noncatalytic condition that is about 25 percent of that for the fully catalytic condition. This very large effect is due to the large boundary layer atom population at the high enthalpy (19,000 Btu/lb) and low pressure (0.007 atm) at which these tests were performed. Typical results are presented in Table 11.

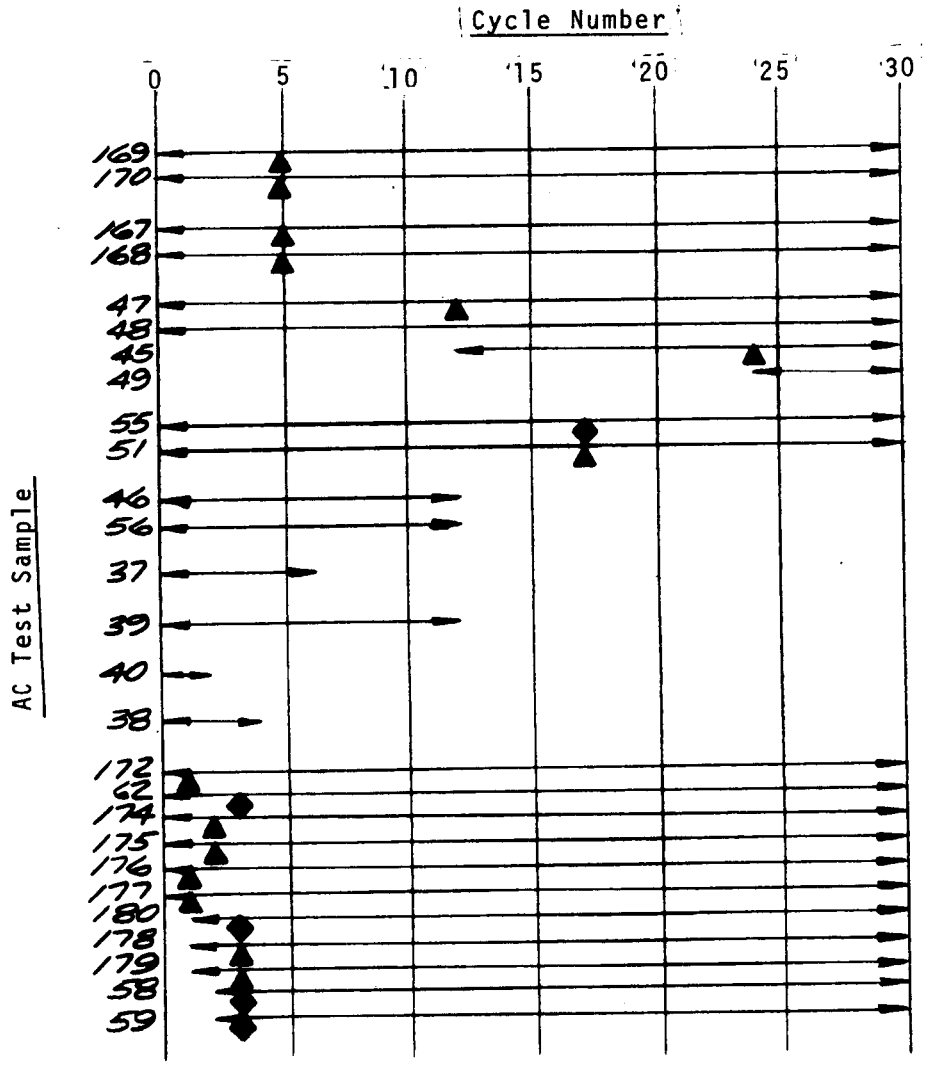

▲ Sample Failed
◆ Insufficient Samples to Continue Tests

Measurements Every 6 Cycles
180°, 360°, or 60° Test Samples

Figure 27 Carbon-Carbon Composites Test Matrix

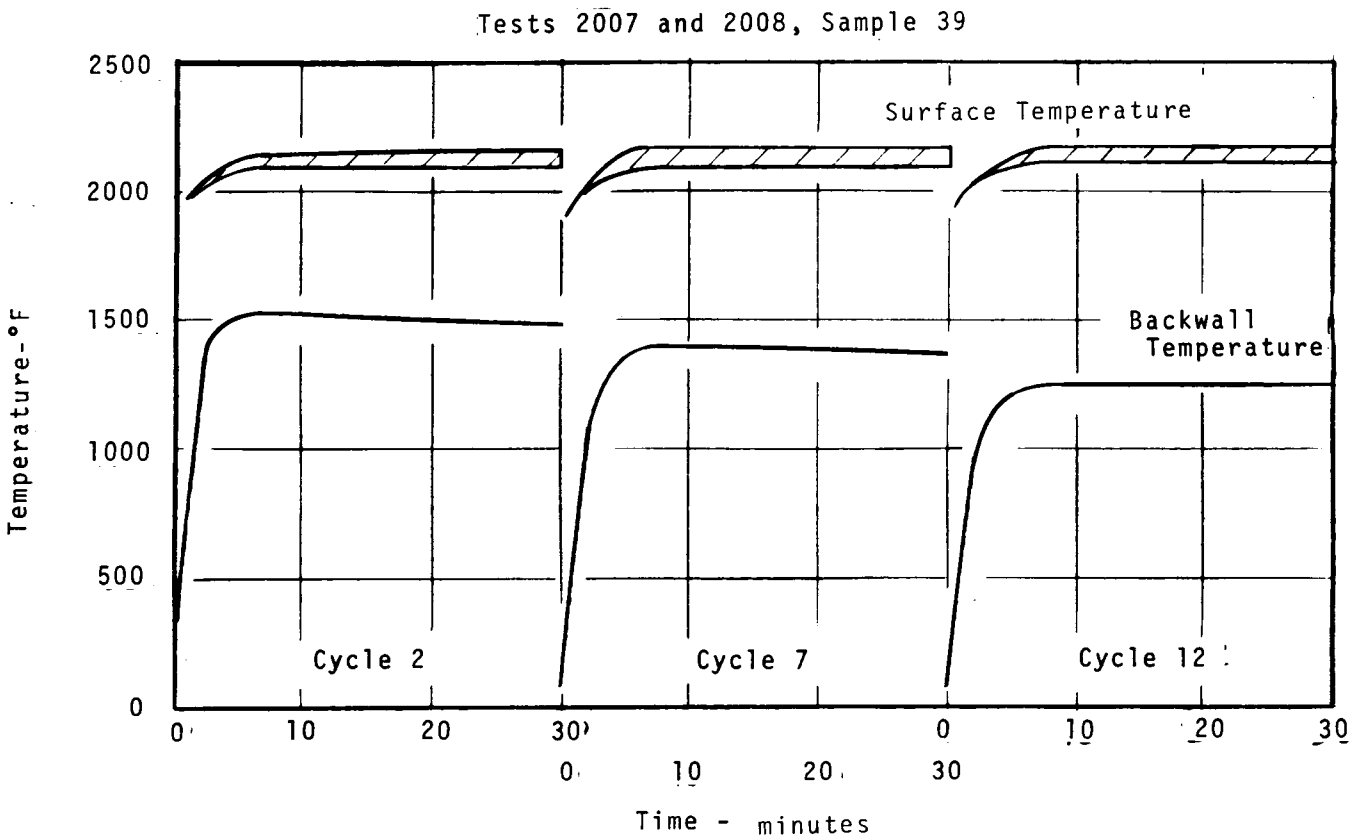

Figure 28 Typical Cyclic Temperature - Time Results for Carbon-Carbon Composites

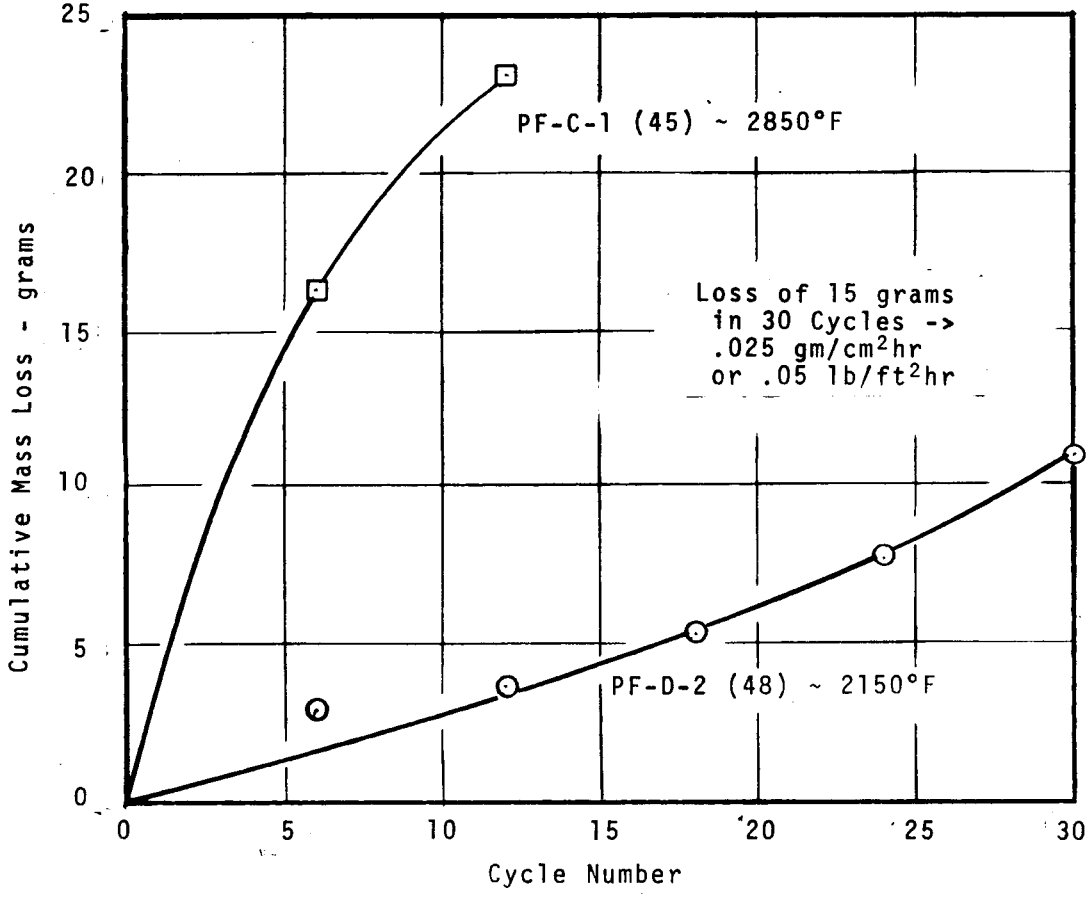

Figure 29 Typical Mass Loss Results for Carbon-Carbon Composites

TABLE 11

SURFACE CATALYCITY AND SURFACE EMISSIVITY FOR CARBON-CARBON COMPOSITES

Sample	Sample Description	Test	Cycle	Cumulative Exposure Time (min.)	Measured Surface Temperature (°F)	Emissivity (-)	Cold Wall Heat Flux (Btu/ft^2 sec)	Total Enthalpy (Btu/lb)	Hot Wall Heat Flux (Btu/ft^2 sec)	Probable Net Heat Flux (Btu/ft^2 sec)	Surface Catalycity Ratio (-)
45	PF-C-1 180°	2001	6	180	2830	.85	76.0	19,000	73.2	47.4	0.65
		2002	12	360	2900		75.9	19,000	72.8	51.6	0.71
48	PF-D-2 180°	1999	6	180	2100		74.1	18,950	72.0	17.4	0.24
		2000	12	360	2100		75.9	18,950	73.7	17.4	0.24
		2001	18	540	2200		76.0	19,000	73.7	20.3	0.28
		2002	24	720	2190		75.9	19,000	73.6	20.0	0.27
		2003	30	900	2150		77.0	18,925	74.7	18.8	0.25

The observed failure modes included:

- Local coating failure and the subsequent severe in-depth oxidation of the carbon-carbon subsurface
- Gross coating failure due to cracking
- Severe internal oxidation

Typical qualitative response characteristics which include these failure modes are presented in Figure 30.

4.5 ABLATORS

4.5.1 Test Matrix

A single ablator type with honeycomb reinforcement - SS41 - was tested. The test samples formed the entire test model as shown in Figure 2. The detailed description of the test samples is presented in Appendix A.

The nominal and actual test matrix is presented in Figure 31. The test samples were exposed for 1000 sec and 2000 sec to define the time variation of the response parameters. The two nominal heat flux conditions were 40 and 100 Btu/ft^2sec.

At the high heating rate condition, the 100 Btu/ft^2sec flux was essentially double the maximum heat flux projected at the start of the program, and therefore the conditions at which this flux was achieved were not optimum. The radial distribution of flux on the model was therefore quite nonuniform - a significant drop off to the edge occurred. Although the char thicknesses were relatively uniform at these conditions, the sample response must be considered to have been influenced to some extent by this nonuniformity, resulting in a somewhat optimistic indication of the sample response.

4.5.2 Test Results

Typical test results for the ablators are presented below in terms of the surface recession and in-depth charring response, the surface and backwall temperature response, and the failure modes and operating limits. Results not presented are included in Appendix A.

The surface recession and in-depth degradation response at the two test conditions is presented in Figure 32. The char - virgin material interface indicated in the figure corresponds to the boundary below which no visual indication of thermal degradation has occurred which is also the plane of weakest structural integrity. For the high heat flux condition, the char has penetrated essentially to the backwall in 2000 seconds. The surface recession is a factor

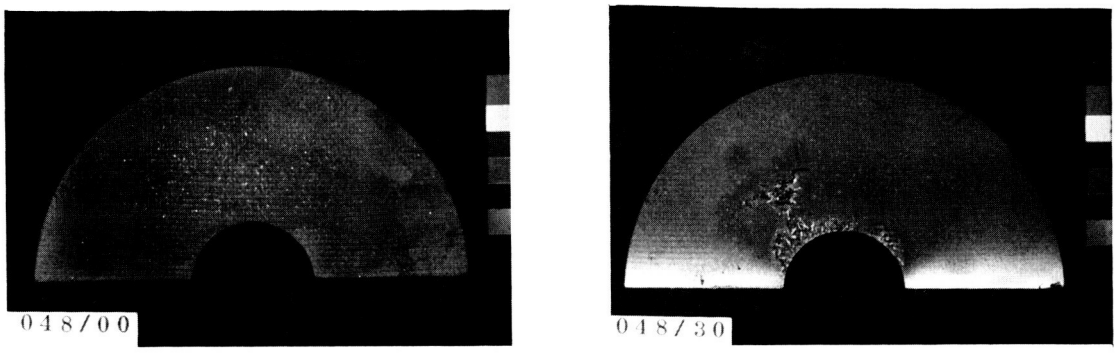

2150°F

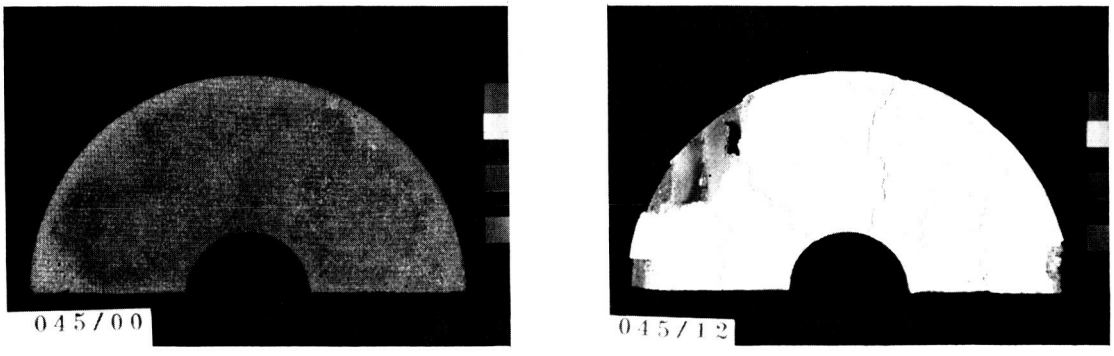

2850°F

75 Btu/ft^{2}sec

000/00 → Sample/Cycle

Figure 30 Response Characteristics of Carbon-Carbon Composites

360° Test Samples

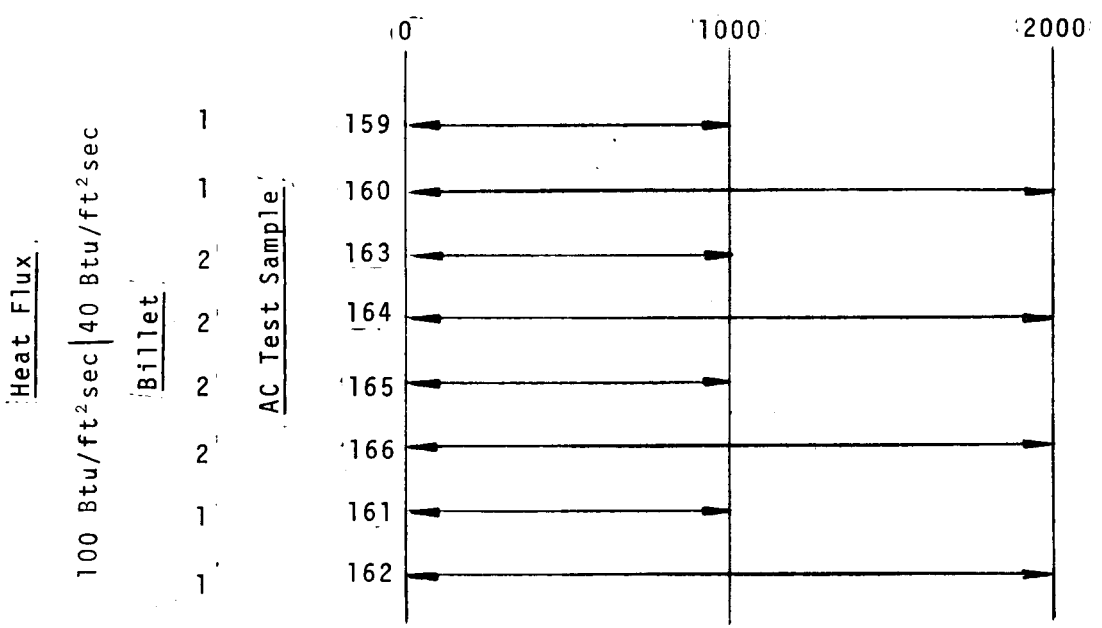

Figure 31 Ablator Test Matrix

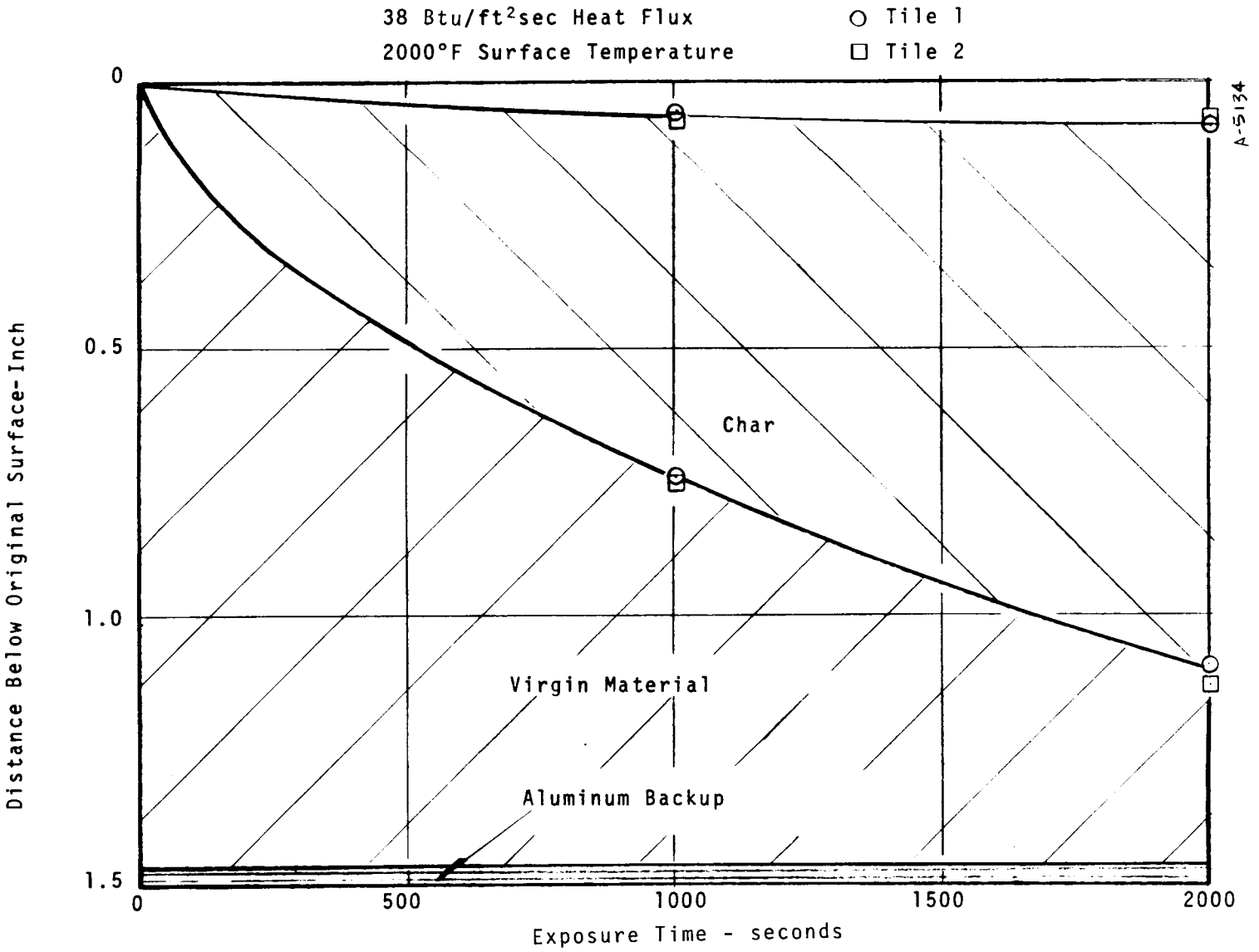

Figure 32 Surface Recession and In-Depth Degradation Response of SS41 Ablator
a) Low Flux Condition

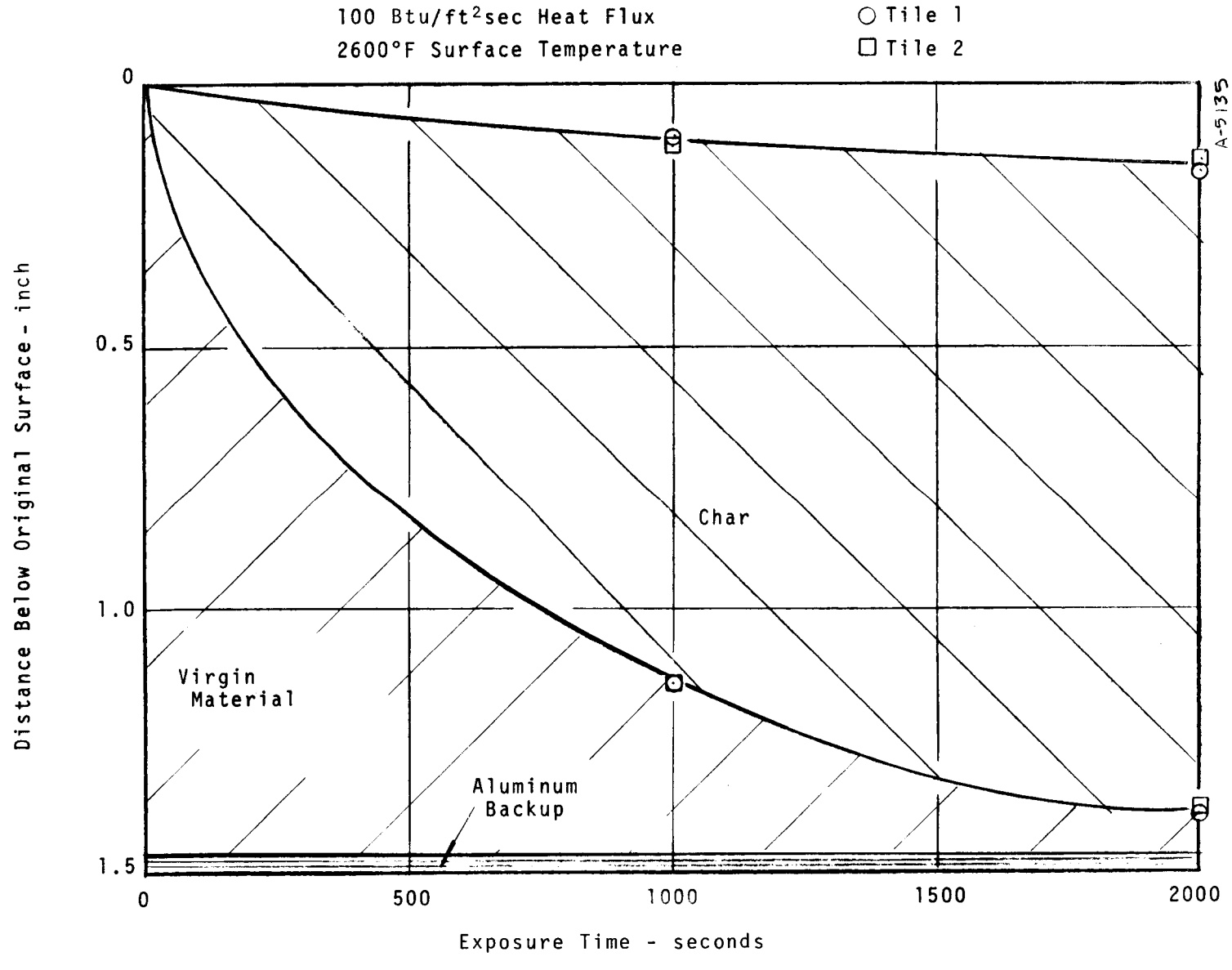

Figure 32 Concluded
b) High Flux Condition

of two higher for the high heat flux condition as compared to the low heat flux condition.

The surface and backwall temperature results for the ablators are presented in Figure 33 for both heat flux conditions. Note that even though charring had occurred to essentially the aluminum backup for the high flux condition, the backwall temperature did not exceed 600°F.

At the low heating rate condition, the material simply charred with no significant dimension change or loss of integrity. At the high heating rate, however, a small amount of silica melt formed on the surface, and a significant preferential mass loss at the honeycomb reinforcement occurred. This response is illustrated qualitatively in Figure 34.

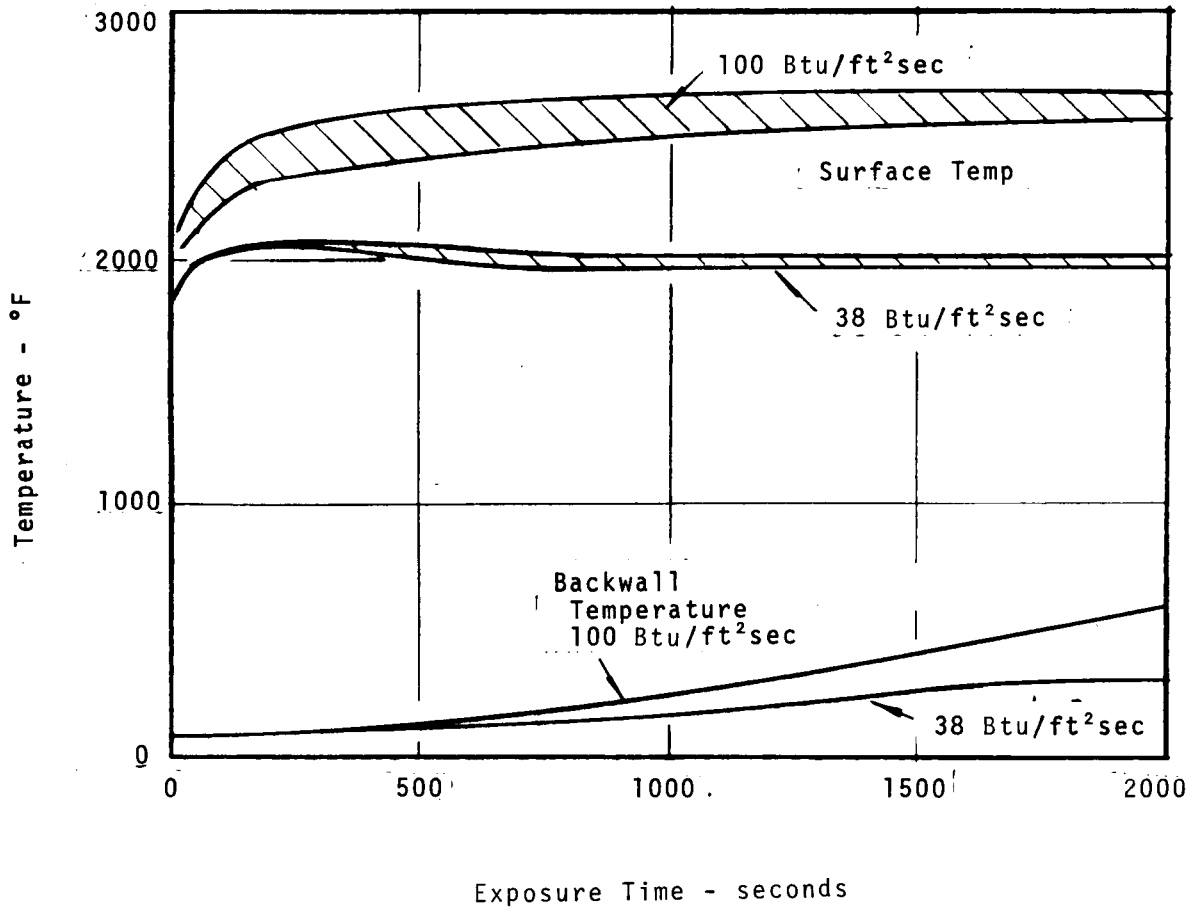

Figure 33 Typical Surface and Backwall Temperature Results for Ablators

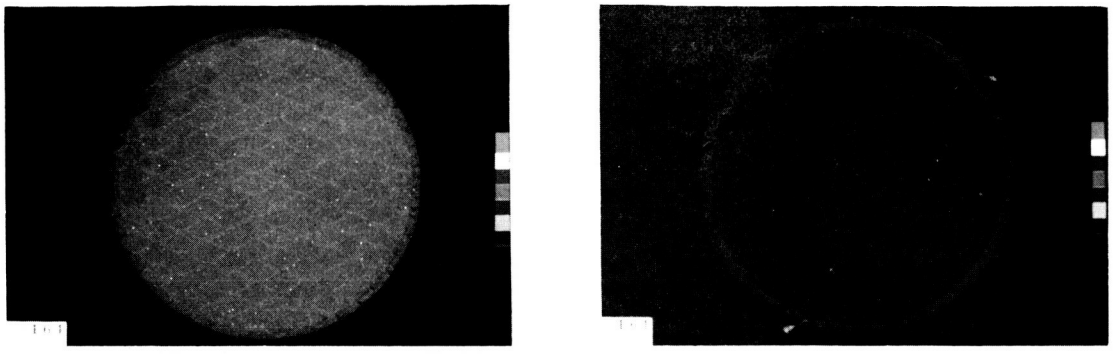

40 Btu/ft^{2}sec

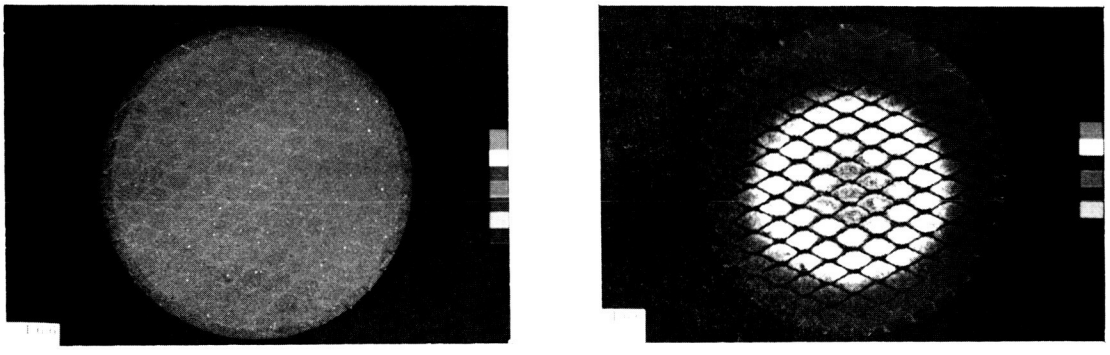

100 Btu/ft^{2}sec

SS 41

Figure 34 Response Characteristics of Ablators

SECTION 5

CONCLUSIONS

Based on the results of 870 sample hours of testing presented above and in Appendix A for the complete spectrum of space shuttle orbiter candidate TPS materials, the following conclusions have been made:

GENERAL

- Accurate measurement of surface temperature requires further evaluation of measurement techniques; accurate measurements of emissivity at the proper wavelengths must be available for pyrometer measurements.
- At conditions of high enthalpy and low surface pressure that result in a high boundary layer atom population, the interpretation of the test results and their application to flight depend critically on an accurate knowledge of the surface catalycity.
- Due to differences in surface catalycity and emittance, tests and comparison of materials should be made at common levels of heating rate, not surface temperature.
- Test model singularity regions which may influence material response and which are not typical of the flight application should be eliminated.
- By testing at maximum efficiency, the test cost can be as low as $70 per hour and with a six sample model configuration this results in a cost of roughly $10 per sample hour of exposure.

SPECIFIC

- Metallics
  - TD NiCr exhibits consistent response characteristics in the temperature ranges of its application (to 2400°F).
  - Flaws in coated Cb are generally self-healing (at 2500°F).
  - Flaws in coated Ta generally grow and can result in catastrophic failure (at 2700°F).

- Surface Insulators
  - Wide range of surface emittance and catalytic activity can be achieved depending on the surface coating.
  - Response is sensitive to singularities.
- Carbon-Carbon Composites
  - A wide range of surface catalytic activity can be achieved depending on the surface coating or surface matrix.
  - Oxidation protection of the internal surfaces of the truss core configuration is required.
- Ablators
  - At high flux, local mass loss at the honeycomb reinforcement is significant.

REFERENCES

1. Winovich, W., "On the Equilibrium Sonic-Flow Method for Evaluating Electric-Arc Air-Heater Performance," NASA TND-2132, March, 1964

2. Schaefer, J. W., Flood, D. T., Reese, J. J., Jr., and Clark, K. J., "Experimental and Analytical Evaluation of the Apollo Thermal Protection System Under Simulated Reentry Conditions," Aerotherm Corporation, Mountain View, California, Final Report No. 67-16, July, 1967.

3. Schaefer, J. W. and Flood, D. T., "High-Enthalpy Reentry Simulation for Planetary Return Missions," Journal of Spacecraft & Rockets, Vol. 5, No. 9, September, 1968, pp. 1108 - 1110.

4. Hiester, N. K. and Clark, C. F., "Feasibility of Standard Evaluation Procedures for Ablating Materials," Stanford Research Institute, Menlo Park, California, NASA CR-379, February, 1966.

5. Boison, J. C. and Curtis, H. A., "On Experimental Investigation of Blunt Body Stagnation Point Velocity Gradients," ARS Journal, Vol. 29, No. 2, February, 1959.

6. Schaefer, J. W., Tong, H., Clark, K. J., Suchsland, K. E., and Neuner, G. J., "Analytic and Experimental Evaluation of Flowing Air Test Conditions for Selected Metallics in a Shuttle TPS Application," Aerotherm Division, Acurex Corporation, Mountain View, California, Final Report No. 72-64, Contract NAS 1-10913, to be published as a NASA low number CR.

7. Private Communication, W. B. Lisagor, NASA Langley Research Center, August, 1972.

8. Rinehart, W. A., Land, D. W., Painter, J. H. and Williamson, R. A., "Cyclical Tests of Selected Space Shuttle Materials in a Plasma Arc Tunnel," McDonnell Douglas Astronautics Company, NASA CR-114459, to be published.